National Défense
Defence nationale

DESIGN OF A TEM CELL EMP SIMULATOR (U)

by

Pete Sevat

DEFENCE RESEARCH ESTABLISHMENT OTTAWA
REPORT NO. 1084

Canada

June 1991
Ottawa

National Defence / Défense nationale

DESIGN OF A TEM CELL EMP SIMULATOR (U)

by

Pete Sevat
Nuclear Effects Section
Electronics Division

DEFENCE RESEARCH ESTABLISHMENT OTTAWA
REPORT N0. 1084

PCN
041LT

June 1991
Ottawa

ABSTRACT

This report is a compilation of design criteria for a Transverse Electromagnetic (TEM) cell, an EMP generator and a terminating network. From this information, two detailed designs are presented, one for a 50 Ω and the other for a 100 Ω cell. Both these designs integrate the three sections mentioned above into one shielded system.

RÉSUMÉ

Ce rapport résume les critères utilisés pour la conception d'une cellule électromagnétique transverse, d'un générateur d'impulsions électromagnétiques et d'un réseau de terminaison. Deux configurations sont étudiés en détails: une cellule de 50 Ω et 100 Ω. Les deux configurations incorporent les trois sections mentionnées pour former un système blindé.

Executive Summary

Electromagnetic Pulse (EMP) Simulators are designed to simulate the EMP generated by a nuclear weapon and, subsequently, are used to harden equipment against the effects of EMP.

At present, the Defence Research Establishment (DREO) has a 1-m, asymmetric, parallel-plate EMP Simulator in use for testing computer size terminals. In addition, a 10-m, parallel-plate, EMP Simulator is under development for testing larger objects such as helicopters.

This report concerns the design of a small, symmetric, co-axial type of EMP Simulator intended primarily for R&D purposes such as; calibration of sensors, precision measurements, design and testing of transient suppression devices etc.

A detailed design is given for a 50 Ω and 100 Ω TEM cell with a inner volume of ℓ x w x h = 2m x 2m x 1m and a test volume of ℓ x w x h = 2m x 0.3m x 0.4m. The pulse generator and terminating network are integrated into the TEM cell to form a completely shielded structure. In this way no interference from the inside of the cell to the outside, or vis versa, will occur.

TABLE OF CONTENTS

1.0	INTRODUCTION	1
2.0	REQUIREMENTS	4
3.0	TEM CELL	4
	3.1 TEM Mode, Higher-Order Modes	4
	3.2 Dimensions	12
	3.3 Impedance	13
	3.4 Resonant Frequencies	13
	3.4.1 CW Applications	13
	3.4.2 Pulse Applications	21
	3.4.3 The Effects of Resonances	21
	3.5 Field Intensity	24
	3.6 Field Distribution	24
	3.7 Test Volume	29
	3.8 Field Enhancement	33
	3.9 Risetime	45
4.0	GENERATOR	45
	4.1 Capacitor	47
	4.2 High Voltage Power Supply	51
	4.3 Spark Gap	51
	4.4 Triggering	55
	4.5 Adapter	57
	4.6 Suppression of Higher-Order Modes	57
5.0	TERMINATION	62
	5.1 Load Resistor	62
	5.2 Voltage Divider	66
6.0	CONSTRUCTION	69
7.0	SAFETY	69
8.0	CONCLUSIONS	71
9.0	ACKNOWLEDGEMENT	72
10.0	REFERENCES	93
APPENDIX A:	Regulated High Voltage DC Power Supply, Glassman ER60R5	95
APPENDIX B:	Ceramic Capacitors; TDK and Murata	97
APPENDIX C:	Non-inductive Resistors; Carborundum	107

1.0 INTRODUCTION

A TEM cell is a square or rectangular coaxial transmission line tapered at each end to form a closed cell. The cell can be fed at one end with a signal generator and terminated at the other end by a resistor equal to the characteristic impedance of the line. Between the inner conductor (the septum) and the enclosure a field propagates from the source to the termination as a planar field in free space, see Figure 1.

The source at the input side can be a CW or a pulse generator. The source and termination can be connected to the cell by coaxial cables. In the case of an EMP simulator the pulser and terminating resistor can be made a part of the coaxial structure and can be integrated with the cell to form a completely closed structure, see Figure 2.

The exterior of the cell is a grounded metal enclosure which contains the internal field that otherwise would radiate into the surroundings and perhaps interfere with associated equipment and, conversely, shields the internal volume from the external electromagnetic environment, e.g. from nearby broadcast transmitters.

One advantage of the TEM cell is that the field is well characterized and reasonably uniform. The primary shortcomings are the upper frequency limit and the restricted working space.

The TEM cell EMP simulator to be designed for DREO, is intended for applications such as:

- susceptibility testing of small equipment;
- calibration of sensors;
- design and testing of countermeasures;
- measurement of transfer functions; and
- research and development (low voltage signal input).

In this report the tools required for the design of a TEM cell, an EMP generator and a terminating network are collected. The report has been prepared as a part of the Consulting Service Contract, attached to letter DREO 3743A-1 (ED/NES) of 22 March 1990.

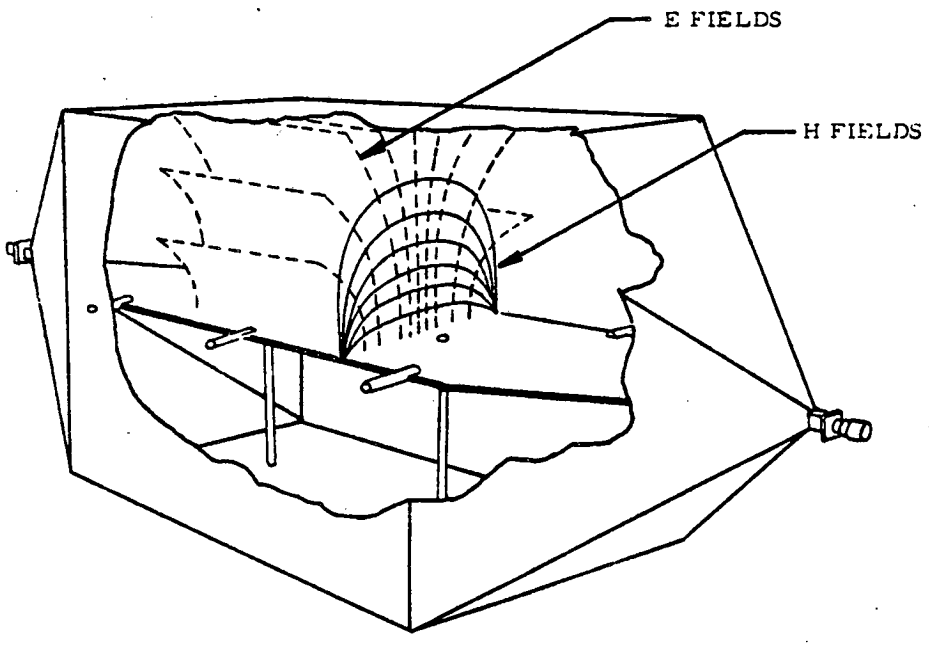

FIGURE 1 Transverse electromagnetic (TEM) field distribution inside a TEM cell

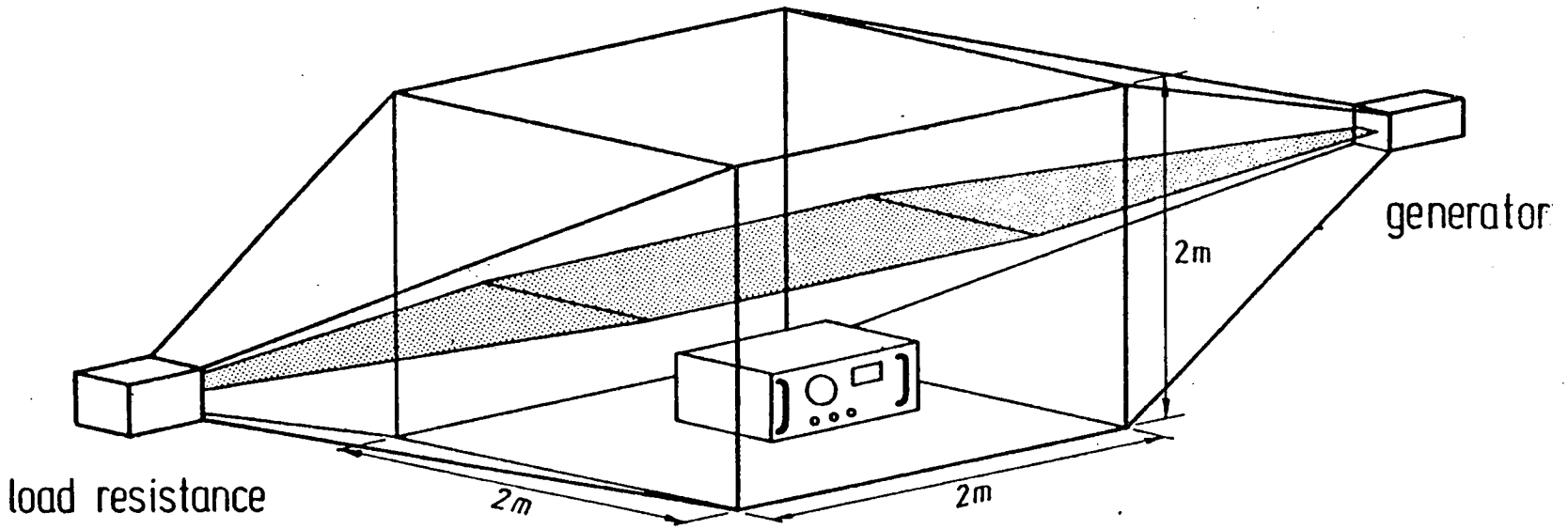

Electromagnetic Pulse Simulator EMIS-1

Operational at the Physics Laboratory TNO, The Hague, since April 1973 (Ref. NATO, AEP-9)

FIGURE 2 A TEM cell EMP simulator. Pulser and load are shielded and integrated in the cell

2.0 REQUIREMENTS

The following characteristics should be implemented in the design:

- simulation of the exo-atmospheric EMP;
- EMP model as described in NATO documents;
- minimum test height 30 cm;
- system impedance 50 Ω;
- adaptor for 50 Ω coaxial input;
- voltage divider output for calibration purposes; and
- negligible outside radiation.

3.0 TEM CELL

The shell of the cell can be square or rectangular in cross section with the septum either midway between opposite walls (a symmetric cell) or offset from the center plane of the cell (an asymmetric cell). The trade-off between test volume and field uniformity determines which cell configuration is best for a given application.

3.1 TEM mode, higher-order modes

TEM (Transverse Electro Magnetic) waves are characterized by the fact that both the electric vector (E-field) and the magnetic vector (H-field) are perpendicular to each other and to the direction of propagation. A TEM cell will not only propagate a single TEM mode at all frequencies, but also a set of Transverse Electric and Transverse Magnetic higher-order modes TE_{mn} and TM_{mn} at frequencies above their respective cutoff frequencies $f_{c(mn)}$. The TEM mode propagates through the tapered ends of the cell without significant alteration. Each higher-order mode, however, is always reflected at some point within the taper where it becomes too small to propagate the mode. This is the point where the cross-section of the taper has narrowed to that of a waveguide whose cutoff frequency is lower than the field frequency. The propagating energy in the higher-order mode undergoes multiple reflections, end to end, within the cell, until it is dissipated.

At certain frequencies a resonance condition is satisfied, in which the cell's effective length for the mode is "p" half guide wavelengths long ($p = 1, 2, \ldots$). At these resonant frequencies $f_{R(mnp)}$, a TE_{mnp} resonant field pattern exists. Thus the TE_{mn} mode in a given TEM cell has one cutoff frequency $f_{c(mn)}$ and an infinite set of resonant frequencies, $f_{R(mnp)}$ with $p = 1, 2, \ldots$. The same is true for the TM_{mn} higher-order modes, although these only occur at higher frequencies.

The total E-field pattern due to the presence of some RF energy in a propagating higher-order mode can be qualitatively understood by adding or subtracting the pattern of the higher-order mode to or from the TEM mode pattern, see Figure 3. TEM cells can be used above the cutoff frequency of the first higher-order mode $f_{c(01)}$ [1].

The resonant frequencies, $f_{R(mnp)}$ are calculated from the values of $f_{c(mn)}$ and the cell's length and taper dimensions, see Figure 4.

$$f^2_{R(mnp)} = f^2_{c(mn)} + \left(\frac{pc}{2L_{mn}}\right)^2 \qquad (1)$$

$$L_{mn} = L_C + X_{mn}L_E \qquad (2)$$

L_C is the length of the uniform-cross-section center part of the cell, L_E is the length (along the center line) of the two tapered ends, and X_{mn} is the fraction of the two ends included in the value of L_{mn}, see Figure 4, Fraction X_{mn} is empirically determined and is different for each cell as well as each mode. It can change from 0.8 for the TE_{01} mode to 0.5 for the TE_{10} and TE_{11} modes.

The TE_{01} mode in a small gap TEM cell has strong gap-fringing fields, while not exhibiting significant fields in the central test area, see Figure 3. Therefore, although the TE_{01} causes the first possible resonance, it is usually not excited unless a large test object or some other perturbation is present [2]. In Figure 5 the cross-section of a TEM cell and in Figure 6 the cutoff wavelengths of some higher-order modes as a function of the TEM cell geometry are given. Figure 7 shows the cutoff wavelength of the first higher-order mode TE_{01} for different characteristic impedances. Note that the width in Figure 7 is "a", not 2a. Figure 8 shows the same for more higher-order modes [7].

Hill made measurements of the higher-order modes [1]. Each of the first three higher-order modes, TE_{01}, TE_{10} and TE_{11} was found to propagate at frequencies above its first resonance, but not between its cutoff frequency and first resonance. The propagating higher-order modes TE_{01}, TE_{10} and TE_{11} altered the TEM mode E-field in the test volume of the measured TEM cells up to <3%, 10-15% and 10-15% respectively.

A TEM cell may be used for field-probe calibration work up to $f_{R(111)}$, except near $f_{R(101)}$. The effects of the TE_{01p} resonances and the propagating TE_{01} and TE_{10} modes can possibly be eliminated by averaging the two calibration curves taken in the center of the test volume at opposite sides of the septum. [1 p.188]

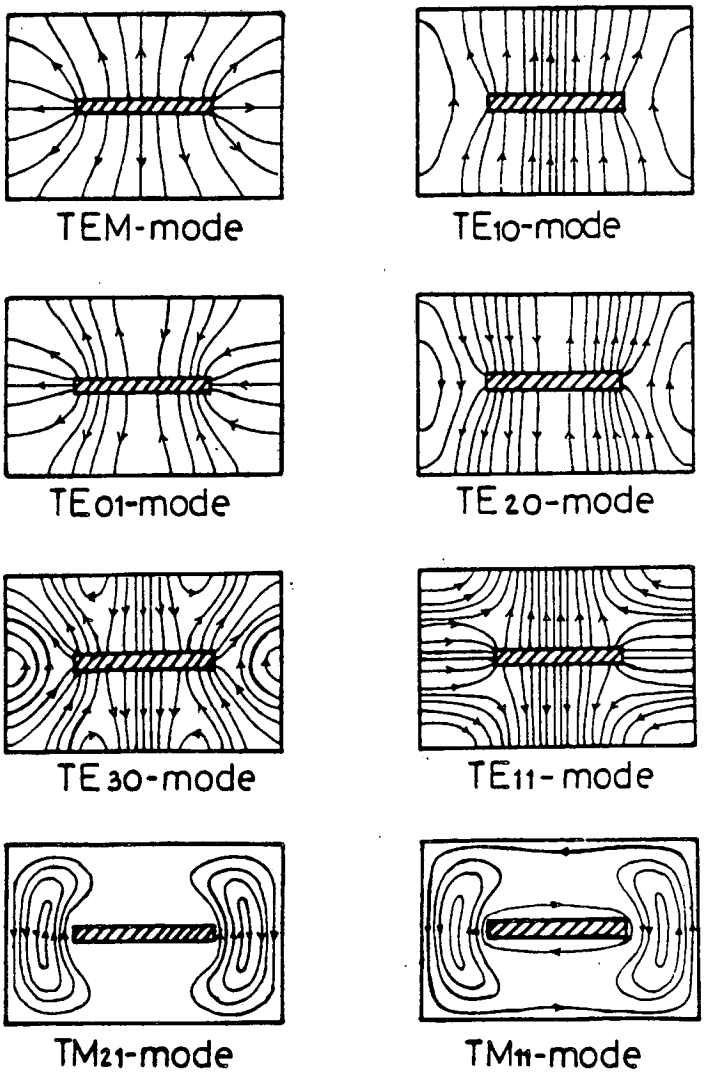

Figure 3 Higher order mode field configurations in symmetric TEM cell. E-field distribution for TEM and TE modes. H-field distribution for TM modes.

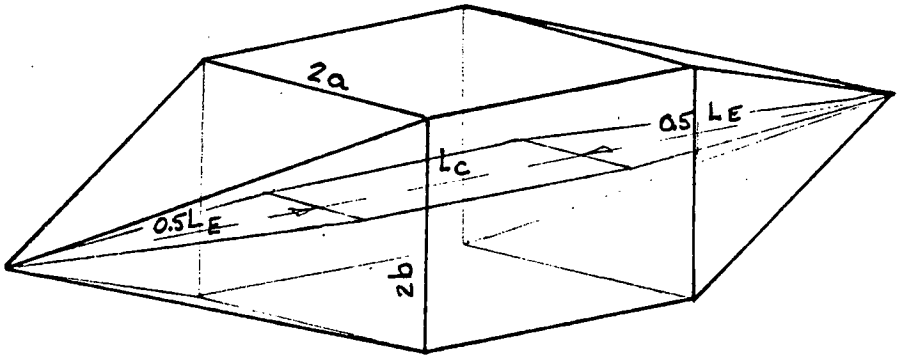

FIGURE 4 . The length of the cell, $L = L_C + L_E$

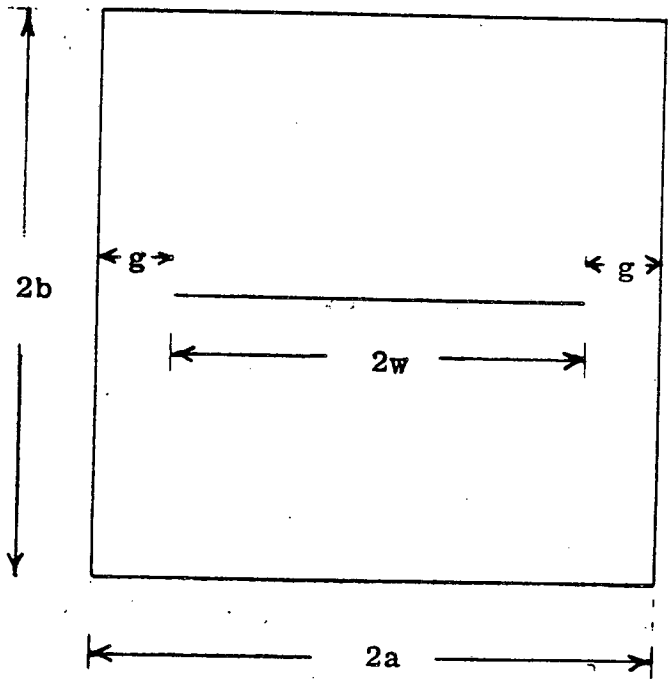

FIGURE 5 Cross-section of a TEM cell

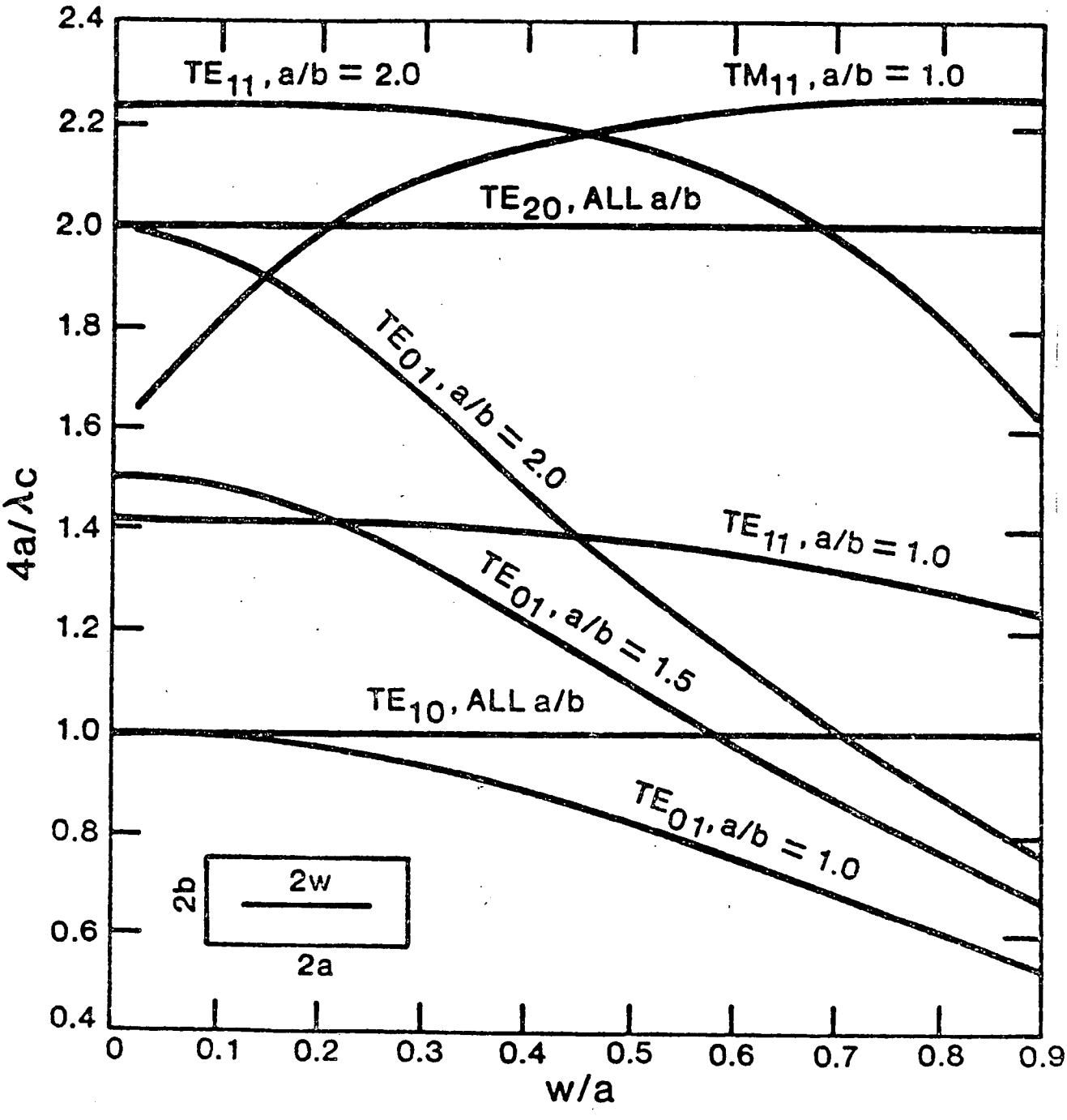

Figure 6 Cutoff wavelengths of some higher-order modes as a function of TEM cell geometry [4].

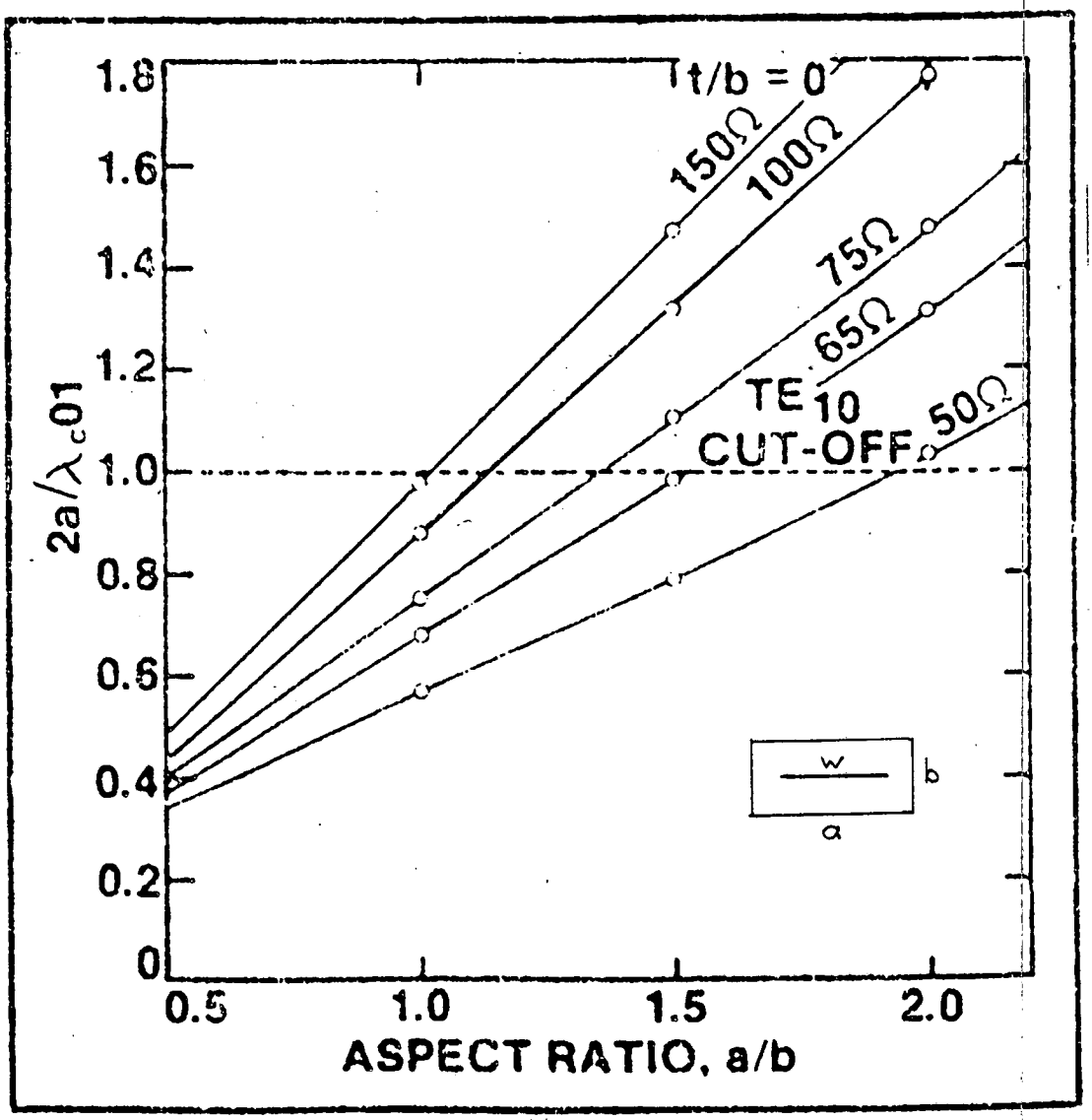

Figure 7 Normalized cut-off frequency versus a/b for the TE_{01} mode in rectangular striplines of different characteristic impedance [4].

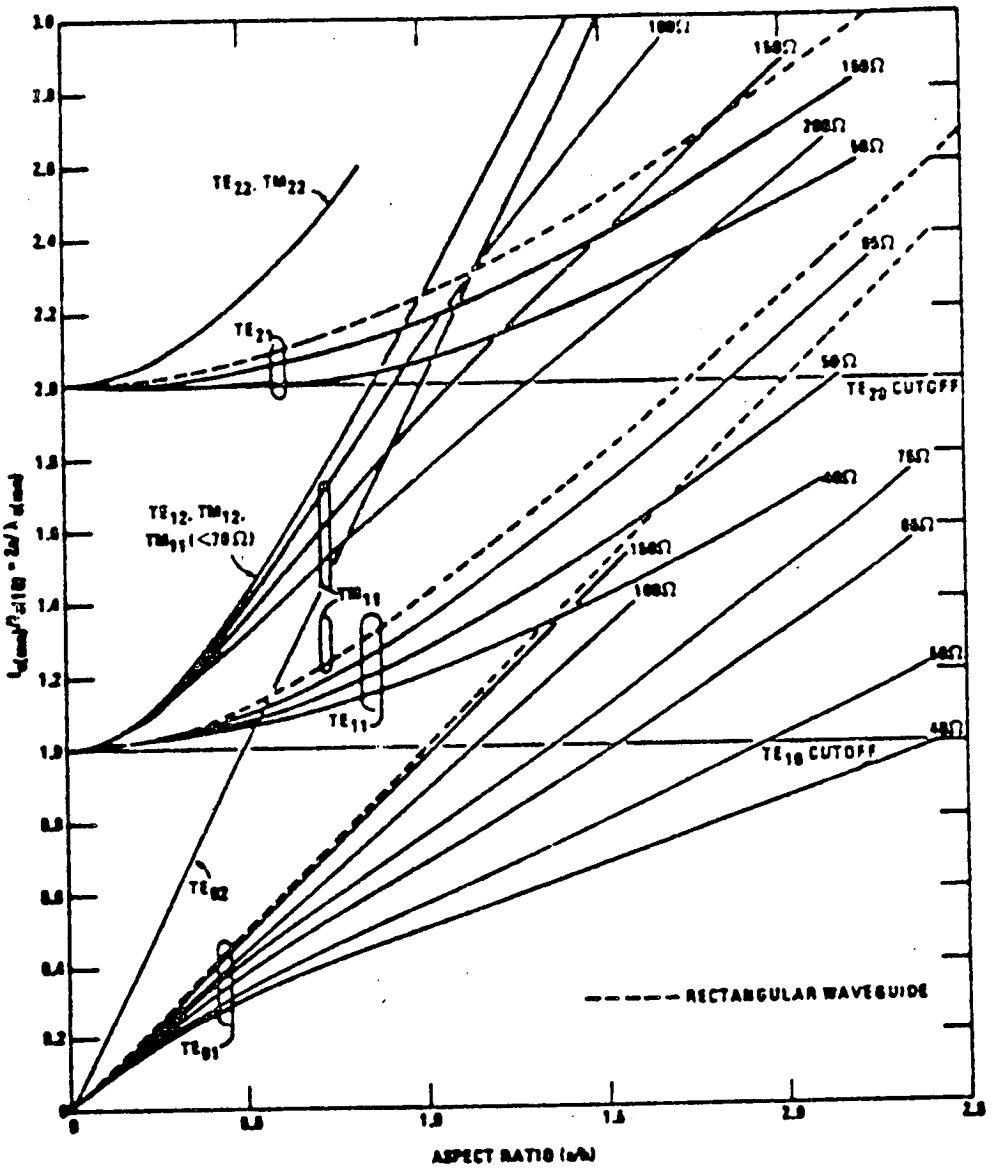

Figure 8 Normalized cut-off frequency versus a/b for the lowest higher-order modes [7].

To design a TEM cell for maximum usable bandwidth, the frequency of the first interacting resonance TE_{101} should be as high as possible. This is accomplished primarily by making cell dimension "a" as small as possible, which causes $f_{c(10)}$ to be as large as possible. To a lesser extent, keeping L_C and L_E as small as possible helps.

For field generation purposes a TEM cell can be operated from zero frequency to the frequency at which higher-order modes appear. However, generating pulsed fields with a width of more than a few hundred nanoseconds does not make sense because the dimensions of the equipment under test (EUT) are too small to couple with very low frequencies. Because of its TEM mode of operation the cell has a linear phase response from zero frequency to near $f_{c(10)}$ and can thus be used for swept frequency measurements.

3.2 Dimensions

The required minimum height of the test volume is 0.3 m. That means that "b" in Figure 5 should be at least 3 x 0.3 m (see section 3.6) for a tolerable field disturbance [3]. Let us choose b = 1 m. For a square structure (a/b = 1) 2a = 2 meters. A rectangular cross-section has a better field uniformity, however, increasing the width to more that 2 m results in a lower cutoff frequency $f_{c(10)}$ and in longer and wider tapers. The optimum geometry for maximum test area and maximum test frequency is one in which b equals a. Therefore, let us choose a larger bandwidth and accept a square cross-section of 2 x 2 m.

For calibration purposes and EMP simulation there are advantages to a symmetric cell. We choose a length of 2 m for both the uniform cross-section (L_C) and the tapers ($L_E/2$). The total length along the center line is 2 + 2 + 2 = 6 m. The length of the tapers is relatively large for a typical TEM cell, however this results in a short rise time (section 3.9) and less distortion of the field caused by reflections at the taper interfaces (section 3.7).

For a square structure (a/b = 1) the TE_{01} mode is always the first higher-order mode for any non-zero value of w/a, see Figure 6 [4]. Extending the frequency range of rectangular structures, basically involves selecting a design such that the TE_{01} mode cannot propagate at frequencies below the TE_{10} mode cutoff. In general, this can be accomplished by reducing the value w/a. This in turn raises the impedance of the line progressively, with a/b = 1 in Figure 7, up to 150 Ω [4]. If the TEM cell would be used only for EMP simulation, a higher impedance than 50 Ω would be a better choice, because it results in a shorter rise time. Furthermore, a higher impedance results in a smaller septum width which generates fewer field enhancement problems.

3.3 Impedance

The characteristic impedance of a TEM cell can be expressed as:

$$Z_0 = \frac{\eta_0 \epsilon_0}{C_0} \quad \text{ohm} \tag{3}$$

where $\eta_0 = 120\ \pi$ ohm, and

$$\frac{C_0}{\epsilon_0} = 4\left[\frac{a}{b} - \frac{2}{\pi} \ln\left(\sinh \frac{\pi g}{2b}\right)\right] - \frac{\Delta C}{\epsilon_0} \tag{4}$$

The term $\Delta C/\epsilon_0$ relates to the fringe capacitance between the edges of the septum and the side walls. If $a/b \geq 1$ and $w/b \geq 0.5$ then ΔC is negligible [5]. The exact value of C_0/ϵ_0 can be read from Figure 9. The term $\Delta C/\epsilon_0$ is dependent on the location along the septum, because the fringe capacitance in the tapers is increasing, resulting in a little larger impedance. If the ratio's a/b and a/w are kept constant over the whole length of the cell the impedance in the tapers will be approximately the same as that in the uniform cross-section of the cell.

Curves for designing a square transmission line with arbitrary cross-section and impedance are shown in Figure 10a and 10b and the effect of the thickness of the septum is shown in Figure 11 [6]. A minimum thickness "t" may be necessary to avoid corona with the application of high voltages.

The last dimension of the cell, the width of the septum, can be read from Figure 11. With $a/b = 1$ and $Z_0 = 50\ \Omega$ the ratio $w/b = 0.83$. For a thickness $t = 0.5$ mm the ratio $t/b \approx 0$. Now, all dimensions of the cell are chosen. They are shown in Figure 12 (top and side view) and Figure 13 (cross-section).

3.4 Resonant Frequencies

3.4.1 CW Applications

With the dimensions of the cell, derived in 3.2, the cutoff frequencies of the lower higher-order modes with their resonant frequencies can be derived. In Table 1, the cutoff and resonant frequencies for $m = 0...2$, $n = 0...2$ and $p = 1...3$ are given. The cutoff frequencies $f_{c(mn)}$ are read from Figs. 6 and 8 [4, 7]. An average value $L_{mn} = 4$ m is used, see Figure 4. The first interacting resonant frequency, the TE_{101} mode, is about 84 MHz. At the frequencies $f_{R(mnp)}$ the cell behaves as a resonant cavity with a high Q. If the cell is fed by a CW source continuous propagating waves and standing waves are produced.

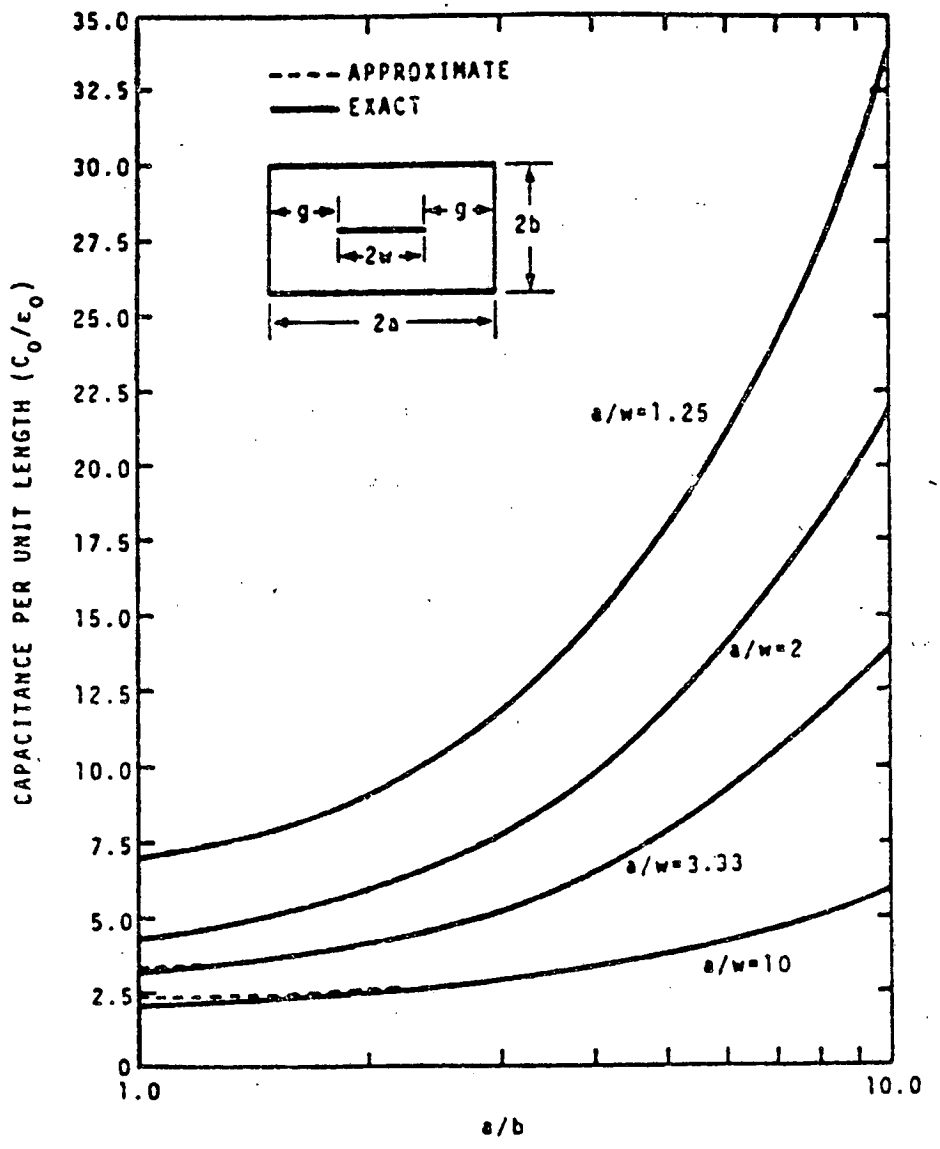

FIGURE 9 Capacitance per unit length of a TEM cell as a function of cell geometry [5]

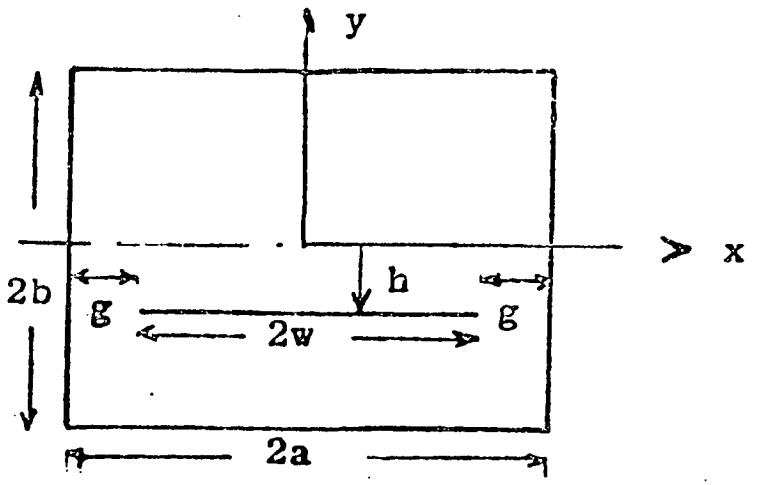
y
x
2b
h
g
g
2w
2a

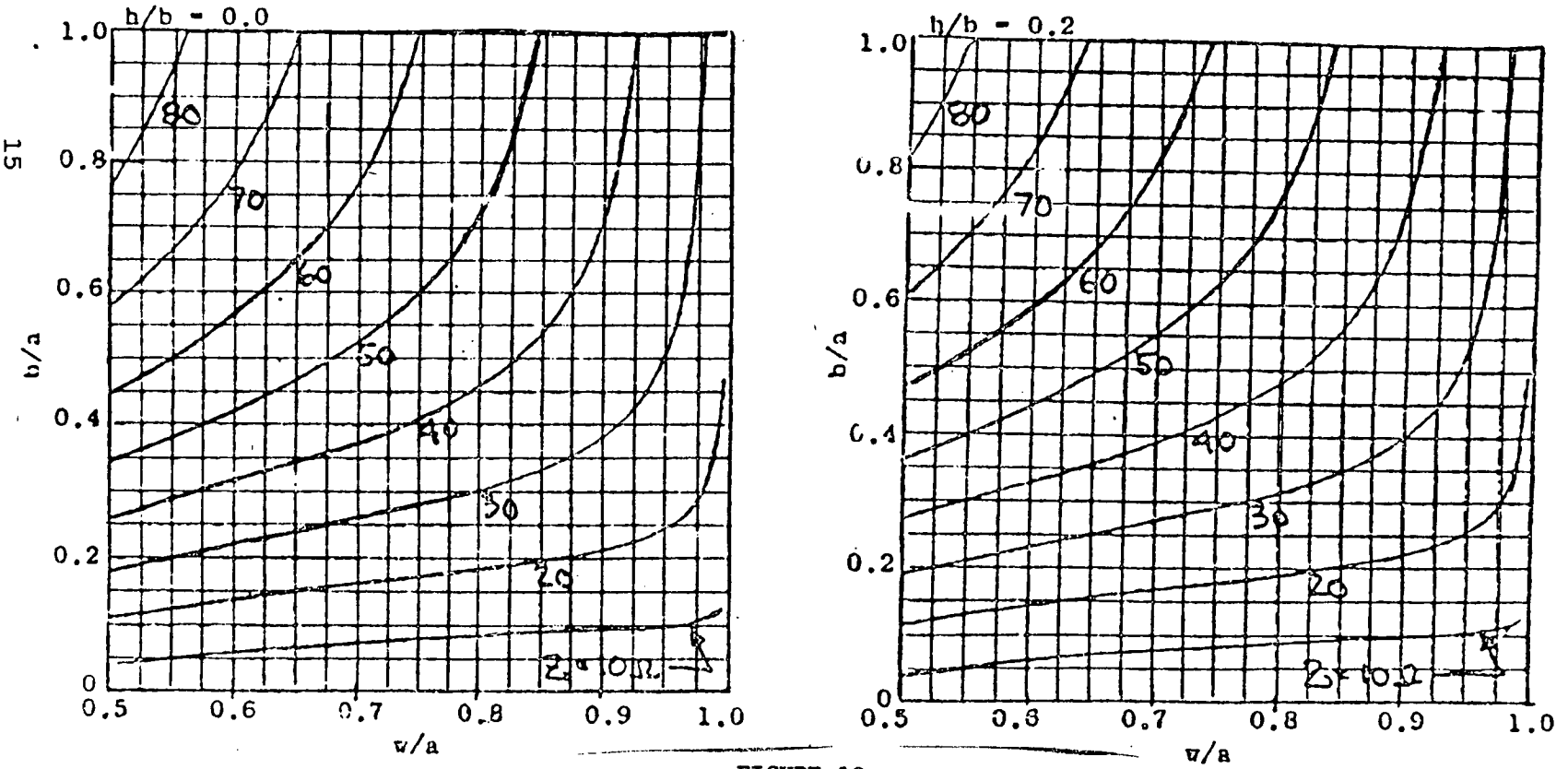
h/b = 0.0
h/b = 0.2
b/a
w/a
80
70
60
50
40
30
20
2a=0.2
0
0.2
0.4
0.6
0.8
1.0
0.5
0.6
0.7
0.8
0.9
1.0

FIGURE 10a

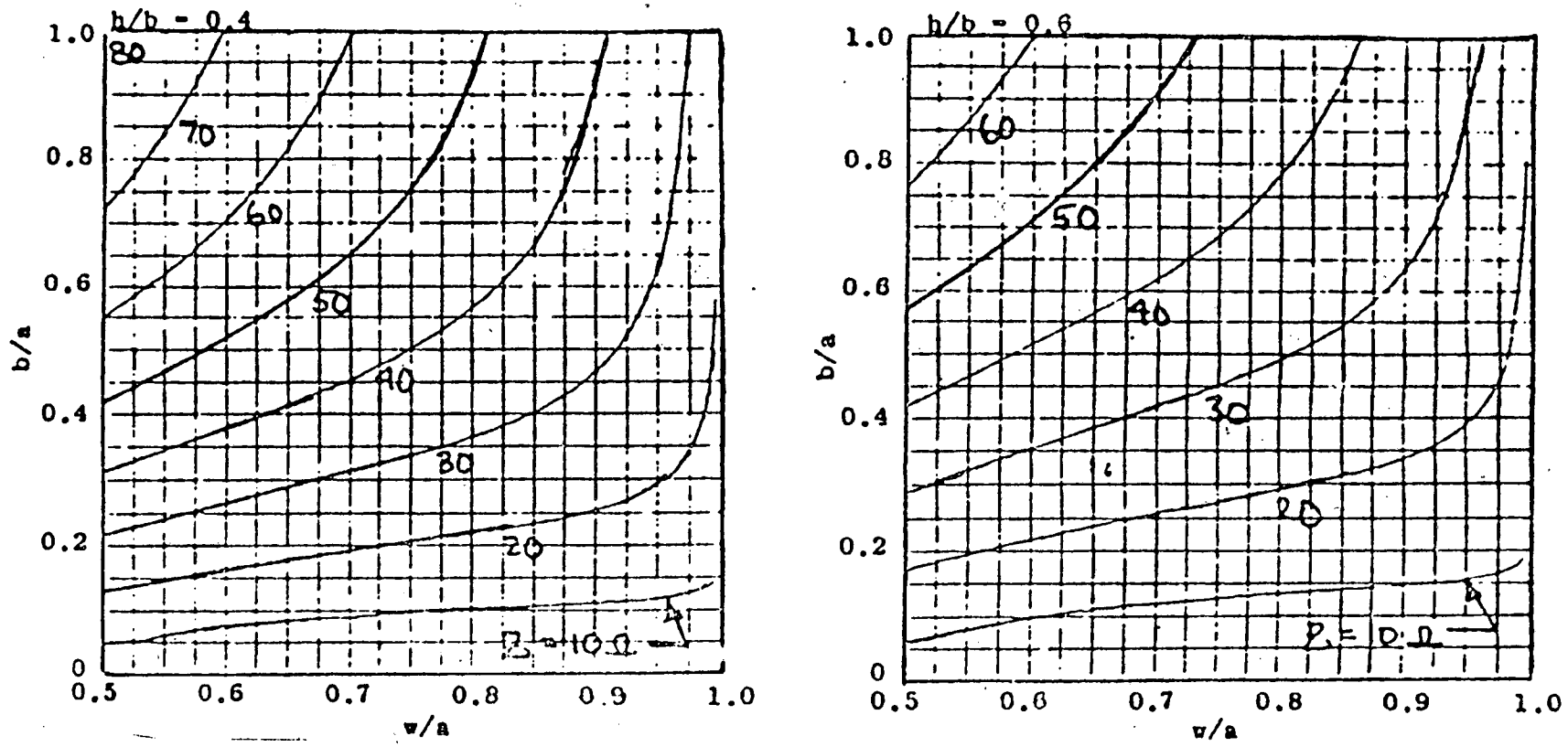

FIGURE 10b Transverse electromagnetic (TEM) cell design curves showing ratio of cell outer conductor dimensions to ratio of center plate width to cell for various transmission line characteristic impedances and vertical center plate locations.

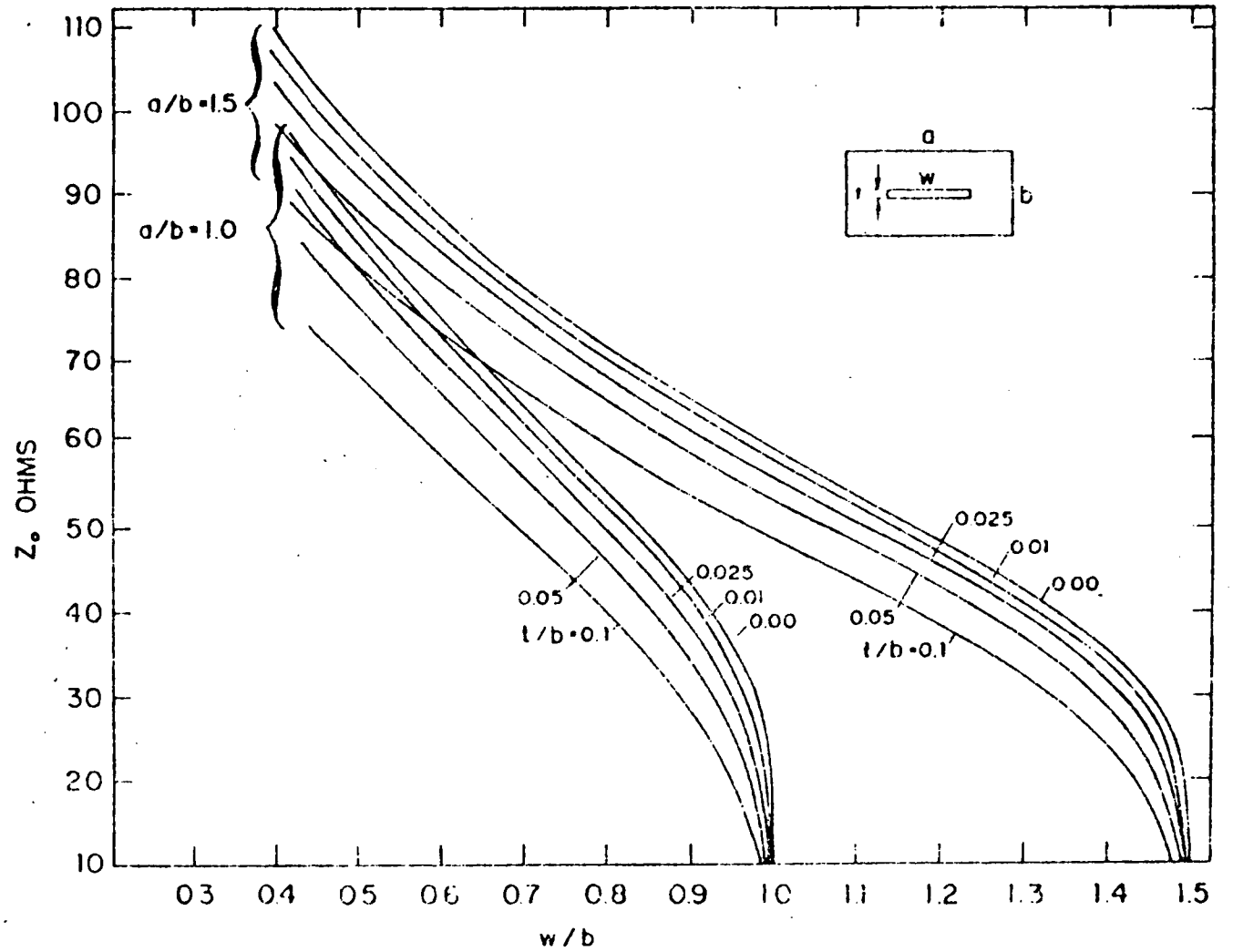

Figure 11 Characteristic impedance for rectangular strip lines with center conductor of finite thickness ($t/b \leq 0.1$) [19].

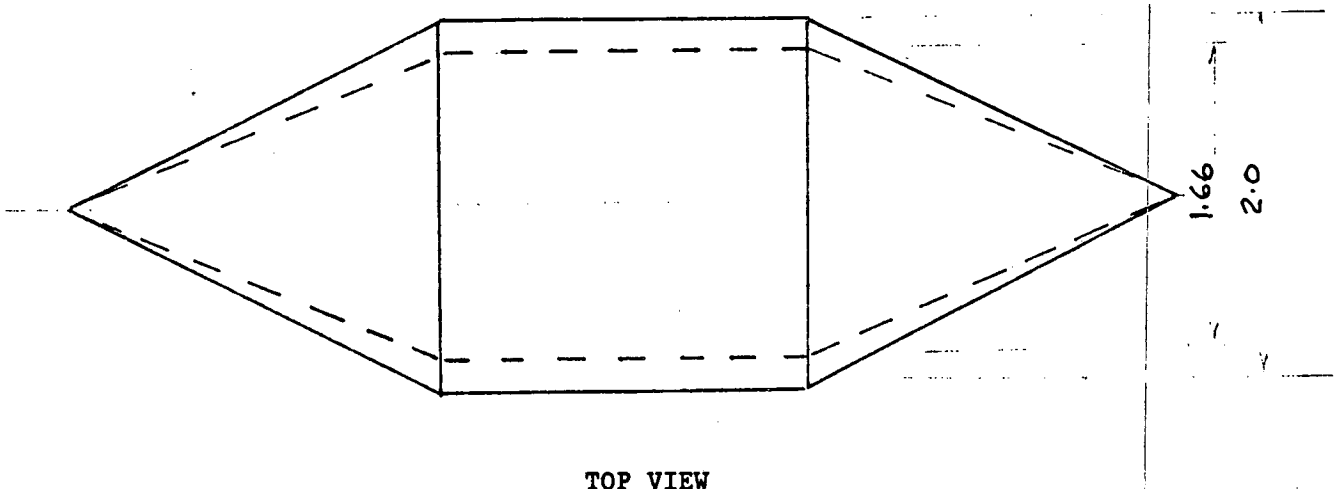

TOP VIEW

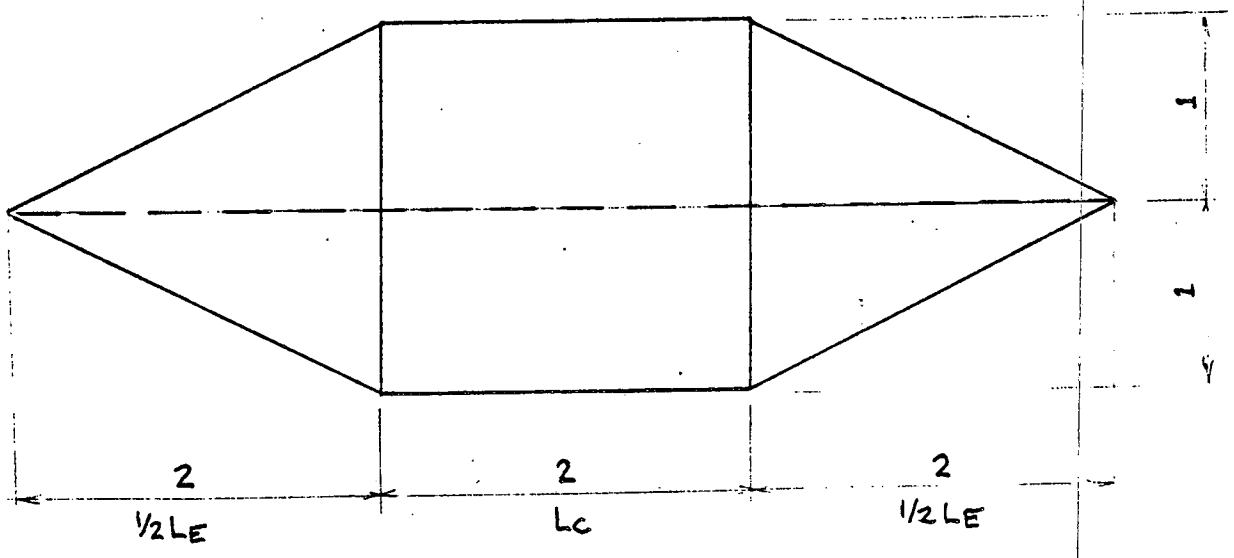

SIDE VIEW

FIGURE 12 Top view and side view of a TEM cell

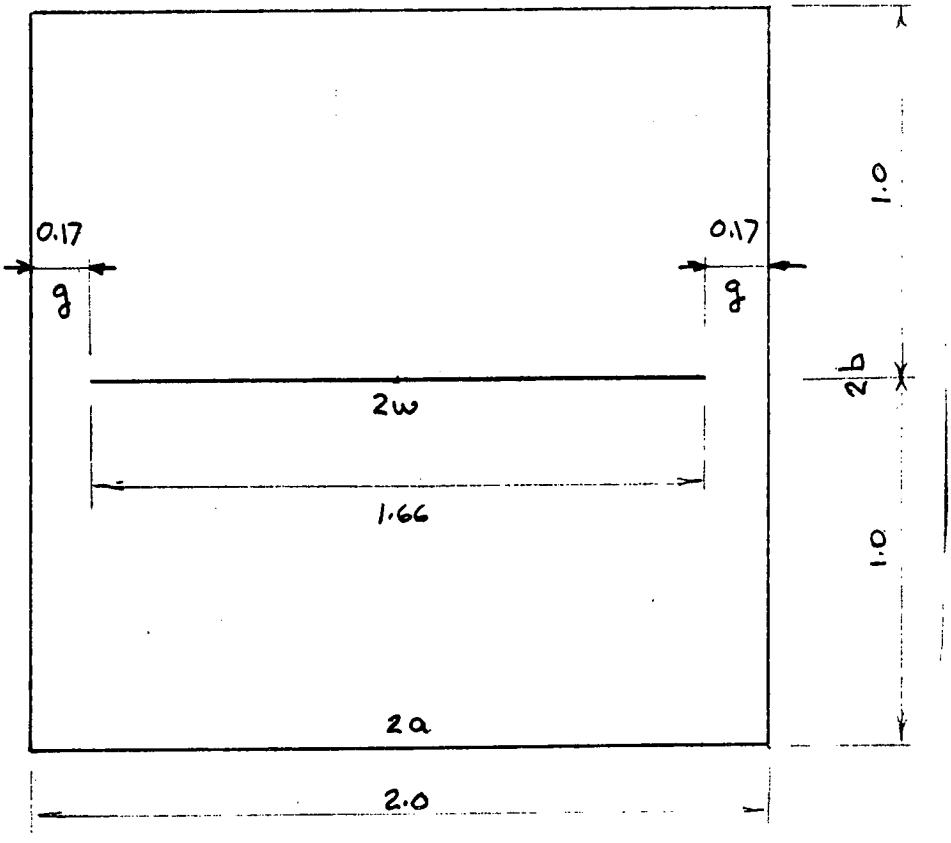

a = 1 m
b = 1 m
w = 0.83 m
g = 0.17 m
t = 1 mm
Z_0 = 50 Ω

a/b = 1
w/a = 0.83
t/b ≅ 0

FIGURE 13 Cross-section of a TEM cell

TABLE 1 Resonance Frequencies f_R (m=0-2, n=0-2 and p=1-3) for TEM Cell with dimensions from Figure 12 and 13.

HIGHER-ORDER MODE			RESONANCE
TYPE	$f_{c(mn)}$ (MHz)	$pc/2L_{mn}$ (MHz)	$f_{r(mnp)}$ (MHz)
TE_{011}	43.5	37.5	57.4
TE_{101}	75.0	37.5	83.9
TE_{012}	43.5	75.0	86.7
TE_{111}	95.25	37.5	102.4
TE_{102}	75.0	75.0	106.1
TE_{013}	43.5	112.5	120.6
TE_{112}	168.0	75.0	121.2
TE_{103}	75.0	112.5	135.2
TE_{113}	95.25	112.5	147.4
TE_{201}	150.0	37.5	154.6
TE_{021}	150.8	37.5	155.4
TE_{211}	154.5	37.5	159.0
TE_{202}	150.0	75.0	167.7
TE_{022}	150.8	75.0	168.4
TE_{121}	168.0	37.5	172.1
TE_{212}	154.5	75.0	171.7
TM_{111}	168.0	37.5	172.1
TM_{112}	168.0	75.0	184.0
TE_{122}	168.0	75.0	184.0
TE_{203}	150.0	112.5	187.5
TE_{023}	150.8	112.5	188.1
TE_{213}	154.5	112.5	191.1
TE_{123}	168.0	112.5	202.2
TM_{113}	168.0	112.5	202.2
TE_{221}	216.0	37.5	219.2
TE_{301}	225.0	37.5	228.1
TE_{222}	216.0	75.0	228.6
TE_{302}	225.0	75.0	237.2
TE_{223}	216.0	112.5	243.5
TE_{303}	225.0	2 Q 12.5	251.6

3.4.2 Pulse Applications

With a single pulse input other types of resonances exist. The dispersion distance (distance between the shortest and longest path in a taper) is:

$$d = \sqrt{(0.5\ L_E)^2 + a^2 + b^2} - 0.5\ L_E = 0.45\ m \qquad (5)$$

For both tapers the total dispersion distance is $2d = 0.9$ m. Assume $2d = \lambda/2$ for the first frequency where the TEM mode is not properly launched. With a wavelength $\lambda = 1.8$ m the corresponding frequency f_0 is $300/1.8 = 167$ MHz. Various resonances (notches) in the field transfer function may occur at about this frequency and above [8]. The closed character of the system will prevent radiation losses. Neglecting ohmic losses in the septum and the enclosure, only coupling to the source and load, or the EUT can damp any resonances.

3.4.3 The Effects of Resonances

What are the consequences of the resonant frequencies with CW and pulse excitation? Let us first look to low voltage, CW applications; such as transfer function measurements. The highest frequency at which the TEM mode exists without interacting higher-order modes is a little less than 84 MHz, depending on the Q-factor of the system (TEM cell with EUT). If a higher upper frequency is desired the width "a" can be made smaller. However, the same test height "b" is only possible at the cost of a higher characteristic impedance Z_0 (for low level measurements an impedance $Z_0 = 50\ \Omega$ is desired). Impedance adaptors at both sides of the cell may be a solution. Furthermore, the length of the tapers can be made shorter for a higher resonant frequency f_R. With an $L_E = 2$m instead of 4m, $L_{mm} = 3$m and $f_{R(101)} = 90.14$ MHz. That is not a big gain. With a width $a = 1$m instead of 2m the first interacting resonant frequency $f_{R(101)} = 158$ MHz!

In the case of EMP simulation (single shot excitation), the second cutoff frequency of the double exponential pulse (Figures 14-17) is about 60 MHz [9]. The calculated upper frequency limit of 167 MHz is probably enough for simulating the exo-atmospheric EMP from Figure 14. For a rise time shorter than $t_r = 5$ ns, the dimensions of the cell should be made smaller, consequently resulting in a smaller test volume and more corona problems. The corona problems can be reduced by choosing a higher impedance than 50 Ω (larger dimension g in Figure 5).

Changing the characteristic impedance Z_0 of the cell can be achieved by adjusting the width of the septum. For a 100 Ω cell the width should be 0.8 m instead of 1.66 m. The term $\Delta C/\epsilon_0$ in Equation (4) is neglected because the curve $a/w = 2.5$ in Figure 9 at $a/b = 1$ does not show any deviation from the exact calculation.

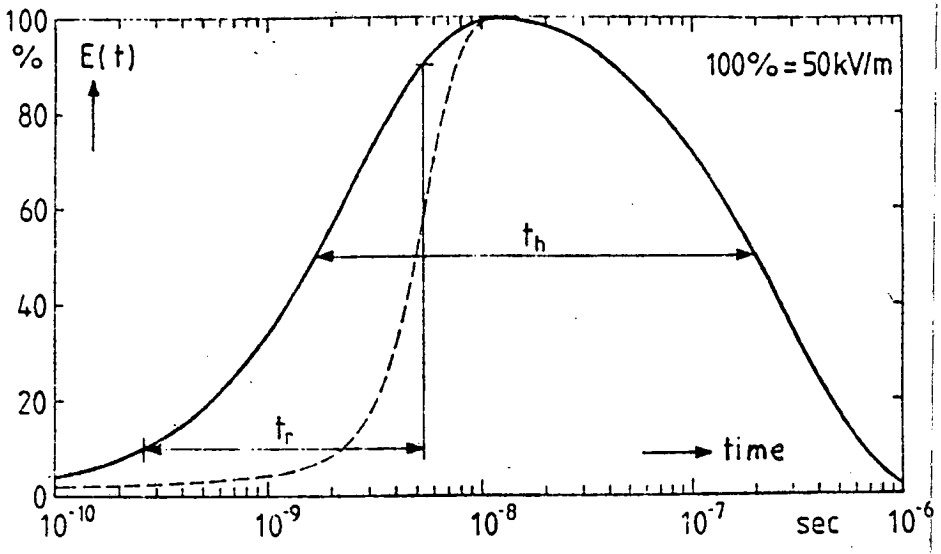

FIGURE 14 Model for exo-atmosphere EMP

$E(t) = E_0 (e^{-\alpha t} - e^{-\beta t})$
$E_0 = 5.28E4$
$\alpha = 3.74E6$ and $\beta = 3.91E8$

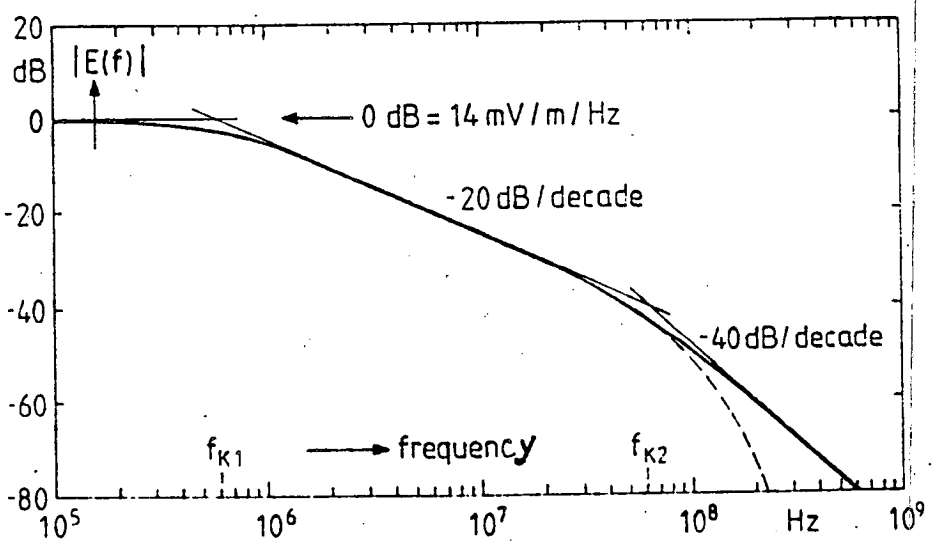

FIGURE 15 Spectrum of model in Figure 14

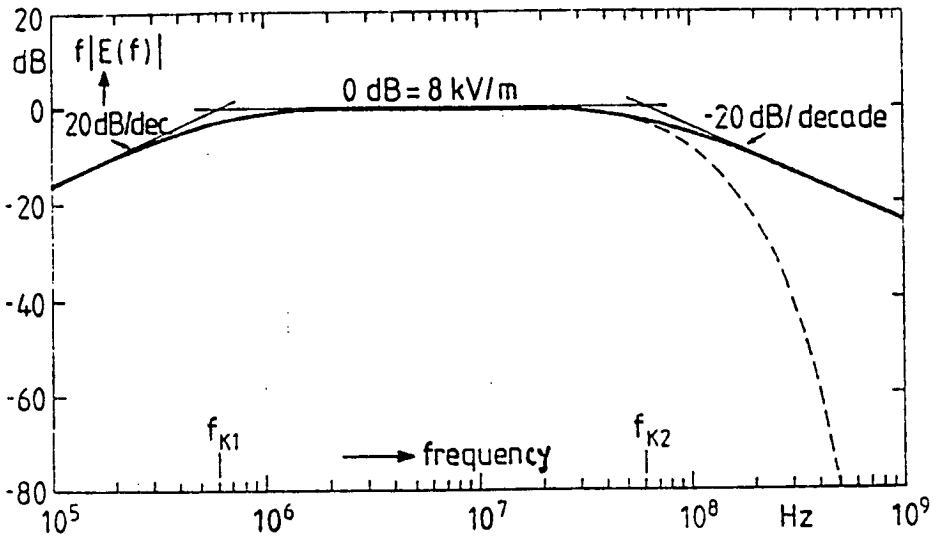

FIGURE 16 First derivative of spectrum Figure 15

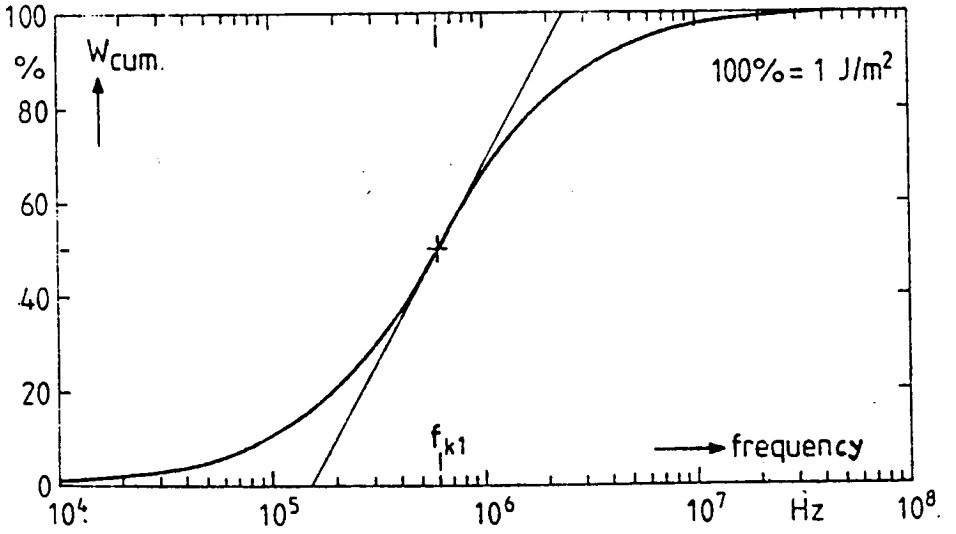

FIGURE 17 Cumulative energy density of model Figure 14

The width of the test volume is a little less than the test height. If more width is required, a characteristic impedance Z_0 of the cell can be chosen somewhere between 50 Ω and 100 Ω.

3.5 Field Intensity

The field intensity, E_o, in the center of the test volume is given by:

$$E_o = \frac{\sqrt{P_n R}}{b} \quad \frac{V}{m} \tag{6a}$$

where P_n is the net power transmitted through the cell, R is the real part of the cell characteristic impedance in ohms and b is half the height of the cell in meters. With a CW source at the input, P_n can be measured. In case of pulsed power input the field strength in the center between septum and bottom is about

$$E_o = \frac{V}{b} \tag{6b}$$

where V is the voltage between the septum and the enclosure. The electric field is polarized normal to the plane of the septum.

3.6 Field Distribution

The general field distribution in a TEM cell is given in Figure 1 and Figure 18. Tables 2 through 5 show the normalized electric field at various transverse positions in a 50 Ω square TEM cell, see Figure 19. The normalized field $\tilde{E}_{x,y}$ is obtained from:

$$\tilde{E}_{x,y} = \frac{E_{x,y}}{V/b} \tag{7}$$

where $E_{x,y}$ is the magnitude of either the vertical or horizontal component of the electric field at the location of interest [10]. V is the voltage between the septum and the enclosure, b is the separation distance between the septum and upper or lower walls. The field distribution from Table 2 through 5 is obtained by using the formulation derived by Tippet and Chang [5, 11].

Figure 20 gives an impression of the electric field strength gradients in an area within which an EUT can be placed. For example, in the shaded area centered between the septum and the lower wall, equal to 2a/3 x b/3, the cell has less than ± 1.4 dB E-field gradient [6].

If a metal box (simulating an EUT) is placed in the center of the test volume,

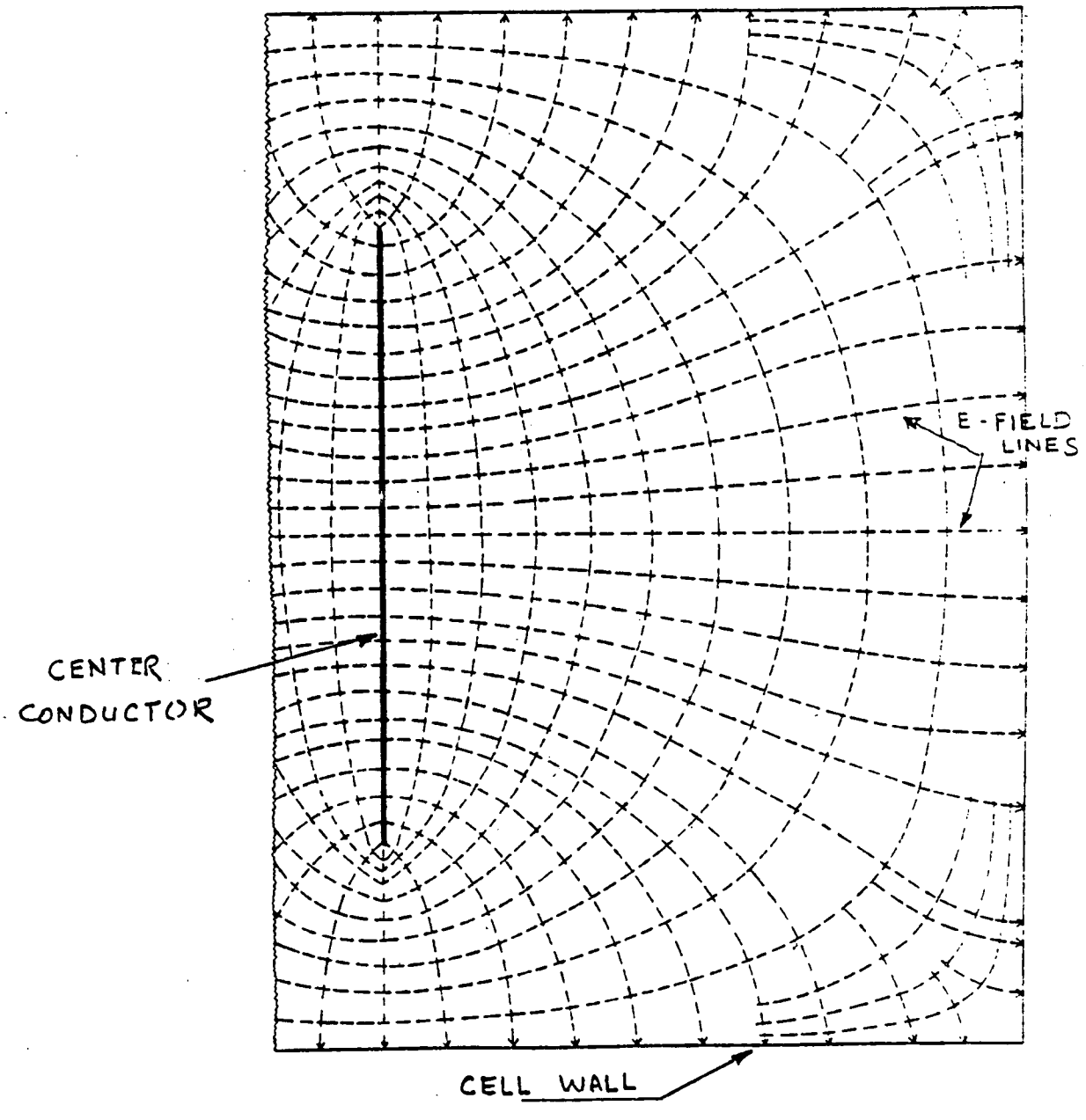

FIGURE 18 General field distribution in a TEM cell

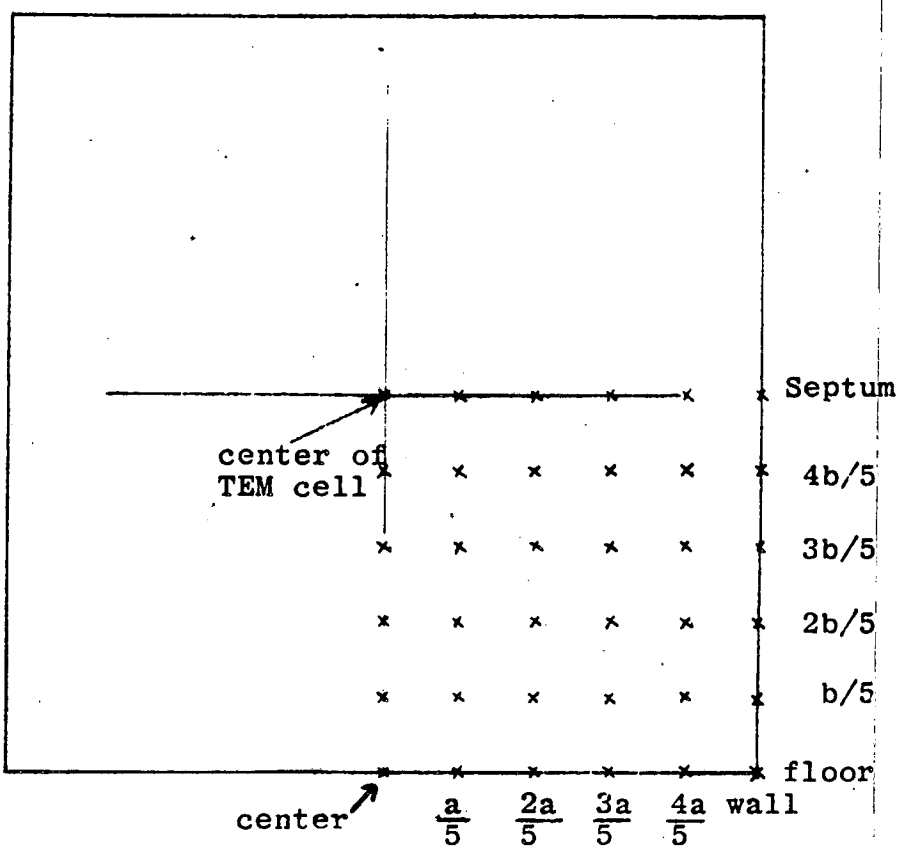

FIGURE 19 Field distribution locations shown in Tables 2-5

Table 2

x-component of the electric field in a square symmetric TEM cell. (Figure 13, a=b, w=0.83a)

Floor	0.000	0.000	0.000	0.000	0.000	0.000
b/5	0.000	0.060	0.129	0.208	0.278	0.307
2b/5	0.000	0.108	0.245	0.422	0.600	0.680
3b.5	0.000	0.127	0.311	0.620	1.029	1.237
4b/5	0.000	0.090	0.248	0.647	1.684	2.285
Septum	0.000	0.000	0.000	0.000	0.000	3.603
	center	a/5	2a/5	3a/5	4a/5	wall

center of TEM cell

Table 3

y-component of the electric field in a square symmetric TEM cell. (figure 13, a=b, w=0.83a)

Floor	0.824	0.793	0.698	0.530	0.289	0.000
b/5	0.853	0.825	0.736	0.568	0.315	0.000
2b/5	0.935	0.917	0.852	0.699	0.410	0.000
3b/5	1.049	1.052	1.051	0.977	0.652	0.000
4b/5	1.153	1.186	1.298	1.499	1.343	0.000
Septum	1.196	1.245	1.431	1.986	6.640	0.000
	center	a/5	2a/5	3a/5	4a/5	wall

center of TEM cell

Table 4

Magnitude of the electric field in a square symmetric TEM cell. (Figure 13, a=b, w=0.83a)

Floor	0.824	0.793	0.698	0.530	0.289	0.000
b/5	0.853	0.827	0.747	0.605	0.420	0.307
2b/5	0.935	0.924	0.886	0.817	0.727	0.680
3b/5	1.049	1.060	1.096	1.157	1.218	1.237
4b/5	1.153	1.189	1.321	1.633	2.154	2.285
Septum	1.196	1.245	1.431	1.986	6.640	3.603
	center	a/5	2a/5	3a/5	4a/5	wall

center of TEM cell

Table 5

Polarization angle of the electric field in degrees in a square, symmetric Tem cell

Floor	90.00	90.00	90.00	90.00	90.00	-----
b/5	90.00	85.86	80.05	69.89	48.54	00.00
2b/5	90.00	83.27	73.97	58.89	34.35	00.00
3b/5	90.00	83.14	73.50	57.60	32.36	00.00
4b/5	90.00	85.64	79.20	66.67	38.56	00.00
Septum	90.00	90.00	90.00	90.00	90.00	00.00
	center	a/5	2a/5	3a/5	4a/5	wall

center of TEM cell

TABLE 2 TO 5 THE ELECTRIC FIELD IN A SQUARE SYMMETRIC TEM CELL

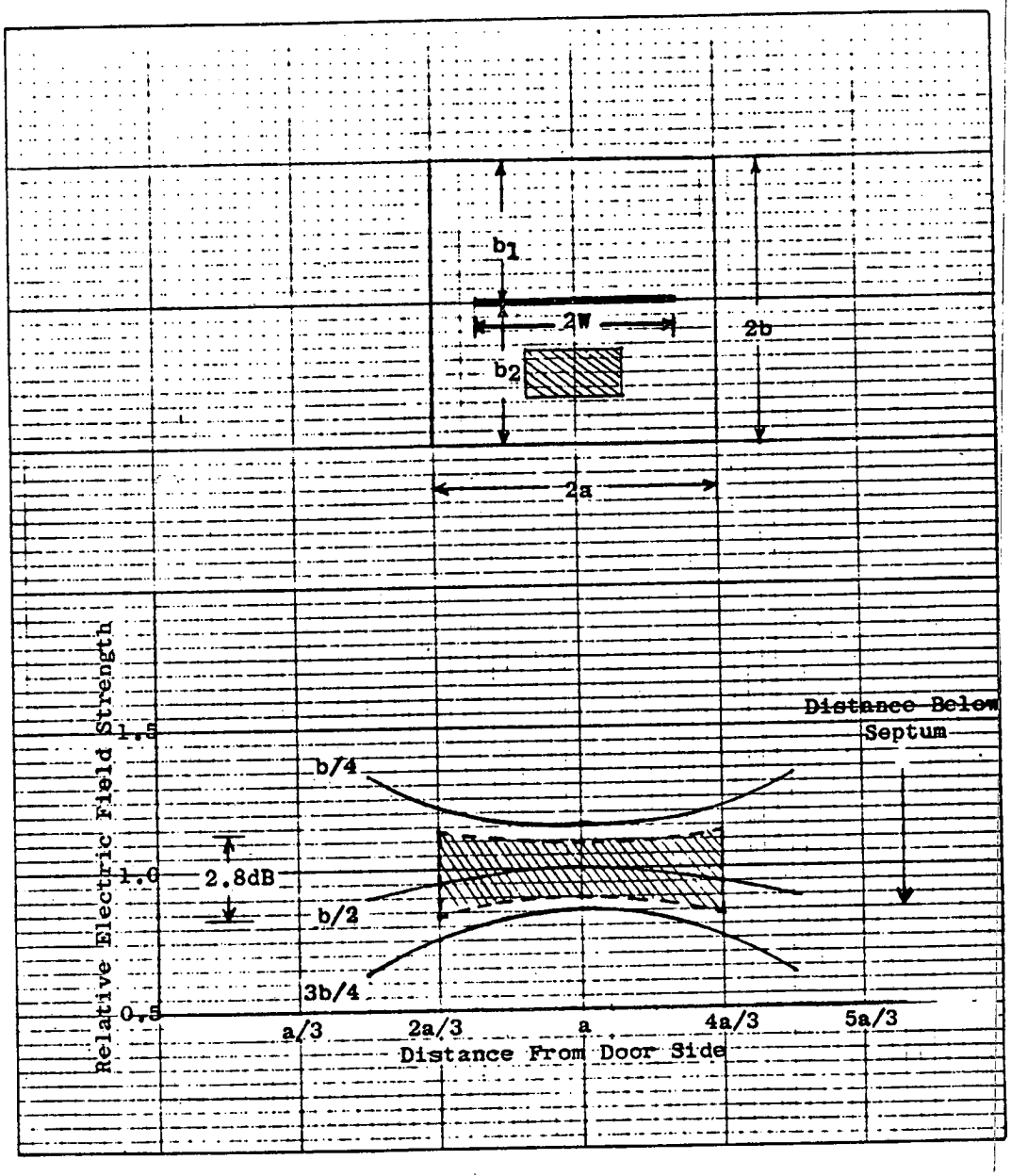

Figure 20 Relative electric field distribution inside symmetric cell. Shaded area corresponds to 1/3 cross-section area shown in top view. Note that this figure corresponds to a 50 Ω cell.

the field distribution is changed. The metal case disturbs the field and has a capacitive loading effect at that location in the cell. Figure 21 shows the relative field distribution with a metal case occupying one third of the volume between septum and outer wall [6]. The field strength has increased by about 3 dB and 5 dB respectively in the regions directly above and below the case and about 1.6 dB and 3.7 dB respectively in front of the case (points 3 and 5). The increase in field strength should be taken into account when determining the absolute test field.

For low frequencies, where the transverse dimensions of the EUT are negligible compared to the wavelength, the discontinuity due to the presence of the EUT is a pure capacitive reactance, and may be regarded as the fringing capacitance of the corresponding electrostatic situation. Under this assumption the ratio of the electric field with and without EUT at the same location has been calculated by Meyer [3]. Figure 22 shows an example of the amount of distortion versus the ratio h/b.

Kanda [3] performed a theoretical as well as an experimental analysis of the loading effect in a TEM cell. He found that the magnetic field distortion due to a perfectly conducting rectangular cylinder is quite small, and much less than the electric field distortion reported by Meyer. However, the electric field distortion is much larger than that predicted by Meyer (a quasi-electrostatic approximation) in case of experiments at 2 and 10 MHz, see Figures 23 and 24.

It can be concluded that to preserve the integrity of the field, the EUT should occupy less than one-third of the septum-to-wall distance. A ratio h/b = ⅓ corresponds to a field enhancement above the EUT of 1/0.66 = 1.5 or about 3.5 dB. Also probes and sensors may cause field enhancements, due to shorting out a part of the field between the septum and the wall. For more accuracy, e.g. with field strength measurements, the probes and sensors should have small dimensions, less than one-third of the septum-to-wall distance.

3.7 Test Volume

The best location of the EUT is in the region where the TEM field is the most uniform. However, if required or desired, the EUT can be placed at almost any location in the cell. Both top and bottom halves of the cell can be used, but generally the lower half is used. This allows the EUT to be supported on the bottom of the cell. The upper half can be used for monitoring purposes with a field sensor mounted in the top of the cell. Hopefully the field in the upper half will not be disturbed by the presence of the EUT in the lower half.

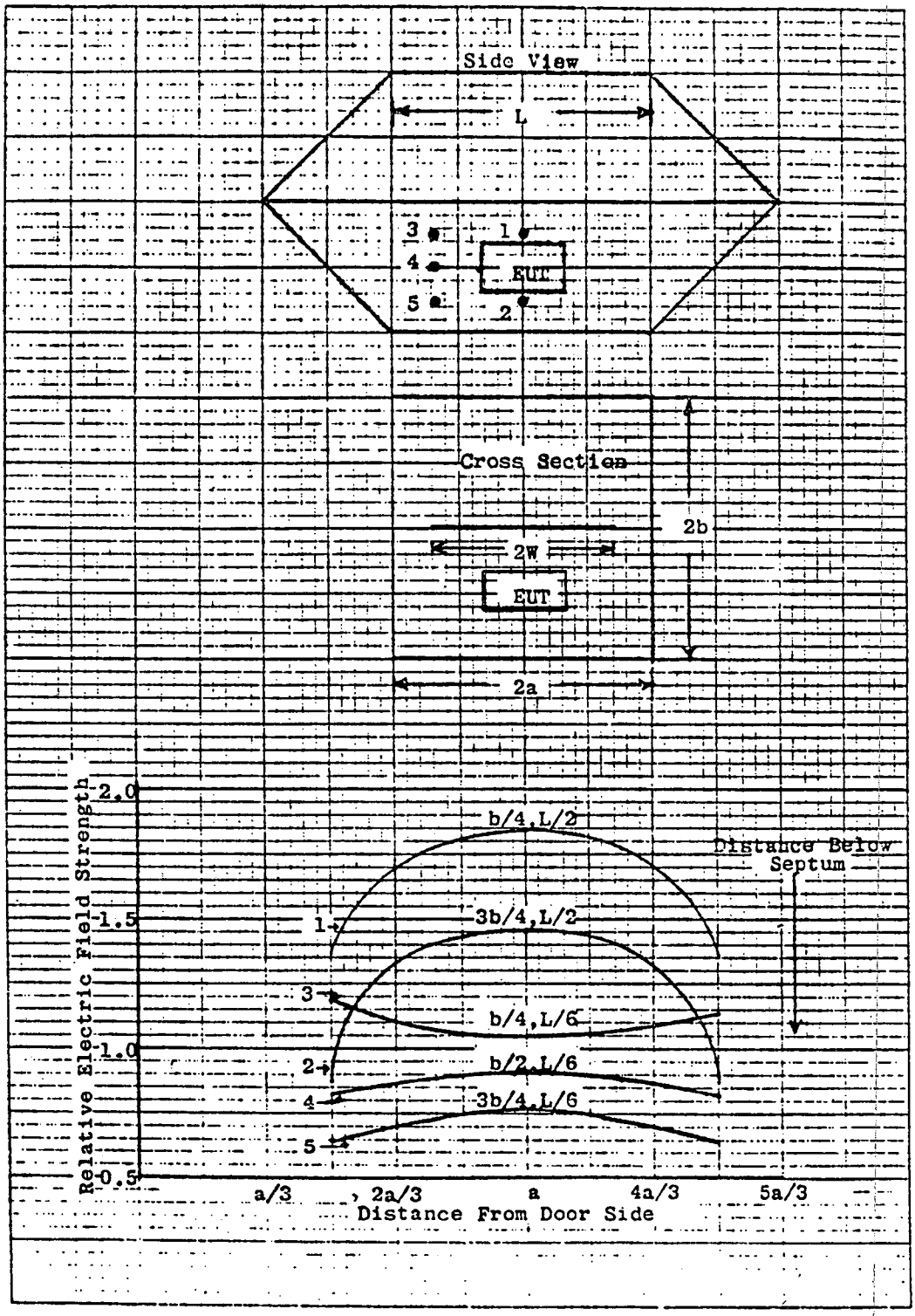

FIGURE 21 Relative electric field distribution inside cell with EUT (metal case) occupying 1/3 vertical separation distance between septum and floor. Cross sectional cuts at center (L/2) and off end (L/6) of EUT as indicated by numbers in top view.

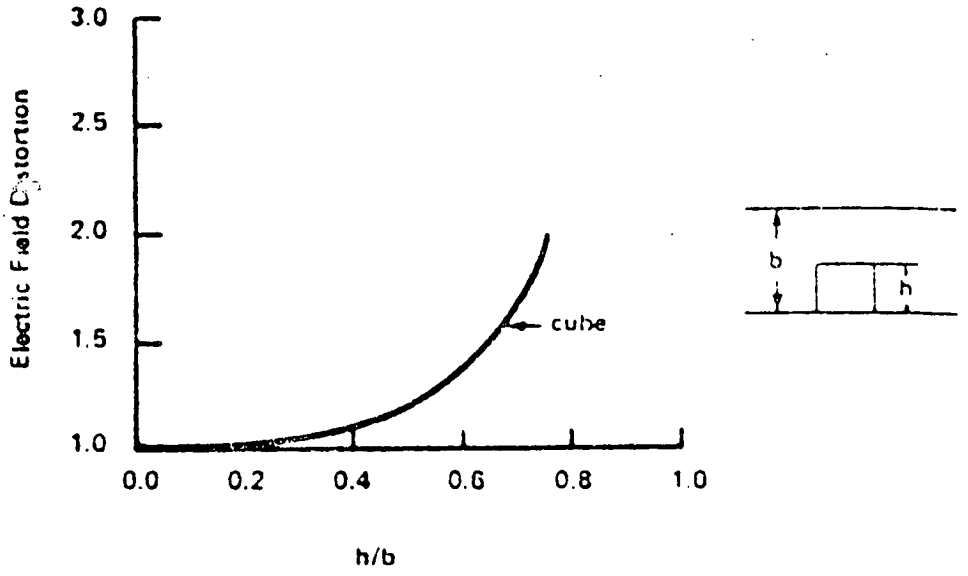

FIGURE 22 Electromagnetic-field distortion due to metallic cube in a transverse electromagnetic cell (electrostatic approximation)

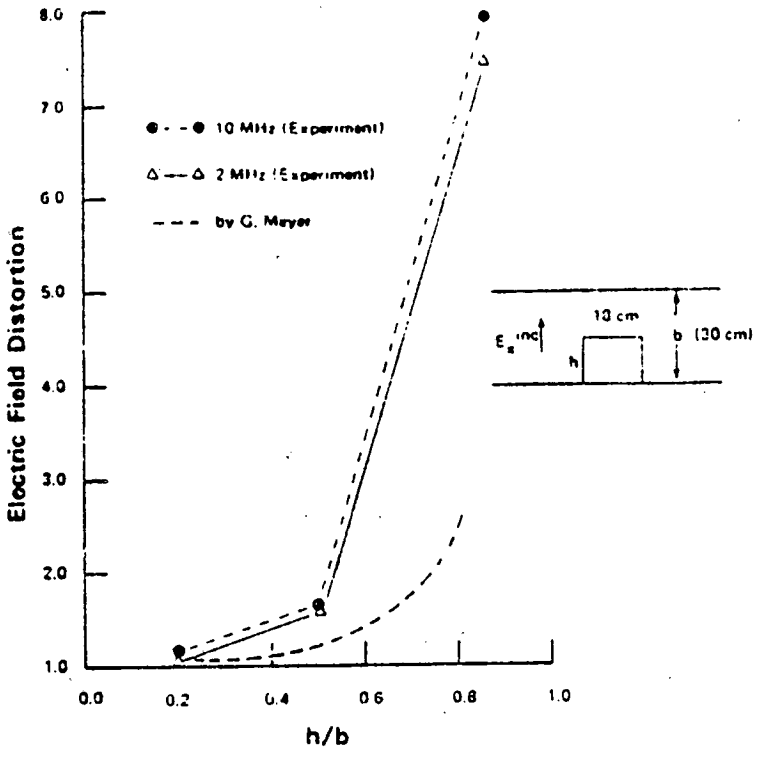

FIGURE 23 Magnetic-field distortion at the center of a top of the cylinder versus the ratio of its height to the separation distance of the parallel-plate waveguide at 2 MHz.

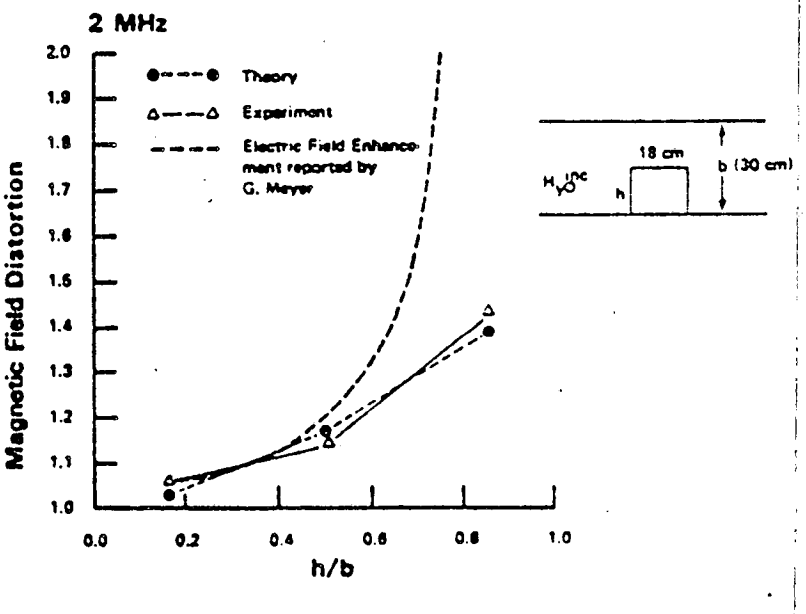

FIGURE 24 Electric-field distortion at the center of the top of the cylinder versus the ratio of its height to the separation distance of the parallel-plate waveguide.

For frequencies with a wavelength equal or smaller than the taper length some reflection from the interface between the input taper and the uniform cross section can be expected [9]. In that case the best position of the EUT is as shown in Figure 25a. Again, for best results, the size of the EUT should not exceed one-third of the dimensions a, b, and l. This prevents excessive capacitive loading which shorts out part of the electric field and distorts the test field pattern.

The best location for EUT's without external connections is shown in Figure 25b. They can be placed upon a non-metallic stand. If external connections to the outside world have to be made, vertical parts in the cabling should be avoided as much as possible. Horizontally positioned, shielded cables are preferred, e.g. to connect the EUT to a power source.

It is better to place EUT's with electrical connections to the outside environment (asymmetric $\dot{D}$-sensors, $\dot{B}$-sensors, etc.) on the bottom plate to avoid pick-up along the vertical parts of the connecting cables, see Figure 25c. Coaxial connectors mounted in the bottom plate are excellent RFI-free connections. Outside measuring equipment connected via coaxial cables to the TEM cell don't have to be shielded against the internal generated EMP field. Asymmetric sensors placed upon the bottom plate, with their connectors passing through a hole in the bottom plate and connected to a coaxial cable, have no vertical cable parts exposed to the field in the cell and have therefore no pick-up.

3.8 Field Enhancement

For EMP simulating purposes a high voltage pulse generator is connected to the input taper of the TEM cell. This may cause corona or even flash-over problems at locations with small gap distances, particularly near the apex of the tapers. At a distance of 20 cm from the apex the gap distance between the septum and the side walls is only $g/10 = 1.7$ cm and the width of the septum at that place is already $2w/10 = 16.6$ cm. That is rather large to connect to the spark gap. At 30 cm distance the gap distance is 2.55 cm, see (Figure 26).

With a DC voltage of 60 kV the DC field strength in the gap without field enhancement is:

$$\frac{V}{d} = \frac{60\ \text{kV}}{1.7\ \text{cm}} = 35.3\ \text{kV/cm} \qquad (8)$$

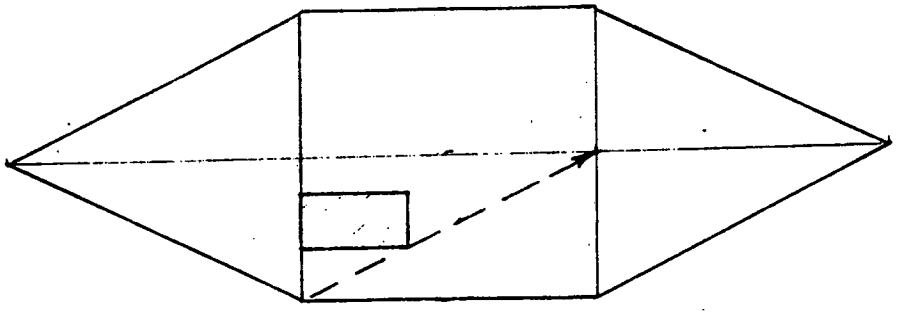

FIGURE 25a EUT outside reflection area

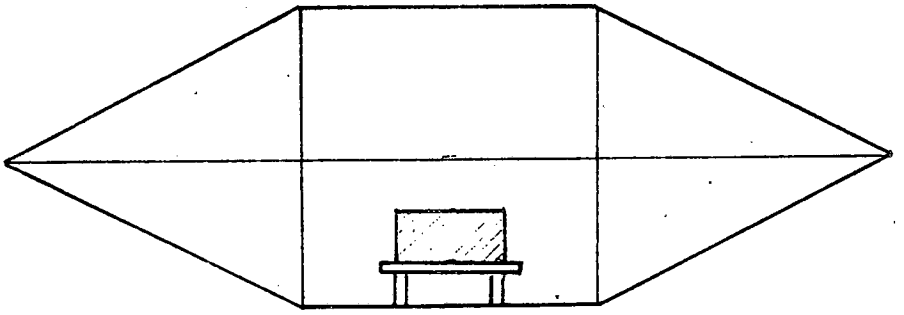

FIGURE 25b EUT without external cabling

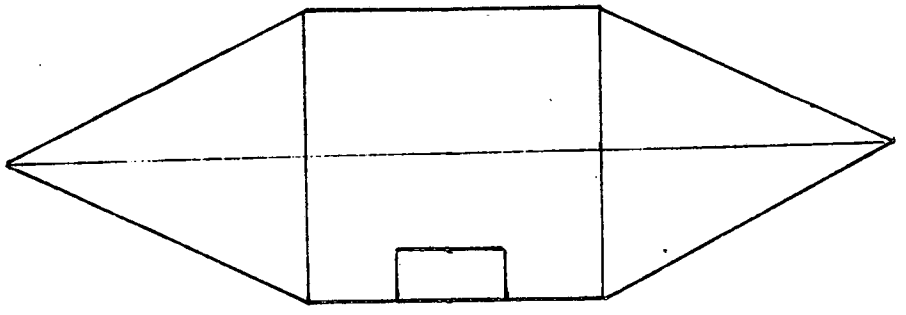

FIGURE 25c EUT with electrical connections

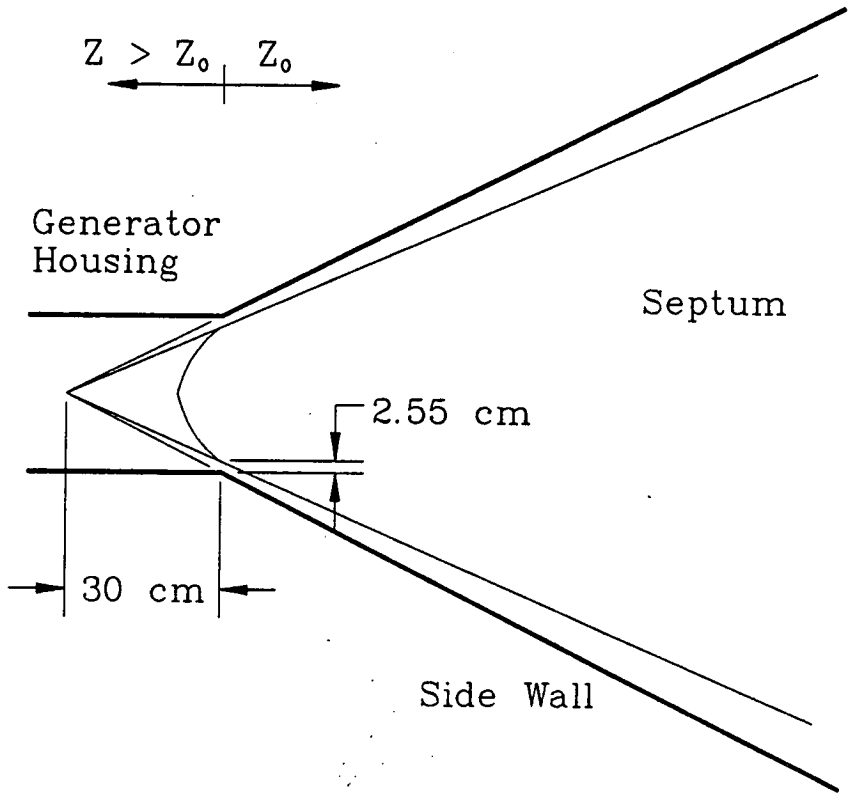

FIGURE 26 Small gap near the apex of the taper (Z_0 = 50 Ω)

The field enhancement between a sphere and a large flat plate can roughly be approximated by:

$$E = 0.9 \frac{V}{d} \frac{r+d}{r} \qquad (9)$$

with r and d in cm's [12], see Figure 27. Assume 2r = 1 mm, d = 1.7 cm and V = 60 kV, then E = 1100 kV/cm. The field enhancement factor f is about 31! Replacing the sphere by a cylinder gives:

$$E = 0.9 \frac{V}{r \ln \frac{r+d}{r}} \qquad (10)$$

with r and d in cm's [12], see Figure 28. The field in the gap is 304 kV/cm and the field enhancement factor f = 8.6.

Miles Burton (DREO) made more accurate calculations of the field enhancement by replacing the cylinder with a rounded-edge plate, see Figure 29 and 30a. The maximum field strength at the surface of the edge of the septum is about 175 kV/cm and the field enhancement factor f = 4.96. See Figures 30a through 30c.

The voltage across the gap during EMP simulation is not a DC voltage, but has a limited time duration. Before flash-over will occur a streamer has to be formed to form a conductive path for the spark. With a half-width time t_h = 200 ns and an avalanche velocity v = 10^5 m/s a distance of at least 2 cm is required. The voltage across the gap after 200 ns is about 30 kV and the field strength 30/60 x 175 = 87.5 kV/cm. That is still a factor 3 larger than the breakdown strength of air. Some provision is needed to lower the field strength in the gap or to increase the distance needed to close the streamer path.

One possibility is enclosing the edge of the septum in plexiglass or other insulating material that at the same time can be used to support the septum, see Figure 31.

Another problem is damage caused by corona (partial discharge). For pulse systems which must have a life expectance of many shots, corona damage should be a dominant consideration.

If two different types of insulating material are used, see Figure 32, or one insulating material and air, the dielectric stress in each layer can be

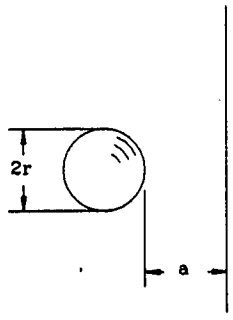

FIGURE 27 Field enhancement between a sphere and a flat plate

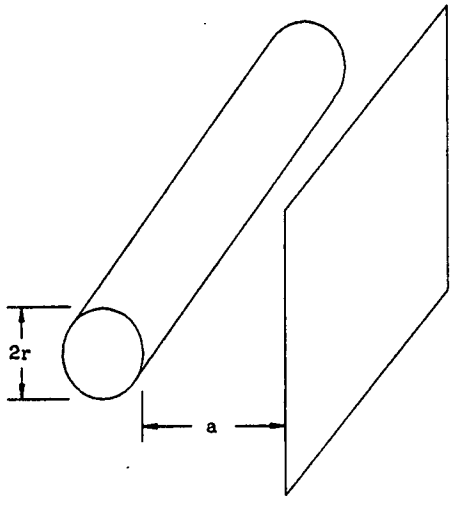

FIGURE 28 Field enhancement between a cylinder and a flat plate

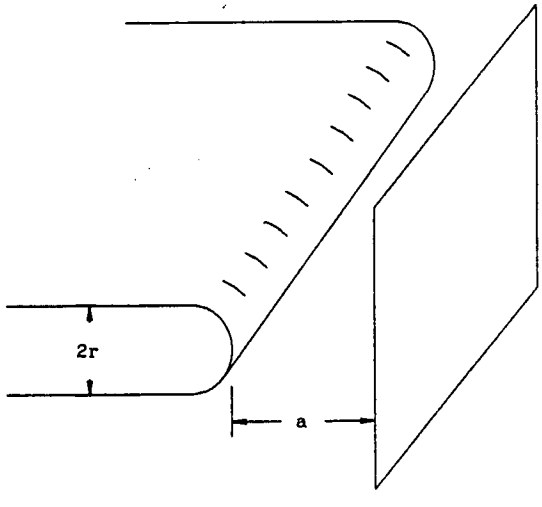

FIGURE 29 Field enhancement between a plate with rounded edges and a flat plate

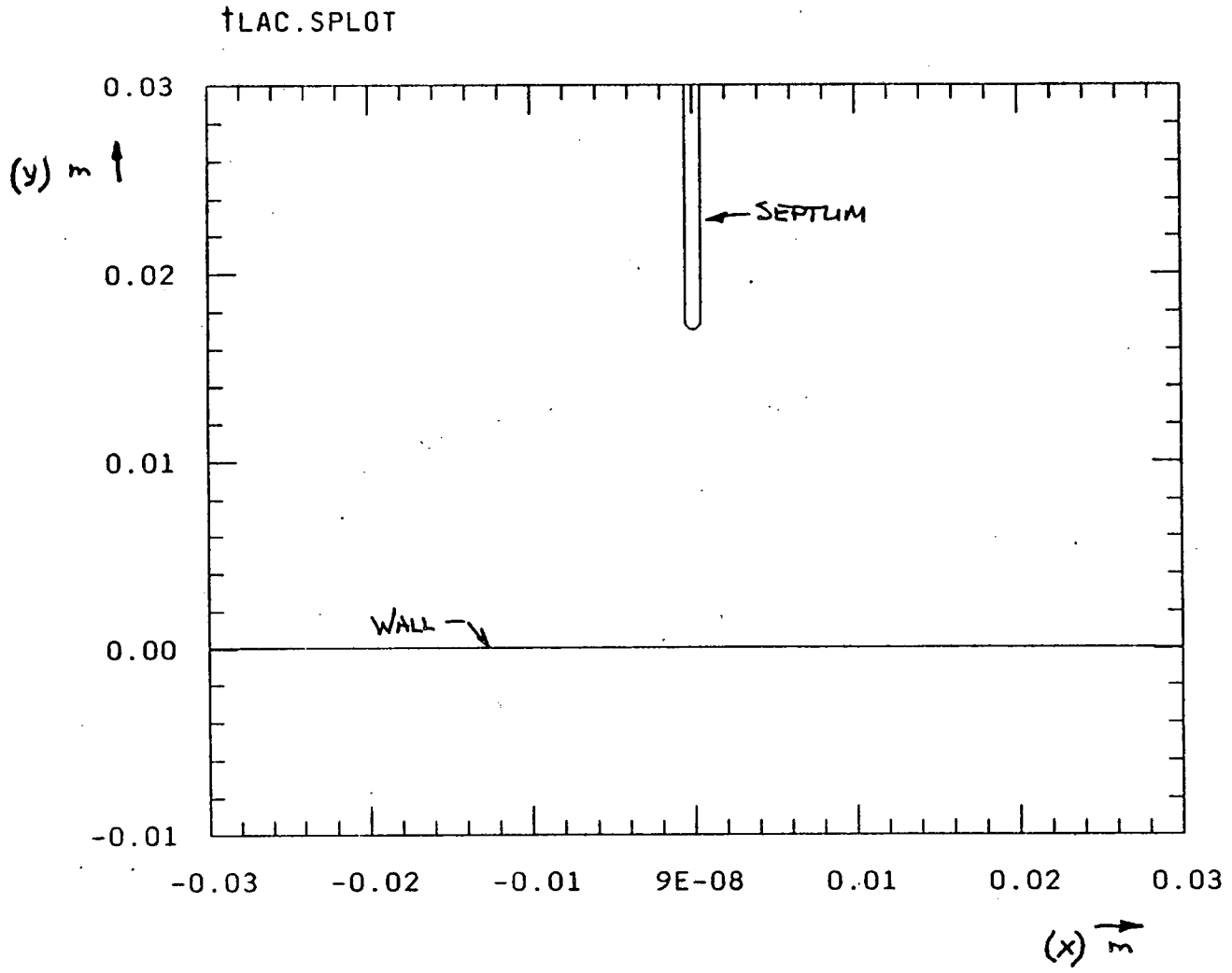

FIGURE 30a Geometry of the wall and septum, gap = 17 mm

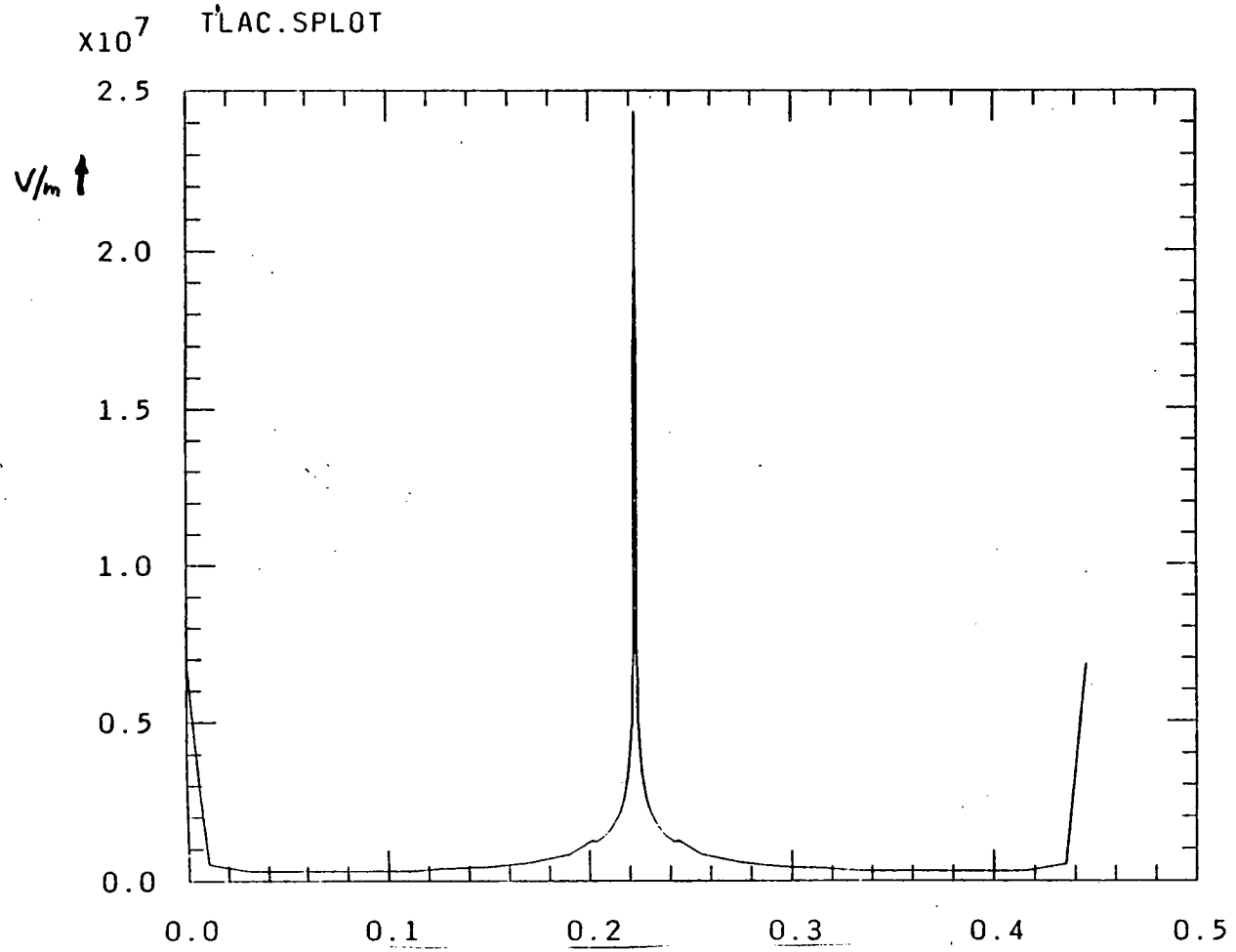

FIGURE 30b Electric field on Spetum, t = 0.5 mm, gap = 17 mm

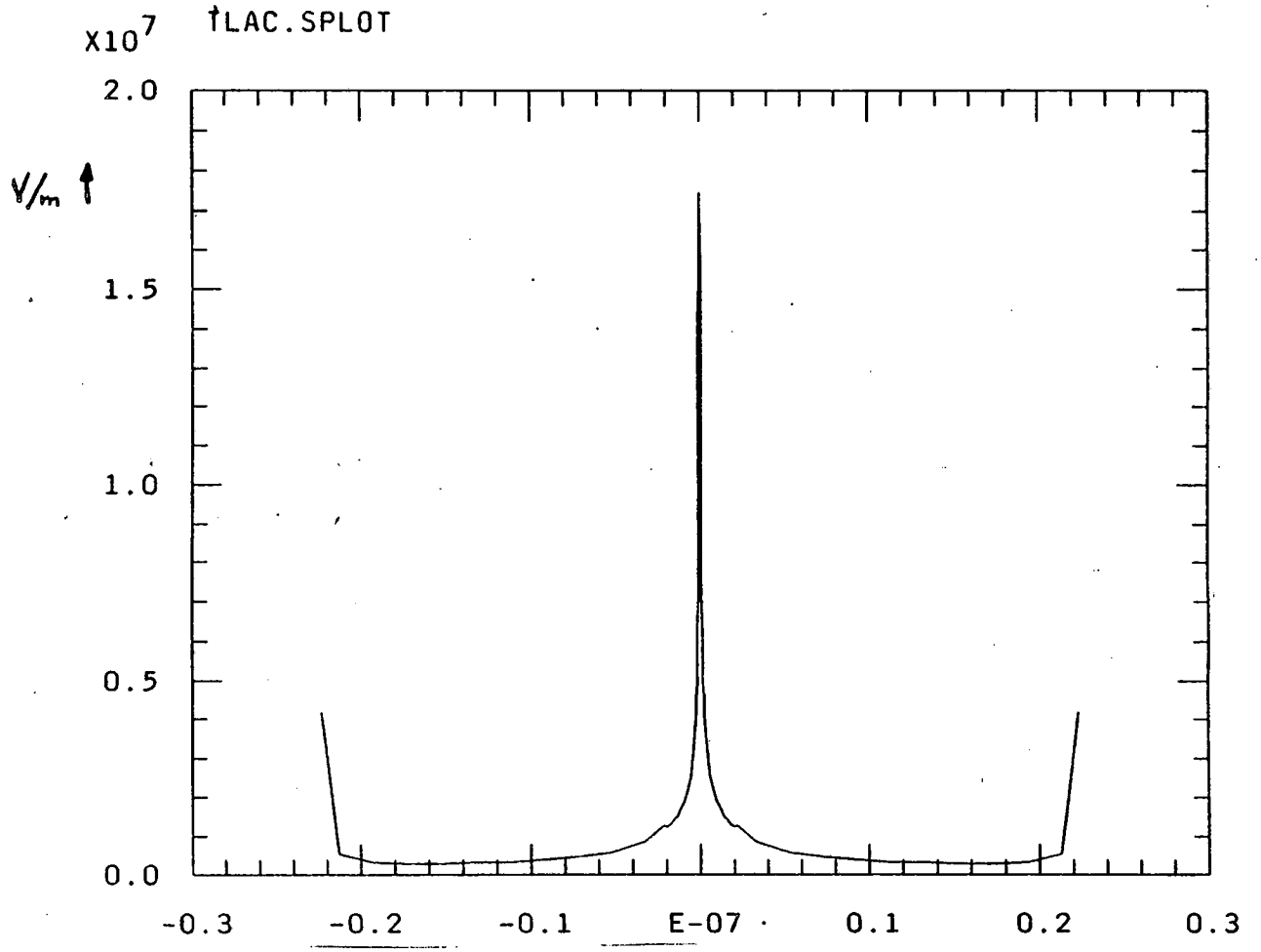

FIGURE 30c Electric field on septum, t = 1 mm, gap = 17 mm

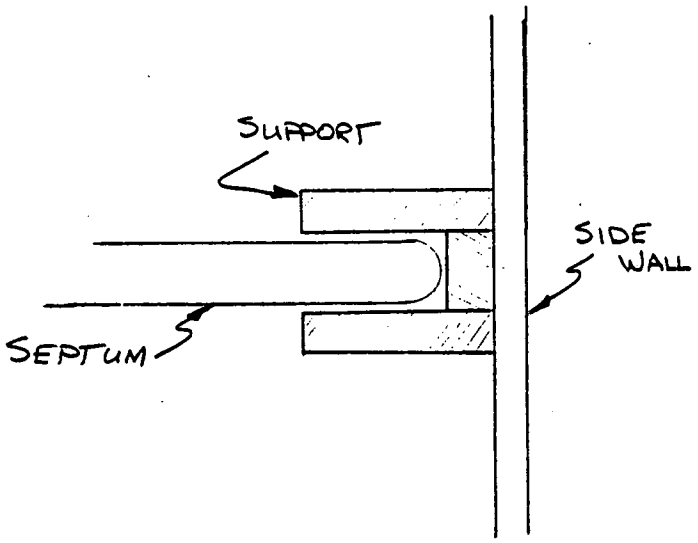

FIGURE 31 Insulation and support of septum

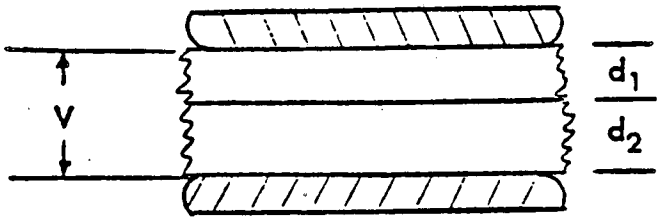

FIGURE 32 Voltage stresses in a two-dielectric insulation

calculated from:

$$E_1 = \frac{V}{d_1 + d_2 (\epsilon_1/\epsilon_2)} \quad kV/cm \tag{11}$$

$$E_2 = \frac{V}{d_1 (\epsilon_2/\epsilon_1) + d_2} \quad kV/cm \tag{12}$$

where V is the total voltage across the gap in kV, E_1 and E_2 are the voltage stresses in materials 1 and 2, ϵ_1 and ϵ_2 are the dielectric constants of materials 1 and 2, d_1 and d_2 are the thickness of materials 1 and 2 [12]. The dielectric constant and DC electric strength of thin sheets or films of commonly available solid, liquid and gaseous insulating materials are given in Table 6. It should be apparent that the dielectric strength of an insulator determines the maximum electric field strength that the insulator can sustain rather than the total voltage applied across the material. That is, the dielectric strength is field-strength dependent rather than voltage-dependent [13].

In reference [12] a listing of some representative materials is given with the relative dielectric constant K and breakdown voltage or "Dielectric strength", V_b, under an impressed DC voltage, see Table 7. The dielectric strength is expressed in volts per mil of dielectric thickness, at a voltage stress level where breakdown is virtually certain within one minute of application of voltage. Note that the dielectric strength for thicker pieces of material is considerably less as a result of bulk impurities, voids, and mechanical flaws.

If, for instance, lucite is used to insulate and support the septum, a dielectric strength can be expected of 500 V/mil = 200 kV/cm. Note that the field strength in the air-seams between the septum and the supporting insulator in Figure 31 is increased. This situation can be deduced from the fact that:

$$(\epsilon_r E)_{gas} = (\epsilon_r E)_{ins} \tag{13}$$

Since the dielectric constant of lucite is a factor 3.3 larger than that of air, the field strength in the air will be the same factor larger! Corona should be avoided in the air of the gaps in the seams to prevent damage or degradation of the insulation, generation of prepulse noise and degrading of the rise time. The best solution is to fill up the gap with insulating compound or oil at locations with a high field strength.

MATERIAL	DIELECTRIC CONSTANT	DIELECTRIC STRENGTH (V/mil)	COMMENTS
Polystyrene (Crosslinked)	2.58 2.55	1,020 500-700	Low heat, solvent resistance
Polyethylene	2.26	1,200	Subject to cold flow
Polyethylmethacrylate (Elvacite)	2.55	4,000	
Polymethylmethacrylate (Acrylic)	2.76	990	Crazes easily
Polypropylene	2.55	650	
Polytetrafluoroethylene (Teflon)	2.1	1,000-2,000	Degraded by voids
Polymonochlorotrifluor-ethylene (Kel-F)	2.3-2.8	3,000-5,000	Degraded by voids
Polyester (Mylar)	3.2	4,000	Sheets only
Mica	5.4	3,800-5,600	Sheets only
Petroleum oil	2.4	350	Liquid
Silicone oil	2.8	450	Liquid
Sulfurhexafluoride	1.0	150-180	Gas, 1 atmosphere
Freon 12	1.0	150-180	Gas, 1 atmosphere
Air	1.0	75	1 atmosphere

TABLE 6 PROPERTIES OF SOME INSULATING MATERIALS

	K	V_b (V/mil)
Air	1.000585	75 (30 kV/cm)
Aluminum oxide	7.0	300
Bakelite (general purpose)	6.0	300
Castor oil	3.7	350
Ceramics	5.5-7.5	200-350
Ethylene glycol	39	500
High-voltage ceramic (barium titanate composite and filler)	500-6000	50
Kapton (Polyamide)	3.6	7000
Kraft paper (impregnated)	6	2000
Lucite	3.3	500(200 kV/cm)
Mylar	2.5	5000
Paraffin	2.25	250
Polycarbonate	2.7	7000
Polyethylene	2.2	4500
Polypropylene	2.5	9600
Polystyrene	2.5	500
Polysulfone	3.1	8000
Pyrex glass	4-6	500
Quartz, Fused	3.85	500
Reconstituted mica	7-8	1600
Silicone oil	2.8	350
Sulfur hexafluoride	1.0	200 (per atm)
Sulfur	4.0	---
Tantalum oxide	11.0	100
Teflon	2.0	1500
Titanium dioxide ceramics	15-500	---
Transformer oil	2.2	250-1000
Water	80	500 (pulse charged in 7 to 10 μs)

TABLE 7 DIELECTRIC CONSTANTS AND BREAKDOWN STRENGTHS OF INSULATORS

3.9 Rise Time

The rise time of the TEM cell can be calculated from the difference in path length the current is travelling in the tapers [9], see Figure 4 and 33. The length x, from the apex to one of the corners at the interface between the taper and the uniform cross-section is:

$$x = \sqrt{L_E^2 + a^2 + b^2} \tag{14}$$

With $L_E = 2a = 2b = 2$ m the length of $x = 2.45$ m. The difference in path length between the shortest and longest path is:

$$\Delta\ell = x - L_E = 0.45 \text{ m} \tag{15}$$

The rise time is then:

$$t_r = \Delta\ell/c = 1.5 \text{ ns} \tag{16}$$

The rise time at the edges of the recommended test volume, see Figure 34, is smaller:

$$x = \left[L_E^2 + \left(\frac{2b}{3}\right)^2 + \left(\frac{w}{6}\right)^2\right]^{1/2} = 2.123 \text{ m} \tag{17}$$

$$\Delta\ell = 2.123 - 2 = 0.123 \text{ m}$$

$$t_r = \frac{\Delta\ell}{c} = 0.38 \text{ ns} \tag{18}$$

The calculated rise time t_r will be degraded a little by geometry mismatches, e.g. at the interfaces.

4.0 GENERATOR

The generator consists of a high voltage power supply (HVPS), a capacitor and a spark gap. The capacitor can be charged by a commercial available HVPS, see Appendix A. The capacitor is discharged via the spark gap and the transmission line into the load resistor. The capacitor and spark gap can be housed in a coaxial structure that can be connected to the TEM cell and matched to the characteristic impedance of the line. In this way the generator can easily be disconnected from the TEM cell and replaced by an adaptor for 50 Ω coaxial connection.

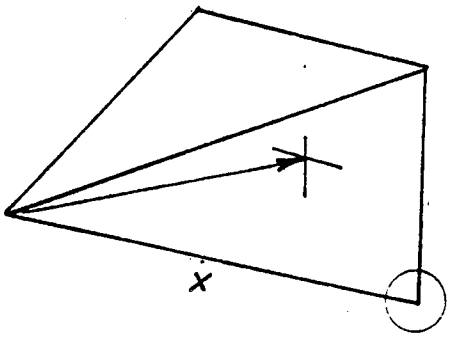

FIGURE 33 The longest path-length x in the taper

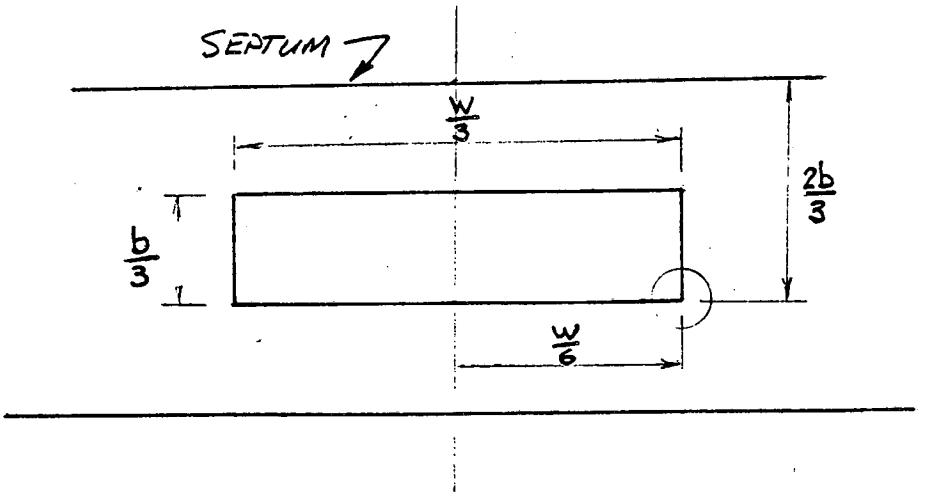

FIGURE 34 The far edge of the test volume

4.1 Capacitor

The required half-width time of the field t_w = 200 ns. The time constant of the discharge circuit should be

$$\tau = RC = t_w/0.7 = 286 \text{ ns} \quad (19)$$

or with $R = Z_o = 50\ \Omega$

$$C = \tau/R = 5.7 \text{ nF}.$$

The HVPS has a maximum voltage of 60 kV. A low inductance, high voltage capacitor is needed. Many factors must be considered in order to make a proper choice. In our case, properties should include: peak voltage, peak current, wave shape, duty cycle, dissipation factor, power factor, life expectancy, temperature coefficient, etc. Other important characteristics are: the equivalent series resistance, impedance, self-resonant frequency, voltage reversal, dielectricum and the dimensions. Detailed discussions on this matter are very complex and beyond the scope of this work. For more information reference [12] should be consulted.

In general, ceramic capacitors have small dimensions, low inductance, low impedance and can handle high voltages. On the other hand they are temperature and voltage dependent. If the temperature of the room is stable and the repetition rate is not too high, ceramic disc capacitors may be a suitable choice. There are several makes of this type, an example is shown in Appendix B. In general the high voltage types have a lower capacitance. If necessary two capacitors of 30 kV in series can be applied. To lower the inductance, three of them can be connected in parallel and can be given a coaxial shape in a square metal housing, see Figure 35. In this case the capacitance of each capacitor $C = 2 \times 5.7/3 = 3.8$ nF. It is recommended to design the generator with a little larger value because the capacitance decreases with increasing temperature, voltage and aging.

The dimensions of the square enclosure can be derived from Figure 36. In case of 4 parallel stacks, approaching a square shape of the capacitor, Figure 37 can be used [14].

At high frequencies, the pulse impedance of a capacitor appears in series with the load and reduces the voltage across the load (in our case only 50 Ω!). If the pulse impedance is more than 10% of the load impedance, the fast rising portion of the output pulse will begin to roll over before reaching 90% of the peak voltage. A pulse impedance of 5 Ω for large capacitors is not uncommon. With the construction of Figure 35 a low pulse impedance is expected.

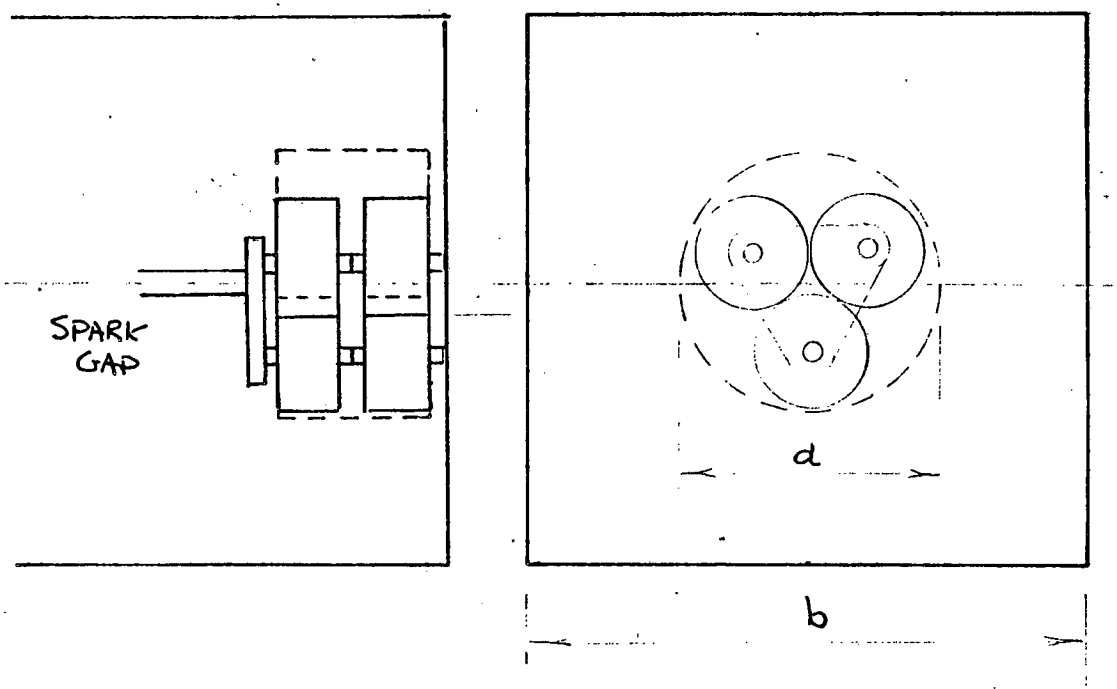

FIGURE 35 Composition of a high voltage, low inductance capacitor (50 Ω)

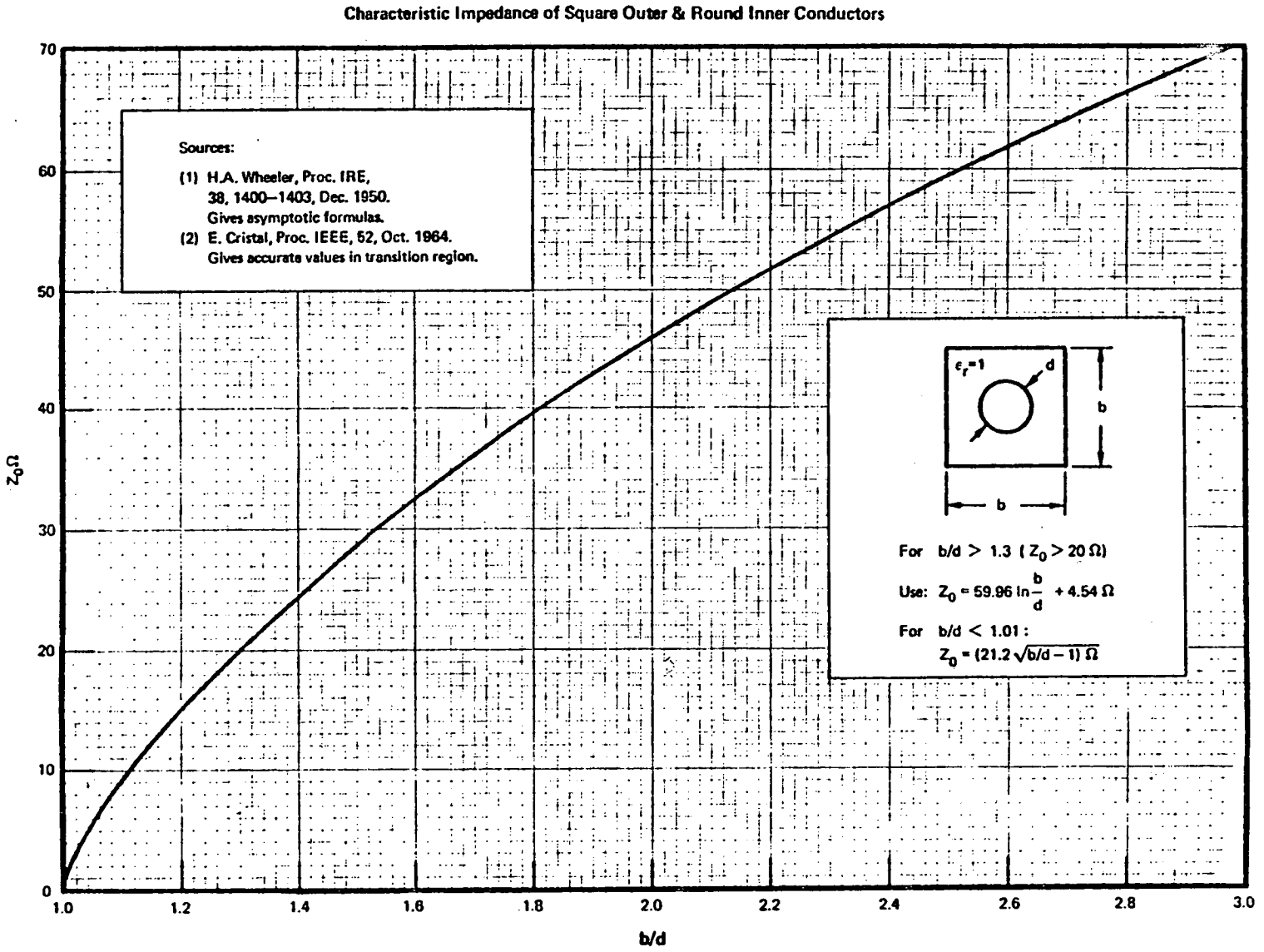

FIGURE 36 Characteristic impedance Z_0 versus b/d

Microwave Engineers'

CHARACTERISTIC IMPEDANCE OF RECTANGULAR COAXIAL TRANSMISSION LINES

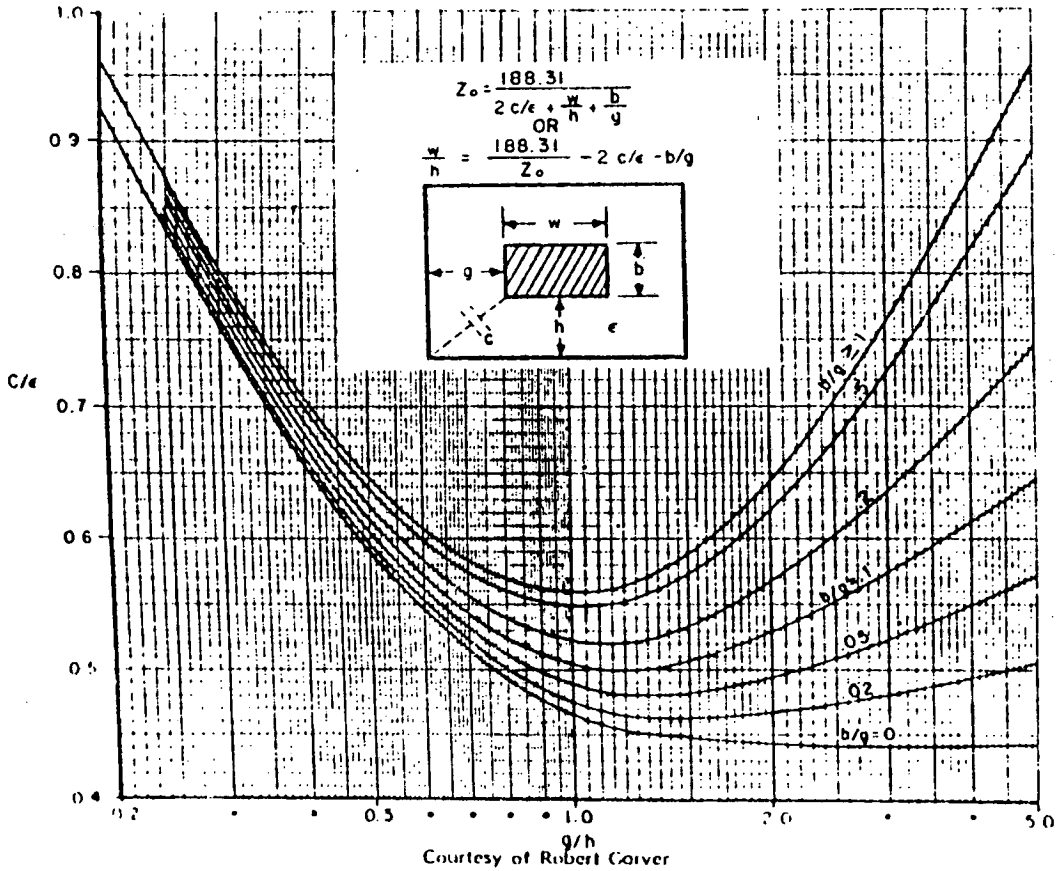

FIGURE 37 Characteristic impedance Z_0 of rectangular structures

4.2 High Voltage Power Supply

The high voltage power supply (HVPS) in appendix A can be adjusted from zero to 60 kV and from zero to 5 mA by two 10-turn potentiometers. The HVPS can be connected to the capacitor via a high-voltage resistor, e.g. 1 MΩ or more.

The time constant of the charging circuit is $\tau = RC = 10^6 \times 5.7 \times 10^{-9} = 5.7$ ms. The capacitor is charged to 99% of the HVPS voltage after $4.5\tau \approx 26$ ms.

The charging time can also be adjusted by the current. With a constant charge current the charging time can be calculated from $i = dQ/dt$. For instance with a capacitor C = 5.7 nF and a voltage V = 60 kV a current i = 0.34 mA is needed to charge the capacitor in one second. The resistor R is needed to isolate the HVPS from the generator during the discharge. A large time constant results in a low prepulse! The polarity of the charge can simply be reversed by changing the connections of the HVPS. Special precautions are needed to prevent spark-over from the end of the high voltage shielded cable to the resistor.

4.3 Spark Gap

The spark gap contains two electrodes in a plexiglass housing that can be filled with air or SF_6 with an pressure of a few atm. (1 atm = 14.7 psig). The electrodes can be made from steel, brass or copper, however these materials are not as good in general as molybdenum and tungsten. The best seems to be copper - tungsten alloys, such as Elkonite 10W3 (57% W, 43%Cu) or 30W3 (66% W, 34% Cu). The charge transfer $Q = C \cdot V$ is only 0.34 mC. The switch can therefore made very reliable with minimum electrode wear and very little maintenance. With an adjustable gap distance the spark gap can be used for different capacitor discharge voltages. Together with an adjustable gas pressure it is possible to have a convenient large field strength adjustment.

The rise time of the spark gap is very dependent on the length of the spark. Therefore the plasma channel must have the shortest possible length. This can be accomplished by the application of a pressurized, high-insulating gas (for example SF_6).

If possible the electrodes should match the transmission line as much as possible. The spark is the switch between the capacitor and the transmission line. The coaxial capacitor is the source from where the TEM wave is launched.

The rise time of the spark gap is dependent on the inductance of the spark gap

and on the resistive phase of the spark.
The inductance of the plasma channel can be calculated from:

$$L = 2\ell\left[\left(\ln\frac{4\ell}{d}\right) - 1\right] \text{ nH} \qquad (20)$$

where ℓ is the length and d is the diameter of the spark channel in cm. Assume ℓ = 1 cm and d = 0.1 mm, then L = 10 nH. With a load impedance of Z_0 = 50 Ω, the time constant τ_L = L/R = 0.2 ns and the corresponding rise time

$$t_L = 2.2\tau_L = 0.44 \text{ ns}$$

With ℓ = 1 cm and d = 10^{-3} cm, L = 14.6 nH and t_L = 0.64 ns. The time constant of the resistive phase can be derived from [16]:

$$\tau_R = \frac{88}{Z^{1/3}\,E^{4/3}}\left(\frac{\rho}{\rho_o}\right)^{1/2} \text{ ns} \qquad (21)$$

where E is the field strength in MV/m, and (ρ/ρ_o) is the ratio of the gas density to that of air at STP (standard temperature and pressure).

With 60 kV across 1 cm and a homogeneous field between the electrodes, E is about 6 MV/m. With dry synthetic air in the spark gap the time constant τ_R is 2.19 ns and the corresponding rise time t_R = 4.82 ns. Applying sulphur hexafluoride gas (SF_6), having a factor $(\rho/\rho_o)^{\frac{1}{2}}$ = 2.5, the gap distance ℓ can be made a factor 2.5 smaller, resulting in a field strength of 2.5 x 6 = 15 MV/m, a time constant τ_R = 1.61 ns and a rise time t_R = 3.55 ns.

Note that it is important to work with a high field strength, E, in the spark gap [9, 14]. With gas pressurization the gap distance can even be made smaller and thus the field strength, E, larger. The total rise time of the spark is the geometric sum of the two rise times t_L and t_R:

$$t_r = \sqrt{t_L^2 + t_R^2} \qquad (22)$$

with t_L = 0.44 ns and t_R = 3.55 ns the total rise time t_r = 3.58 ns.

The resistive term can be converted to an equivalent inductance which can then be added to the geometric inductance. These should be added in quadrature, such that:

$$L_{eff} = \sqrt{L_{geo}^2 + L_{res}^2} \qquad (23)$$

The resistive time constant $\tau_R = L/R = t_R/2.2 = 3.55/2.2 = 1.6$ ns. With a load impedance R = 50 Ω is $L_{res} = 1.6 \times 50 = 81$ nH.

L_{geo} contains the inductance of the capacitor, the connections of the spark gap and of the spark itself. Assume L_{geo} is 20 + 20 + 10 = 50 nH. The effective inductance is then:

$$L_{eff} = \sqrt{50^2 + 81^2} = 95 \text{ nH}$$

The effective time constant:

$$\tau_{eff} = \frac{L_{eff}}{R} = \frac{95}{50} = 1.9 \text{ ns}$$

leading finally to an expected rise time:

$$t_r = 2.2 \times \tau_{eff} = 4.2 \text{ ns}$$

In this calculation it is assumed that the load impedance is 50 Ω resistive!

In this case, it can be concluded that the resistive phase of the spark plays a dominating role in the total rise time. By applying more pressure to the insulating gas in the spark gap, the rise time can be made smaller. With external triggering (eg. laser beam) the resistive phase can be made shorter and the total rise time even more smaller. However, for a rise time t_r = 5 ns dry synthetic air with a few atm of pressure may be sufficient. The recommended triggering of the spark gap is described in section 4.4.

A suggestion for the construction of the spark gap is given in Figure 38. The electrodes can be made from brass or stainless steel. There is no need for much maintenance, since the energy transfer is only $W = \frac{1}{2} CV^2 = 10.3$ J. The peak current I_{pk} = 60 kV/50 Ω = 1.2 kA, the charge transfer Q = CV = 5.7 nF x 60 kV = 0.34 mC. Cleaning and polishing of the electrode surfaces are recommended every 2000-4000 shots.

One of the electrodes, at the side of the septum, can be made adjustable. A gap spacing of 0-1 cm is sufficient. The inductance of the spark gap can be reduced by making the length of the electrodes in Figure 38 shorter. However flash-over on the outside of the enclosure should be prevented. The enclosure can be made from lexan or plexiglass. The spark is then visible and can be observed. Because of the pressure the different parts of the enclosure should be sealed with O-rings. A provision for inlet and outlet of the gas is needed.

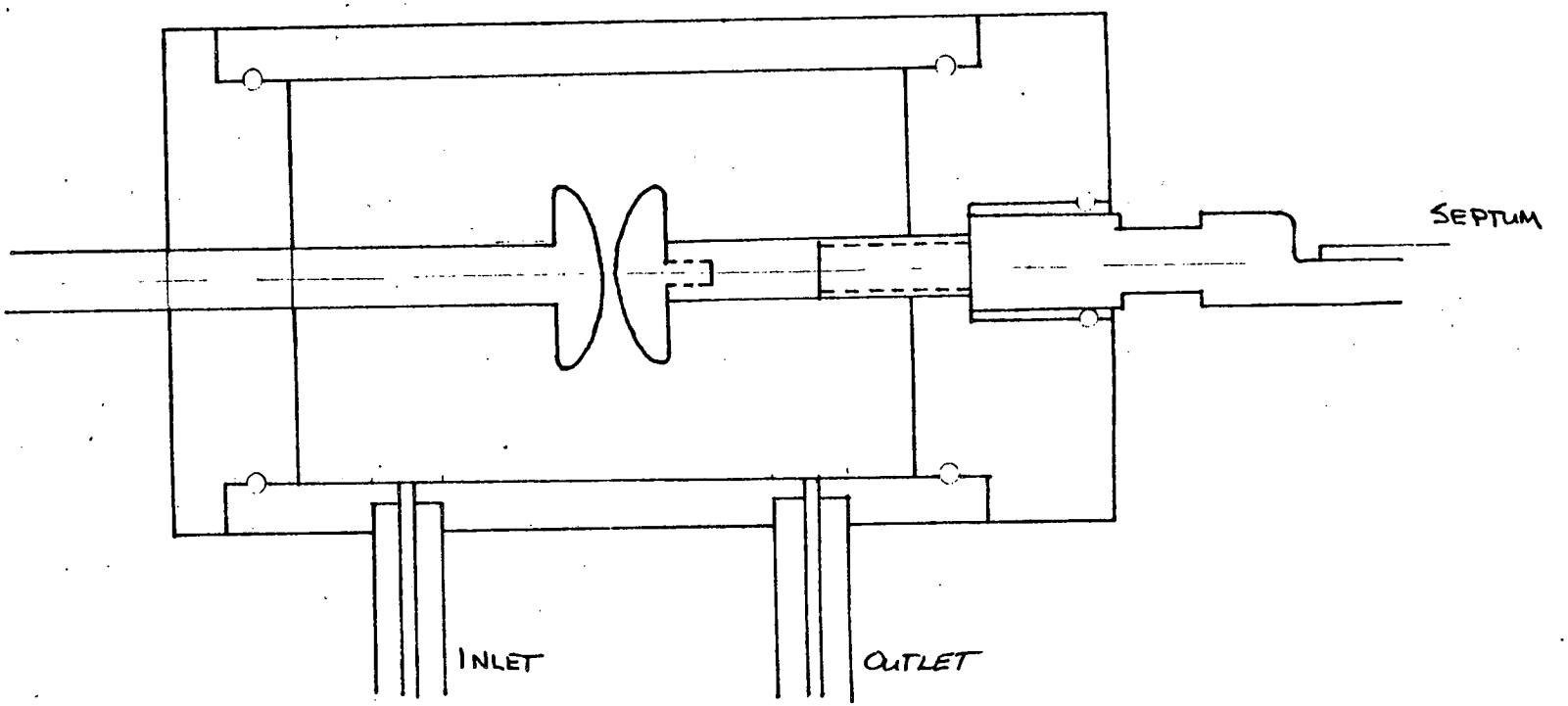

FIGURE 38 Draft for an adjustable spark gap

The high pressure dry air is stored in a cylinder. The specifications of the gas (air or SF_6) are tabulated in Table 8. A reducing valve at the top of the bottle regulates the pressure to approximately 100 psig. With a gas control valve and meter the pressure can further be reduced to the required level between 0 and 100 psig.

4.4 Triggering

A very simple procedure for triggering the discharge of the capacitor in the transmission line is suggested.

- Adjust the gap distance and the gas pressure for the desired charge voltage of the capacitor. For a short rise time choose a small gap distance with a high pressure.

- Select a gas pressure about 10-20% higher than the breakdown voltage of the spark gap. A diagram of the breakdown voltage versus the gas pressure at different gap distances can be prepared in advance.

- Charge the capacitor to the desired voltage (field strength, Eqn. 6b)
  At maximum voltage V = 60 kV the capacitor is fully charged after 30 ms.

- Close the inlet of the spark gap and open the outlet. The escape of the gas causes the discharge.

This simple way of triggering has the advantage of exactly knowing the charging voltage and, therefore, also the field strength. For accuracy of the charge voltage see the specifications of the Glassman HVPS in Appendix A. The output voltage of the generator is determined by the pulse impedance of the capacitor and the voltage across the spark gap. The pulse impedance can be a few ohms in series with the load impedance Z_o = 50 Ω, the spark gap has a typical 150 V arc drop. The ratio of the charge voltage and the peak output voltage can be calibrated in advance. Filling up the spark gap with fresh air removes old gas particles of the spark. This improves the repeatability of the wave shape.

The charge cycle at maximum voltage and 1 MΩ charge resistor is about 30 ms. That is relatively slow, so that no prepulse can be observed. If necessary the charge cycle can further be slowed down by increasing the charge resistor value. This resistor should be sufficiently long to withstand the maximum voltage. Also

INTERNAL GAS SPECIFICATION TABLE	
GAS TYPE	SPECIFICATION
DRY SYNTHETIC AIR	
NITROGEN	79% by volume
OXYGEN	21% by volume
Density	1.29 ± 0.1 g/liter (0°C, 760 mm Hg)
Water content	< 5 ppm by volume; dew point -65°C or lower
Hydrocarbon content	< 10 ppm total
Particle size	< 5 microns
Carbon dioxide	0
SULFUR HEXAFLUORIDE (SF_6)	
Grade	Dielectric
Purity	99.8% minimum
Water content	< 5 ppm by volume, dew point -50°C or lower

TABLE 8 GAS SPECIFICATION

the diameter should be sufficiently large to prevent corona (60 kV for seconds or more!). By selecting a lower gas pressure than needed to prevent breakdown, the generator can be made repetitive.

4.5 Adaptor

The generator housing, containing the capacitor, charge resistor and spark gap forms an integral part of the TEM cell construction. It can be made so that it can be separated from the TEM cell and replaced by an adaptor for connection of low level, 50 Ω internal impedance, signal sources (see Fig. 39). The 50 Ω coaxial connector at the apex of the input taper is then the launching point of the TEM cell. To keep a minimum distance between the septum and side walls and to match the shape of the apex to the connector dimensions, the width of the adaptor septum can gradually be decreased. This means the characteristic impedance of the adaptor is increasing a little towards the apex. This discontinuity in impedance will not be seen by the launched wave as long as the length $\ell < 0.1\ \lambda$, e.g. with a length of 30 cm up to 100 MHz. Moreover, the characteristic impedance, Z_o, is also increasing towards the connector by the increasing fringing capacity term $\Delta C/\epsilon_0$ in equation (4). Fine adjustments of the shape can be made with a TDR measurement, if necessary.

The length, ℓ, of the adaptor is dependent on the length of the generator housing, which contains the capacitor and spark gap, see Figure 26. In this case the capacitor is the launching point. The apex will be somewhere between the capacitor and the spark in the spark gap.

Any type of coaxial connector can be used, except for VHF purposes, where a better quality than that of an N- or BNC connector is recommended.

4.6 Suppression of Higher-Order Modes

The cutoff frequencies $f_{c(mn)}$ and the resonance frequencies $f_{R(mnp)}$ of the TEM cell are briefly discussed in section 3.1. These frequencies depend purely on the cell geometry (dimensions a,b and w for f_c; and a,b,w and L_{mn} for f_R).

A transmission line has an infinite number of possible modes of transmission. Each of the modes has its own distinctive configuration of electric and magnetic fields, and they all satisfy Maxwell's equations and fit the boundary conditions imposed by the particular transmission line. In a two conductor transmission line only one TEM wave can exist, the TE and TM waves are both infinite in number.

The TEM wave has no field components in the direction of energy flow. This

principal mode transmits energy at all frequencies down to and including zero hertz. The TE and TM modes have a magnetic and electric field, respectively, in the direction of energy propagation and have low-frequency limits or cutoff frequencies below which energy will not be transmitted along the line. The attenuation will increase rapidly with decreasing frequency as the cutoff frequency is approached.

A practical transmission line is nearly always designed so that it is able to carry energy in only one mode of transmission. For this reason, the line is restricted in size so that only the lowest order mode, the TEM wave, can transmit energy, and the line is then below cutoff for all the infinity of higher order modes.

In our case, the center part of the TEM cell has a cross-section with large dimensions. This results in energy flow carried by higher-order modes starting at relatively low frequencies (TE_{01},TE_{10} and TE_{11} modes from approximately 57, 84 and 102 MHz). At the generator connection a double exponential pulse is launched with a spectrum from 0 Hz to more than 1 GHz, see Figure 15. It contains several above cutoff modes. If some of the power entering the cell is coupled into higher modes and is superimposed upon the principal mode, the field configuration of the TEM wave will be degraded.

In the uniform-cross-section center part of the cell the TEM wave as well as the TE and TM waves above cutoff are propagated. In the taper sections however, the TE and TM waves are reflected at a distance X_{mn} $\frac{1}{2}L_E$ from the center part section, where the cross-section of the taper becomes too small for the field frequency. Factor X_{mn} is dependant on frequency. Different frequencies from a pulsed higher mode wave are reflected at different distances in the taper. The reflections will arrive at different times in the test volume causing pulse dispersion of the reflected wave.

If the pulse dispersion is neglected, the first reflection of a transient field in the center of the test volume can be expected after a clear time of approximately 2x2m/c = 13.3 ns. That is just after t_{peak} in Fig. 14. The polarization of the reflected wave is changed by the reflection. The waveform of the reflected higher mode wave is dependent on the quality factor $Q = f_o/\Delta f$ of the damped cavity resonances. Multiple reflections appear with an interval time equal to the clear time. However, higher-order modes are not very well guided in the TEM cell.

At certain frequencies reflections back and forth between the two tapers may build up resonances, see Eqn. (1) and (2). Resonant low-loss transmission lines,

like a TEM cell, can have a Q of hundreds in the VHF range. For instance, with CW excitation at $f_{R(101)}$= 84 MHz and a Q = 500, the 3 dB bandwidth of the resonance is only 0.17 MHz. The amplitude of the TE_{10} mode is increasingly attenuated approaching $f_{c(10)}$= 75 MHz. Neglecting the interaction of the TE_{01} mode, it means that in our case no propagating higher-order modes (traveling waves) are present below approximately 84 MHz.

Since the excitation from the EMP generator is a single pulse, the reflections will vanish due to losses inside the cell. No cavity resonances (standing waves) are built up because the losses are not replenished by incoming power as in the case of continuous wave (CW) excitation.

Higher-order modes degrade the pure TEM wave, cause standing wave patterns in the case of CW excitation and cause reflections in case of pulse excitation. It is therefore important to prevent the generation of higher-order modes or to suppress them if they cannot be avoided. Higher-order modes can be launched or excited at the feed point or set up at discontinuities in the transmission line.

If there is a discontinuity in the transmission line, e.g. an abrupt change in cross-section, or a sharp bend at the connection of the taper sections to the central portion of the TEM cell, above cutoff and below cutoff modes will be excited at the discontinuity. The latter are localized and contribute to the fringing fields at the discontinuity.

In our case the tapers are relatively long compared with the height and the width. The angle between the taper and the mid-section is about 153°. This discontinuity can be made more gradual be gluing metal foil on the inner side of the cell and to shape the septum at that point. If higher-order modes due to discontinuities cannot be avoided, e.g. in the case of reflections from an object being tested in the TEM cell, damping material in the output taper can be used. The relatively long tapers also help a little in stretching the reflected EMP field.

Any physical structure that launches a traveling wave in a transmission line will generally excite a large number of modes at the point of excitation. These higher-order modes can be suppressed by making the physical dimensions of the launching point small compared with the half wavelength of the highest frequency content of the generator output pulse. If the physical dimensions (principally the spacing between the septum and the upper and lower wall of the taper at the feed point) are made sufficiently small, the small cross-section of the taper acts as a high-pass filter for the higher-order modes (It has a cutoff frequency below which higher-order modes cannot effectively propagate). Only the TEM wave

is passing through this "filter". The higher modes attenuate rapidly with distance from the point of excitation and are usually negligible at a distance roughly equal to the transverse dimensions of the input cross-section. They may be of large amplitude in the immediate vicinity of the launching structure (the capacitors and spark gap of the EMP generator). At sufficiently low frequencies, far below cutoff, they add to give the fringing fields that are predicted by static field theory.

At 20 cm distance from the quasi apex the space between the septum and the taper enclosure is 10 cm. A half wavelength of 10 cm corresponds to a frequency f = 1500 MHz. That is a factor of 18 higher than the resonant frequency $f_{R(101)}$ of the first interacting higher-order mode.

The generator can be given a coaxial structure, see Figures 38a and 38b, that can be coupled to that of the TEM cell. The problems of exciting waves in a coaxial system are not simple field problems. The field pattern inside the exciting source should be studied. Concentrated sources will not in general excite a pure TEM wave, but all waves that have field components in a favorable direction for the applied components (capacitors, HVPS cable, spark gap, connections). That means that one wave alone will not suffice to satisfy the boundary conditions of the generator, so that many higher-order waves must be added for this purpose.

The TEM wave, if completely absorbed at the termination, will represent a resistive load on the source. The higher-order modes that are excited, if all below cutoff, will be localized in the neighbourhood of the source and will represent purely reactive loads on the source. The real part of the load, representing the TEM wave, should be matched to the source [17,18].

If possible the excitation should be introduced with the field components in the direction of the transverse electro-magnetic wave in the line. A choice can be made from the Figures 38a and 38b. The orientation of the capacitors in Figure 38b results in a horizontal electric field and a transverse magnetic field. The electric field component in the direction of propagation causes TM modes. However, TM modes appear at higher frequencies than TE modes. The first TM resonance is TM_{110} with $f_{R(110)}$= 168 MHz. The taper spacing at the launch point is small enough to suppress the TM modes.

The TEM wave and higher-order waves are launched forwards and backwards. For that reason the connection of the capacitors to the backside of the generator housing should be made as short as possible, see Figure 35. The spark gap, forming a short circuit during the discharge of the capacitors, should have horizontally

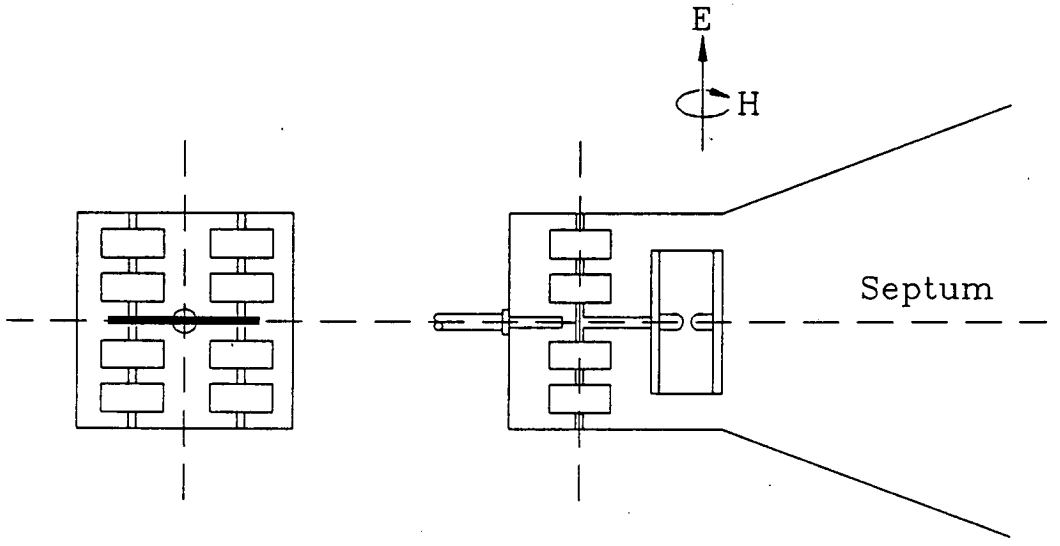

Figure 38a: Vertical orientation of the capacitor unit

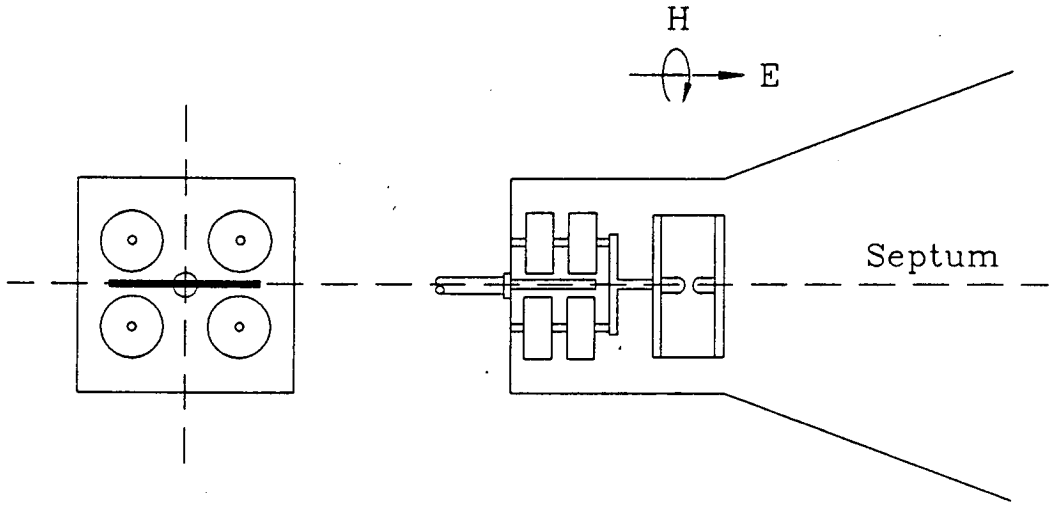

Figure 38b: Horizontal orientation of the capacitor unit.

dominating dimensions. The horizontal shape limits the vertical electric field lines.

The interface between the spark gap and the septum can be given a gradually changing shape. The HVPS cable can enter the generator housing through the center of the back side, with the shield of the coaxial cable connected to the housing and the dielectric material ending at the connection of the inner conductor to the capacitor. In that way the cable is horizontally positioned and concentrically connected to the capacitor unit.

5.0 TERMINATION

The transmission line (input taper - mid section - output taper) is matched to a non-inductive load resistor with value $R = Z_o$. If well designed, all energy arriving at the end of the transmission line will be absorbed in the termination and no reflections will be observed in the test volume.

For low-level CW applications an adaptor as in Figure 39 can be used. However, in the case of EMP simulation, problems with flash-over and corona in the taper, the coaxial connector, the cable and the power absorber are expected. It is therefore better to place the load inside the cell and to make it an integral part of the simulator. In this way all parts of the simulator, except the HVPS, are shielded by the enclosure of the cell.

5.1 Load Resistor

Because of the high peak voltage of 60 kV, the load resistor should have a minimum length of about 20-30 cm, dependent on the construction and the connection of the resistor. This offers the possibility not only to match the line impedance, Z_o, but also the wave impedance over this length. Figure 40 shows how the impedance of the line can gradually be matched to the local resistor value, from 50 Ω to 0 Ω. Figure 41 shows the same for $Z_o = R = 100$ Ω. It is obvious that $Z_o = 100$ Ω is a better choice for an EMP simulator.

The characteristic impedance of a transmission line with a square outer - and a round inner conductor can be calculated from:

$$Z_o = 60 \ln \frac{b}{d} + 4.54 \ \Omega \qquad \text{for } Z_o > 20 \ \Omega, \ \epsilon_r = 1 \qquad (24)$$

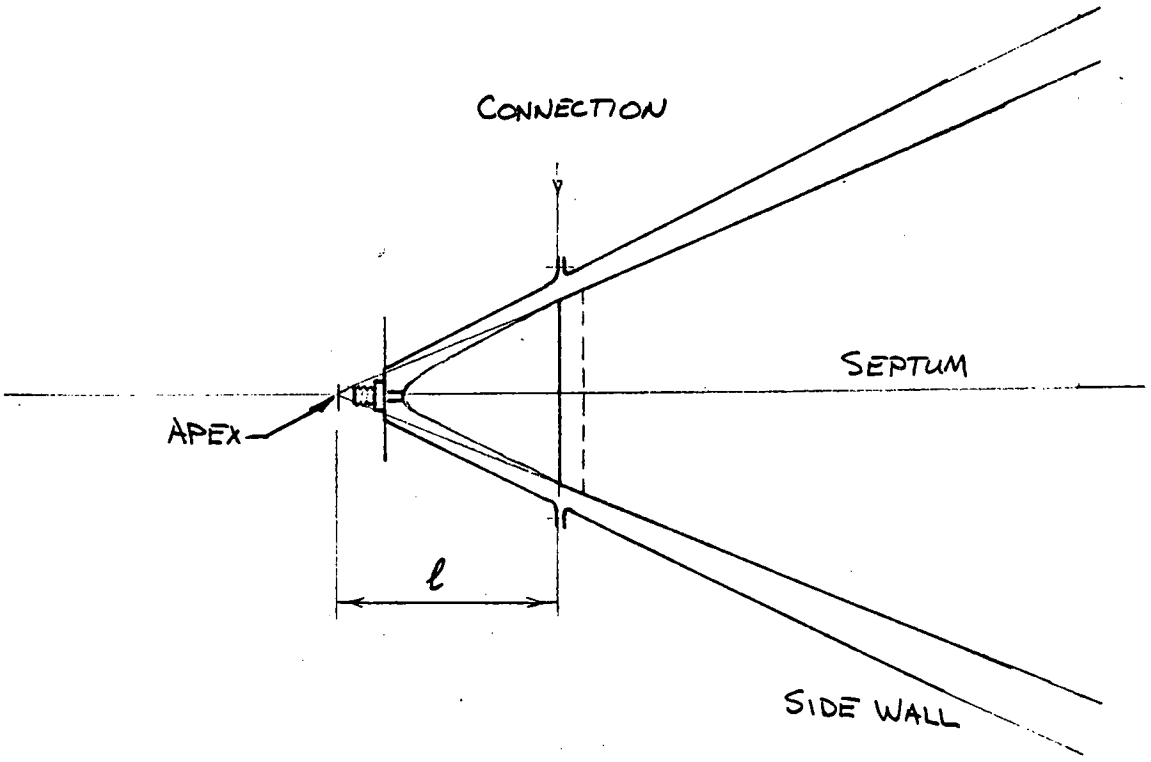

FIGURE 39 Low voltage 50 Ω adaptor (top view)

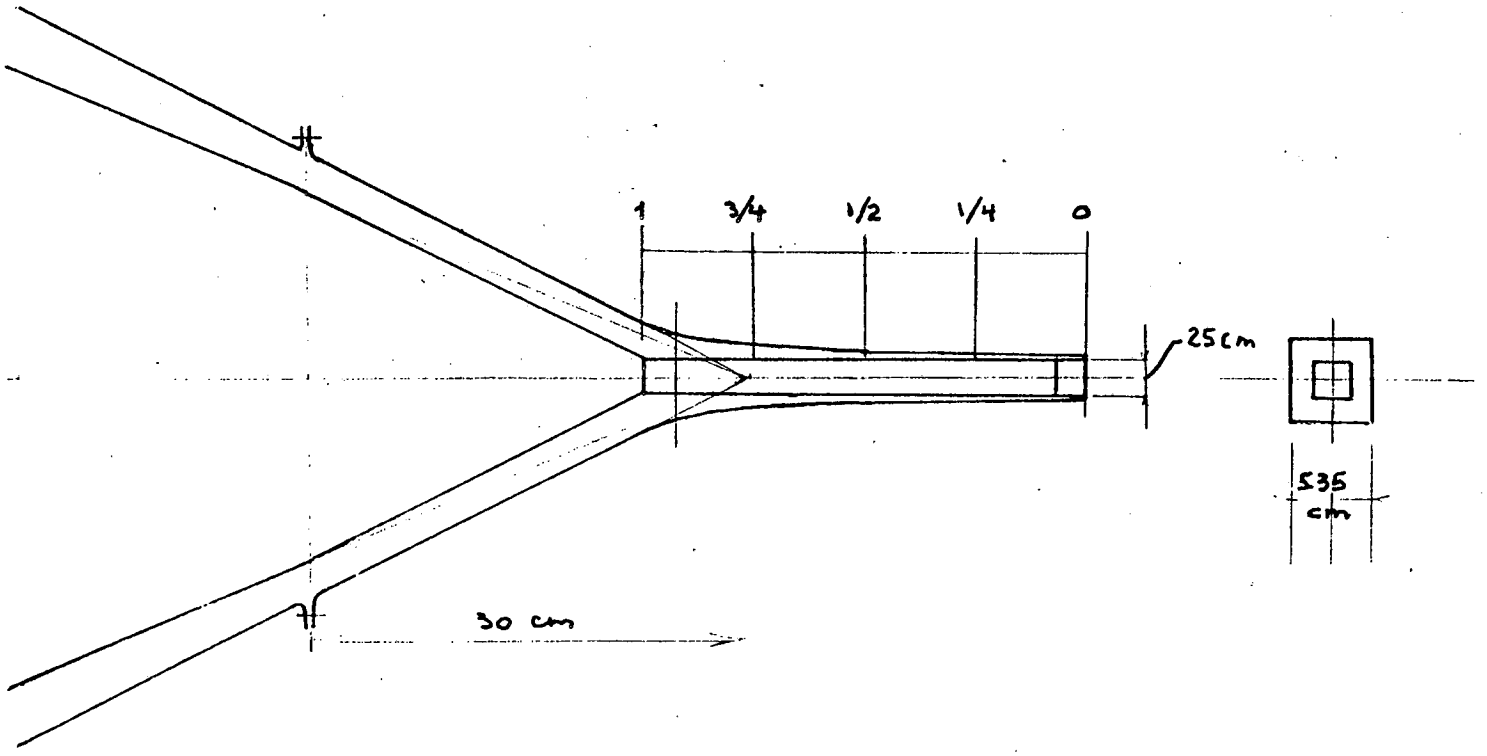

FIGURE 40 Terminating resistor R = 50 Ω, length l = 30 cm, ϕ = 2.5 cm

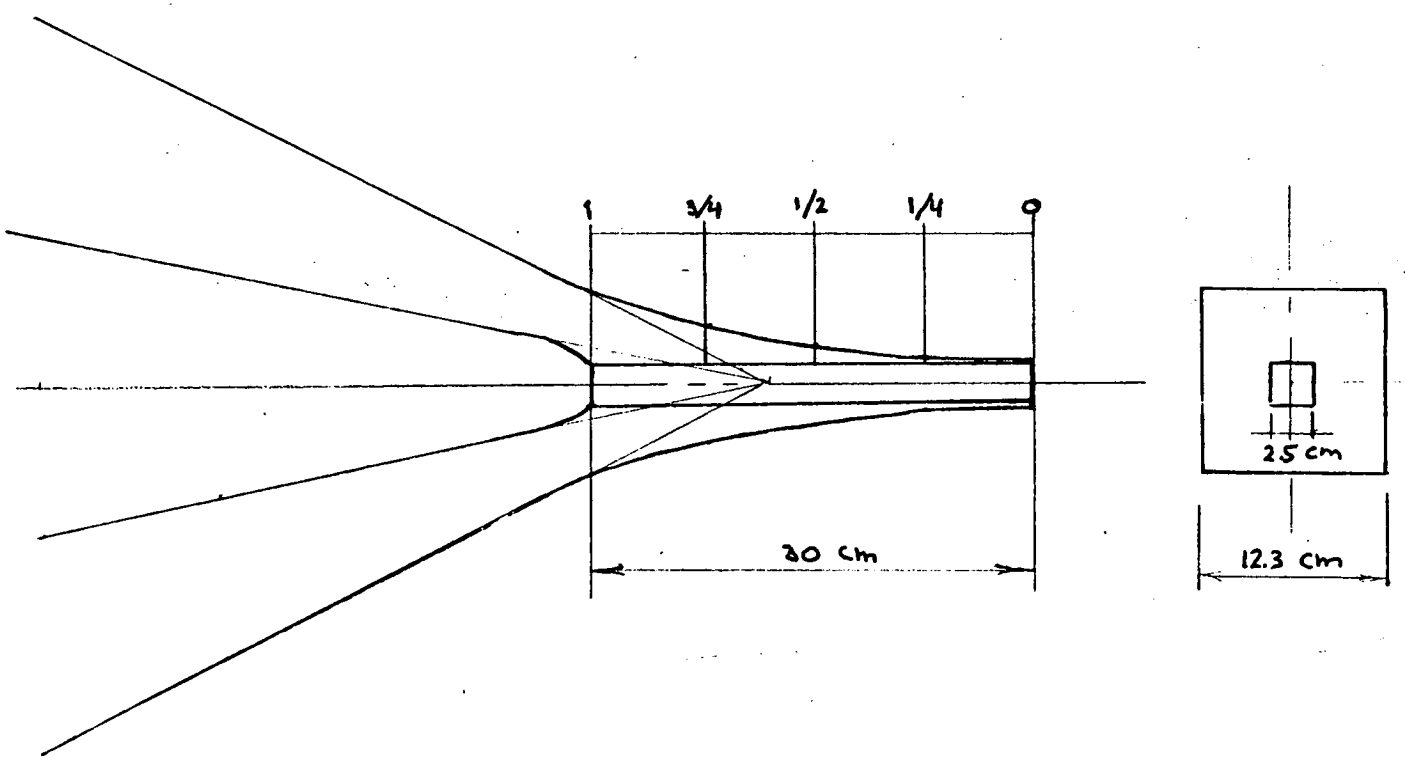

FIGURE 41 Terminating resistor R = 100 Ω

where b is the edge of the cross-section of the enclosure and d the diameter of the round inner conductor [14]. Figure 36 shows a diagram of Z_o versus b/d. The gap between the resistor and the square outer conductor can be read from Table 9.

The requirements for the non-inductive load resistor can be summarized as follows;

- resistive value 50 Ω, ± 2%;
- temperature coefficient 0.2% per degree C;
- peak voltage 60 kV;
- peak current 1.2 kA;
- peak energy 10 J in 1 μs;
- average power 40 W; and
- duty cycle 1 PPS.

The average voltage and current during 200 ns is about 45 kV and 0.9 kA, resulting in 40.5 MW. Assume about this power should be dissipated in 1 μs and the repetitive rate of the pulse generator is maximum 1 pulse per second, then the average power is about 40 W.

A Carborundum ceramic non-inductive resistor, type 889 AS 500 J is a good choice, see Appendix C.

5.2 Voltage Divider

For a high voltage application, as EMP simulation, it is advantagous to combine the terminating resistor with a voltage divider. The voltage divider can then be used to monitor the output voltage and for calibration purposes. For low-level measurements (CW and pulse) commercial available attenuators, connected to the coaxial connector of the adaptor in Section 4.5, may be applied.

To avoid parasitic inductances and stray capacitances the voltage divider should be a part of the coaxial structure. A suggestion is given in Figure 42. To simulate the extension of the terminating resistor, to form a voltage divider, the output resistor can be distributed around the periphery of the terminating resistor. The connection between the two resistors and the output connector can also be made coaxial.

The peak voltage is 60 kV. A voltage division of more than about 1 to 50 is not recommended because of the capacitive coupling at high frequencies. Ten resistors of 10 Ω in parallel are suggested. The maximum output voltage is then about 1200 V. A second voltage divider can be connected to the outside of the cell.

TABLE 9 Gap Distance g in mm Between Inner and Outer Conductor of the Termination.

ℓ	Ω	b/d	g	b
1	100	4.91	48.9	122.8
3/4	75	3.24	28.0	81.0
1/2	50	2.14	14.25	53.5
1/4	25	1.42	5.25	35.2
0	0	1.0	0	25.0

ℓ	Ω	b/d	g
1	50	2.14	14.25
3/4	37.5	1.74	9.25
1/2	25	1.42	5.25
1/4	12.5	1.16	2.0
0	0	1	0

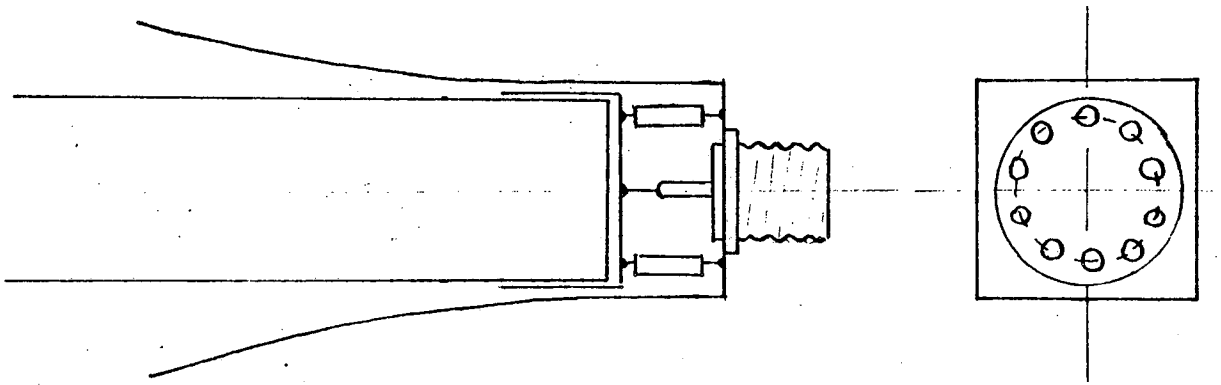

scale 1:1

FIGURE 42 Voltage divider combined with terminating resistor

6.0 CONSTRUCTION

Mechanical details will not be discussed in this section, only some electrical consequences and ideas for application are given. The walls of the TEM cell and the housing of the generator and termination can be used as a shield, if they are constructed as one solid shell, without leaking seams. This shielding enclosure can be constructed from metal sheets, such as tinned iron. Since, standard dimensions are 3' or 4' by 8', many overlapping seams are needed. Tinned iron sheets with a thickness of 0.5 mm are easily soldered and have sufficient shielding effectiveness. For mechanical reasons, thicker material may be needed. If it is convenient or necessary the length L_c can be made a little shorter, without electrical consequences. The septum can be made from thicker material, e.g. 1 mm brass or thicker. The edges should be rounded.

To enter the cell a hatch is needed, e.g. with dimensions of 1 x 1 m, in the lower part of the cell, see Figure 43. Around the four sides of the hatch fingerstock can be mounted, primarily for shielding purposes. The metal sheets of the cell near the hatch can be bent around a wooden frame, outside the cell, to form a flat, solid wall on the inside. The cell can be mounted in a wooden frame outside the cell and placed upon a wooden buck or pedestal, see Figure 43. If necessary the metal sheets can be nailed against this frame. To observe the spark in the generator a small hatch can be made in the generator enclosure that can be shifted horizontally to open and close a viewing hole. The same can be done at the termination end. The small hatch at the generator side is also desirable if the spark gap distance has to be adjusted, without removing the generator.

Coaxial connectors mounted in the bottom of the cell form an ideal connection with the coaxial cables going to the external data recording equipment. The shielding effect of the enclosure will not be degraded. In the upper half of the cell a D-sensor can be mounted against the ceiling with the coaxial connector through the wall. This sensor can be used for monitoring purposes.

7.0 SAFETY

Because of the high voltage, max. 60 kV, special safety precautions are needed. The cable from the HVPS to the generator (the charging resistor) should be shielded (coax cable) as far as possible. A provision should be made to discharge the capacitor before opening the cell. The hatch can be provided with a switch that prevent charging the capacitor when the hatch is removed. Only authorized personnel should be allowed to work with the simulator.

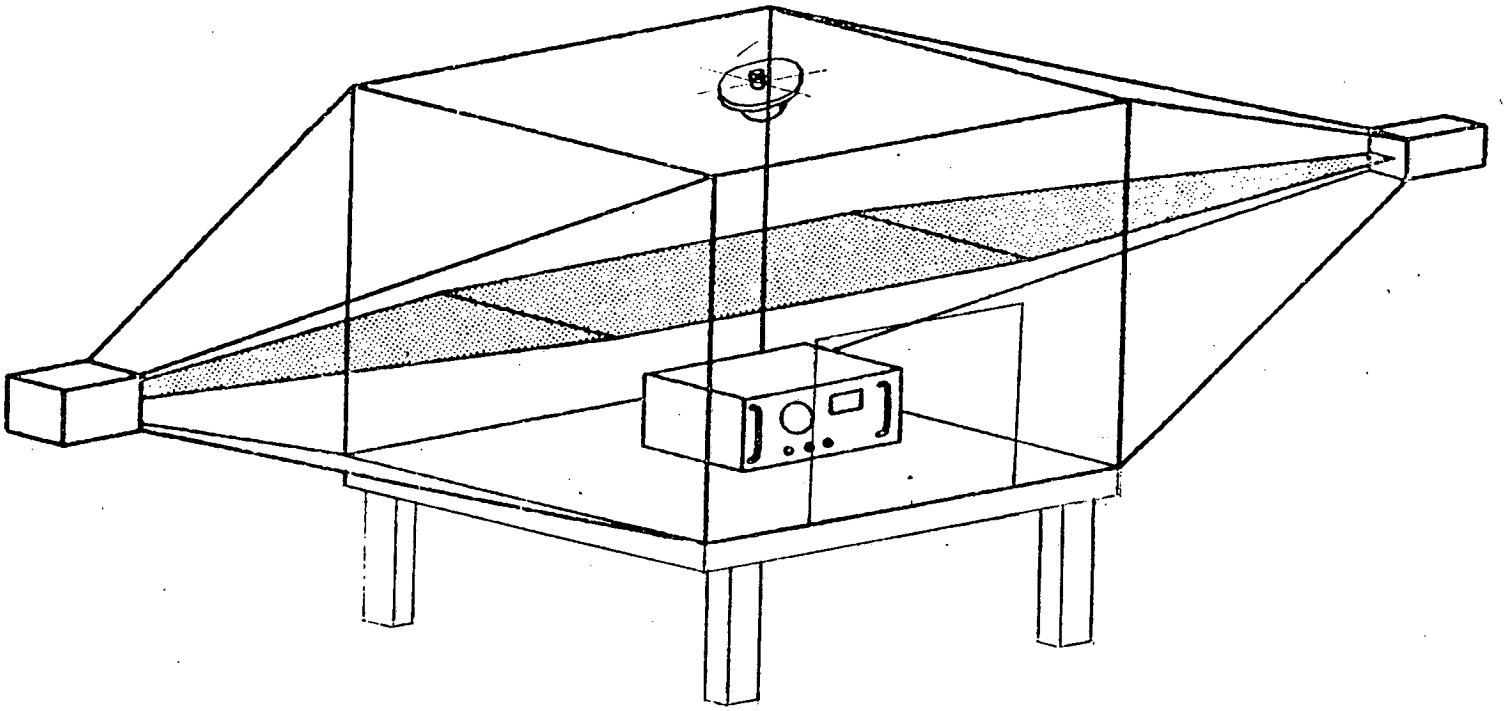

FIGURE 43 TEM cell placed upon a wooden trestle

8.0 CONCLUSIONS

It can be concluded that the construction of a low impedance (50 Ω) TEM cell for high voltage applications may cause some problems with respect to corona and flash-over near the apex of the two tapers, see section 3.8: Field Enhancement and section 5.1: Load Resistor.

To solve this problem the gap distance in the apex of the tapers can be increased, the edges of the septum can be given a larger radius, or an insulating material can be used in the gap. However, every deviation from an ideal matching of both ends of the cell will result in more interacting higher-order modes and in reflections. A compromise between correct matching and high voltage insulation should be made.

Another solution to the problem is to increase the impedance of the cell, resulting in a smaller width of the septum and a larger gap between the septum and the side walls. If the width of the septum is decreased to 1 m, the impedance Z_o will be 83 Ω, or in case of Z_o = 100 Ω the width is 80 cm. Decreasing the width will consequently result in a smaller width of the test volume. However, related to the available test height of about 30 cm, a width of ½ x 2w = 40 cm looks acceptable. It should be noted that reducing the width of the septum will result in a slightly more interacting TE_{01} mode.

In MIL-STD 462, Interim Notice 5 (NAVY) a parallel plate line with an impedance Z_o = 100 Ω is recommended for testing the radiated susceptibility of equipment. Chapter RS-05, section 5.4 of this document recommends TEM cell radiators. Since an impedance Z_o = 100 Ω is an acceptable design and is in agreement with MIL-STD 462, it is recommended for the TEM cell EMP simulator.

Increasing the impedance Z_o from 50 Ω to 100 Ω has additional advantages: a shorter rise time t_r, larger output voltage from the generator, a smaller generator capacitance and a higher first higher-order cut-off frequency ($f_{c(01)}$ = 67 MHz instead of 57 MHz).

For low level measurement applications, the adaptors described in section 4.5, should be equipped with 100 Ω connectors and impedance matching networks are needed to connect the 100 Ω cell to the 50 Ω measuring equipment. Another possibility is to convert the 100 Ω cell into a 50 Ω cell by placing metal sheets over the smaller septum. In that case normal 50 Ω connectors can be used and no impedance matching networks are needed.

The specifications for a 100 Ω TEM cell EMP simulator are collected in Table 10.

The dimensions of the TEM cell are balanced against the first higher-order cut-off frequency (maximum test volume with the highest first interacting resonant frequency).

The generator and termination are integrated with the TEM cell, thus forming one solid shell enclosure. In this way RFI can be avoided from the outside to the inside during measurements inside and from the inside to the outside during testing. Data recording equipment without extra shielding can be used near the simulator.

9.0 ACKNOWLEDGEMENT

I would like to thank Dr. Satish Kashyap and Joe Seregelyi for their encouraging discussions, Miles Burton for the calculations of the field enhancement and Miss Robin Mann for typing the manuscript.

TABLE 10 Specifications for the 100 Ω TEM Cell EMP Simulator

1.0 TEM CELL

dimensions:	width 2a = 2m, height 2b = 2m, Figure 4, total length L = L_E + L_C = 4 + 2 = 6 m, Figure 4, septum width 2w = 0.8 m, Figure 13, septum thickness t = 1 mm, Figure 11
test volume:	ℓ x h x w = 2m x 0.3 m x 0.4 m
impedance:	Z_0 = 100 Ω, eq. (3)
$f_{C(01)}$:	cut-off frequency of the first higher-order mode is 66.8 MHz, Figure 6
$f_{R(011)}$:	resonant frequency of the first higher-order mode is 76.6 MHz, eq. (1)
$f_{R(101)}$:	first interacting resonant frequency is 83.9 MHz
rise time:	TEM cell, t_r = 1.5 ns, Figure 33, eq. (16) test volume, t_r = 0.4 ns, Figure 34, eq. (18)

2.0 GENERATOR

capacitor:	C = 2.86 nF, 6 capacitors of 1.9 nF (2 stacks of 3 parallel capacitors in series), Figure 35. Advise: order 6 x 2 nF (e.g. TDK UHV-9A, App. B)
charging time:	t = 4.5 τ = 1 sec, 99% of the output HVPS
time constant:	τ = RC = 0.22 sec
charging resistor:	R = 78 MΩ, 5 mA charge current, section 4.2
maximum PRR:	1 pulse per second
spark gap:	electrode distance d = 0 to 1 cm, Figure 38
gas type:	dry synthetic air, Table 8
gas pressure:	0 - 1 to 2 atm. pressure, ref [9, p.20] 1 atm = 14.7 psig
τ_I:	inductive time constant is 0.1 ns, eq. (20)
τ_R:	resistive phase time constant is 1.74 ns, eq. (21)
τ_{eff}:	effective time constant is 1.81 ns, eq. (23)
rise time:	total rise time generator t_r = 3.98 ns (@ 1 atm.)
output voltage:	Appr. 57 kV maximum
output control:	10% to 100% of maximum
HVPS:	voltage range 1 to 60 kV, App. A current range 1 to 5 mA, App. A
triggering:	adjustable with gas pressure

3.0 TERMINATION

resistor:	R = 100 Ω, low inductive, Figure 41
voltage divider:	1 to 50, Figure 42

TABLE 10 Specifications for the 100 Ω TEM Cell EMP Simulator (con't)

4.0 OVERALL CHARACTERISTICS

field strength:	E_{pk} = 6 to appr. 57 kV/m
pulse shape:	double exponential, Figure 14
rise time:	$t_r \leq 5$ ns, (10%-90%), 4ns in test volume
half width time:	t_h = 200 ns (50%-50%)
fall time:	t_f = 660 ns (100%-10%)
field distribution:	± 2.5 dB E-field gradient, Figure 20
pre pulse:	≤ 1% of E_{pk}
oscillations:	≤ 5% of momentary amplitude
polarization:	vertical
polarity:	reversible
field enhancement:	input taper, Figure 44 through 49
	termination, Figure 50 through 61

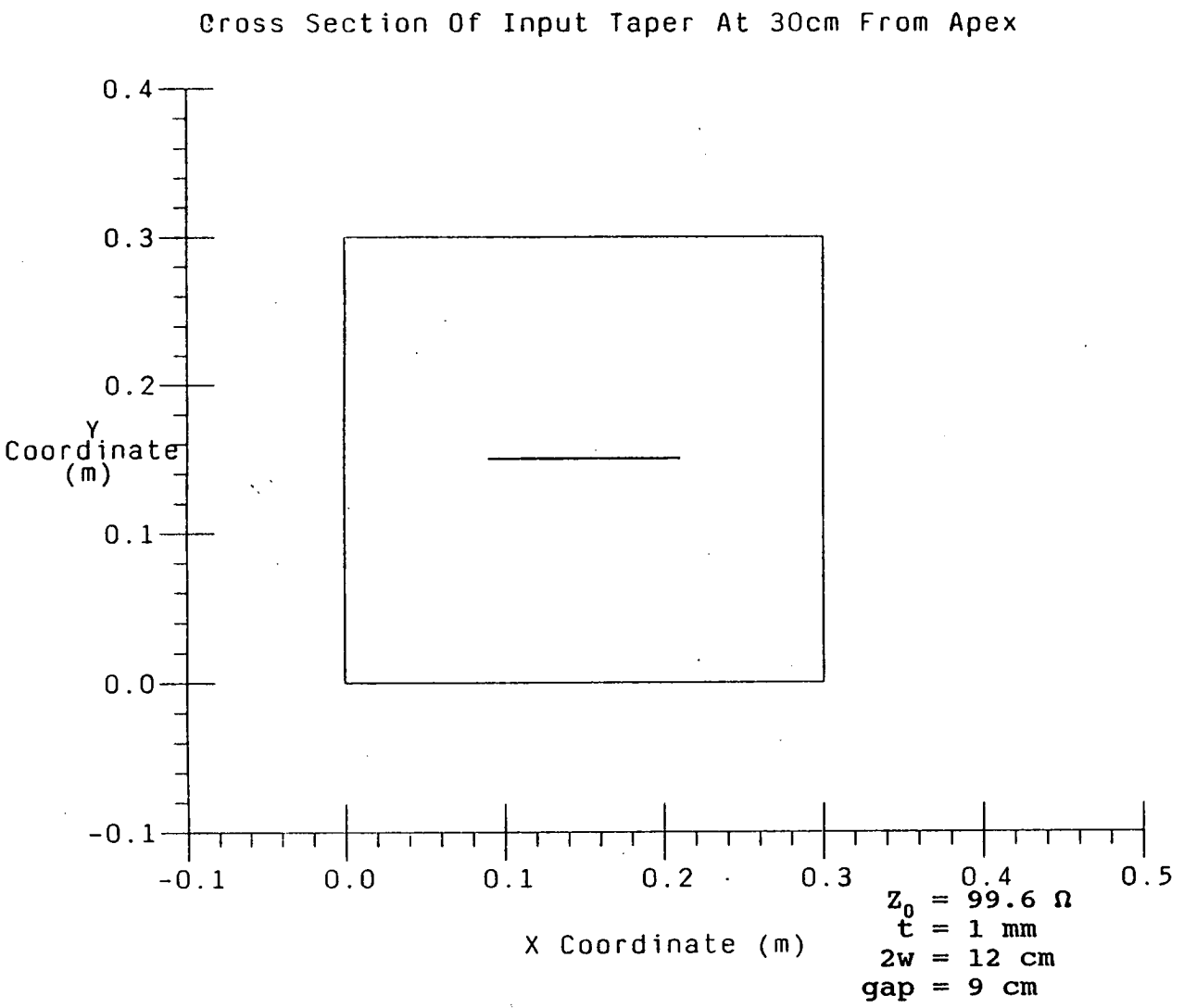

FIGURE 44 Cross-section of input taper at 30 cm from apex

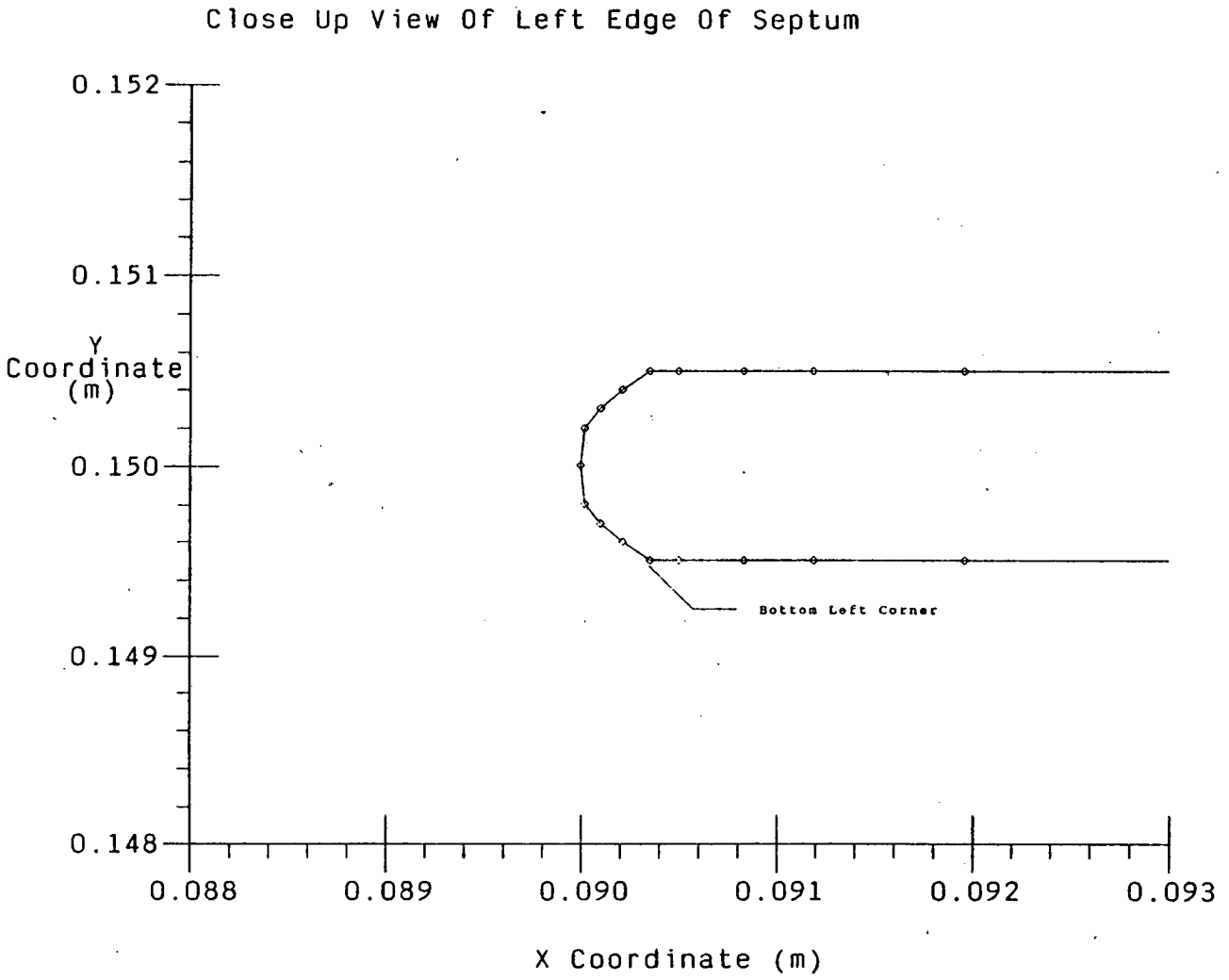

FIGURE 45 Close up view of left edge of septum

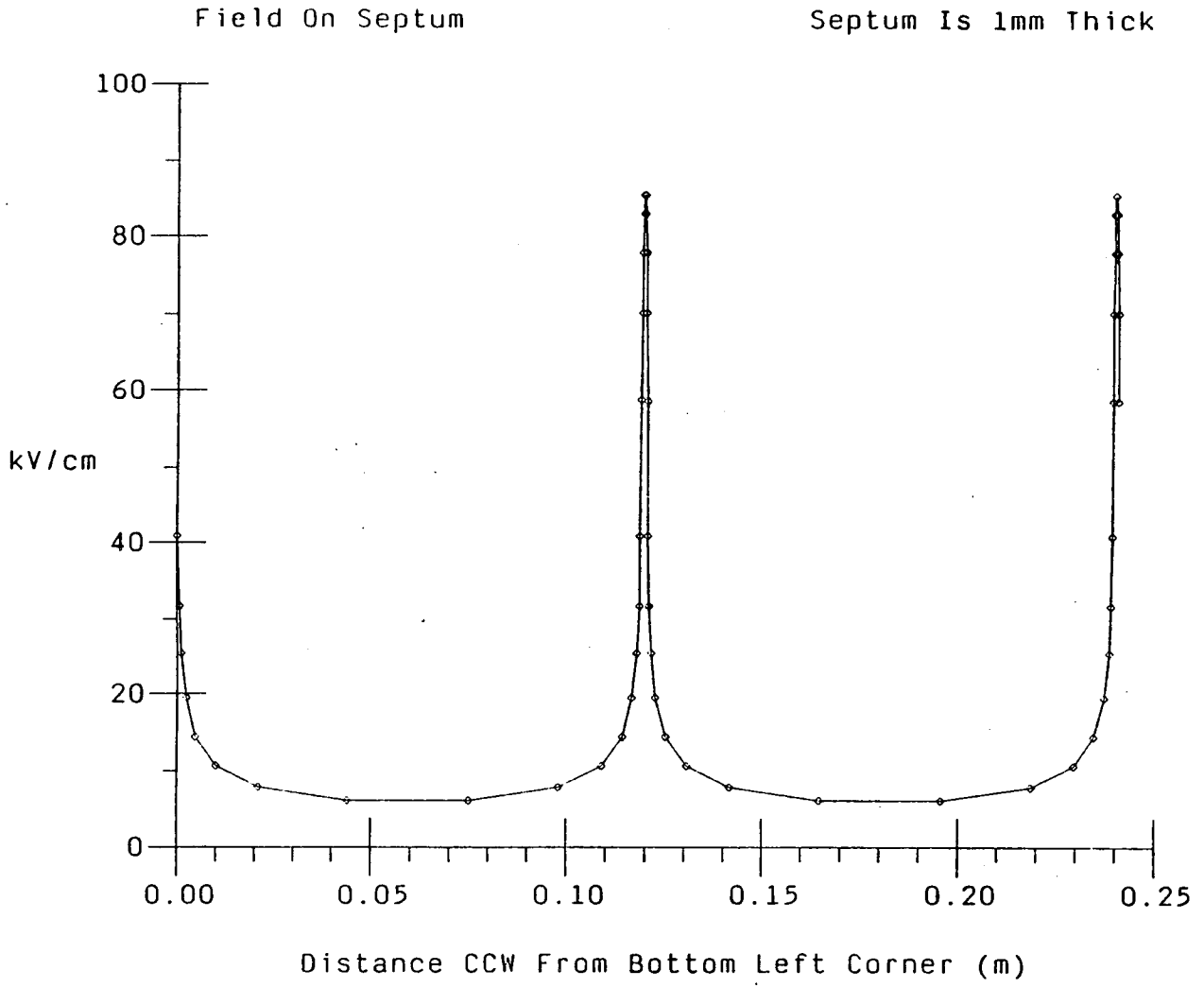

FIGURE 46 Fieldstrength on surface of septum, t = 1 mm, Z_0 = 99.6 Ω

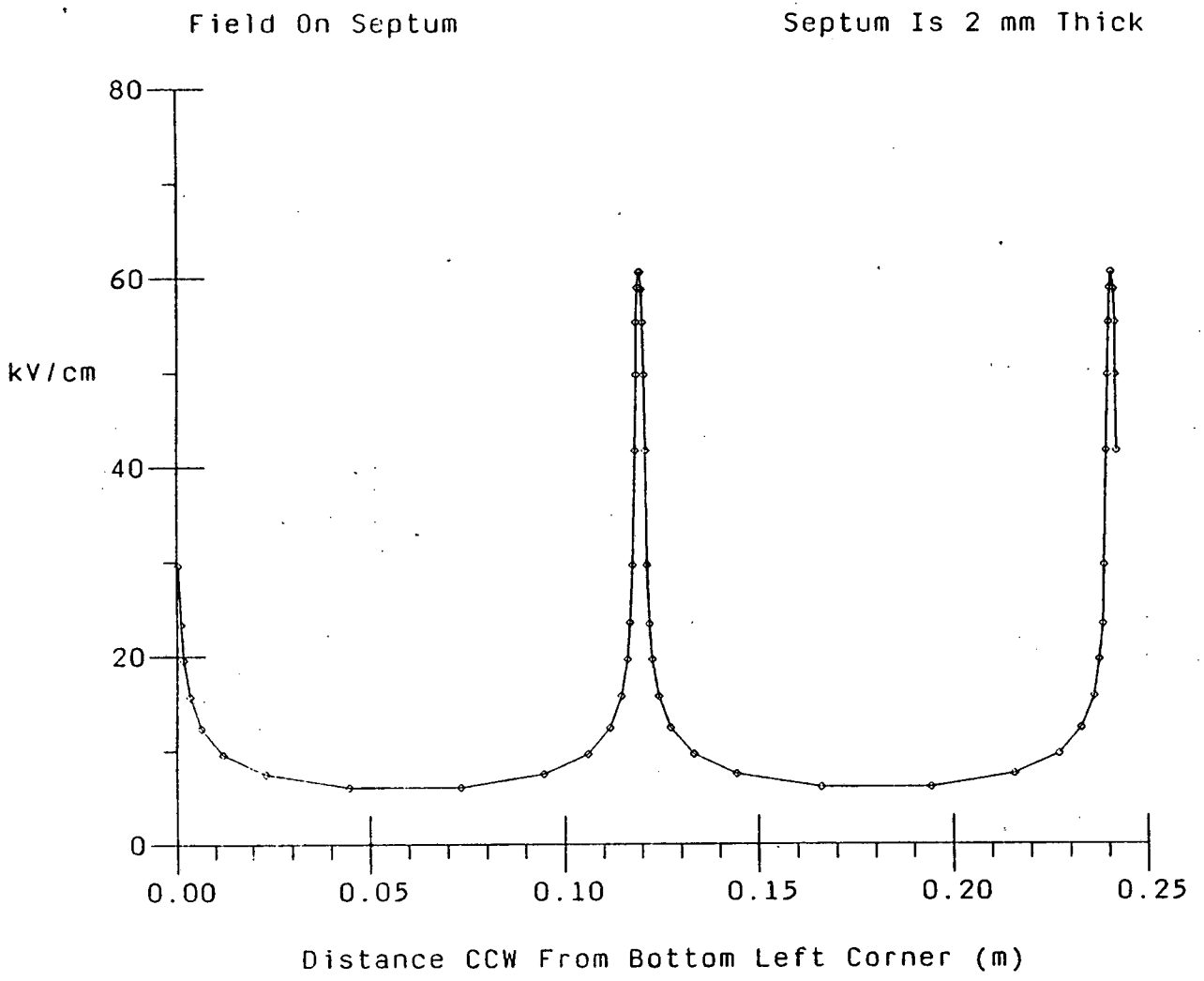

FIGURE 47 Fieldstrength on surface of septum, t = 2 mm, Z_0 = 98.1 Ω

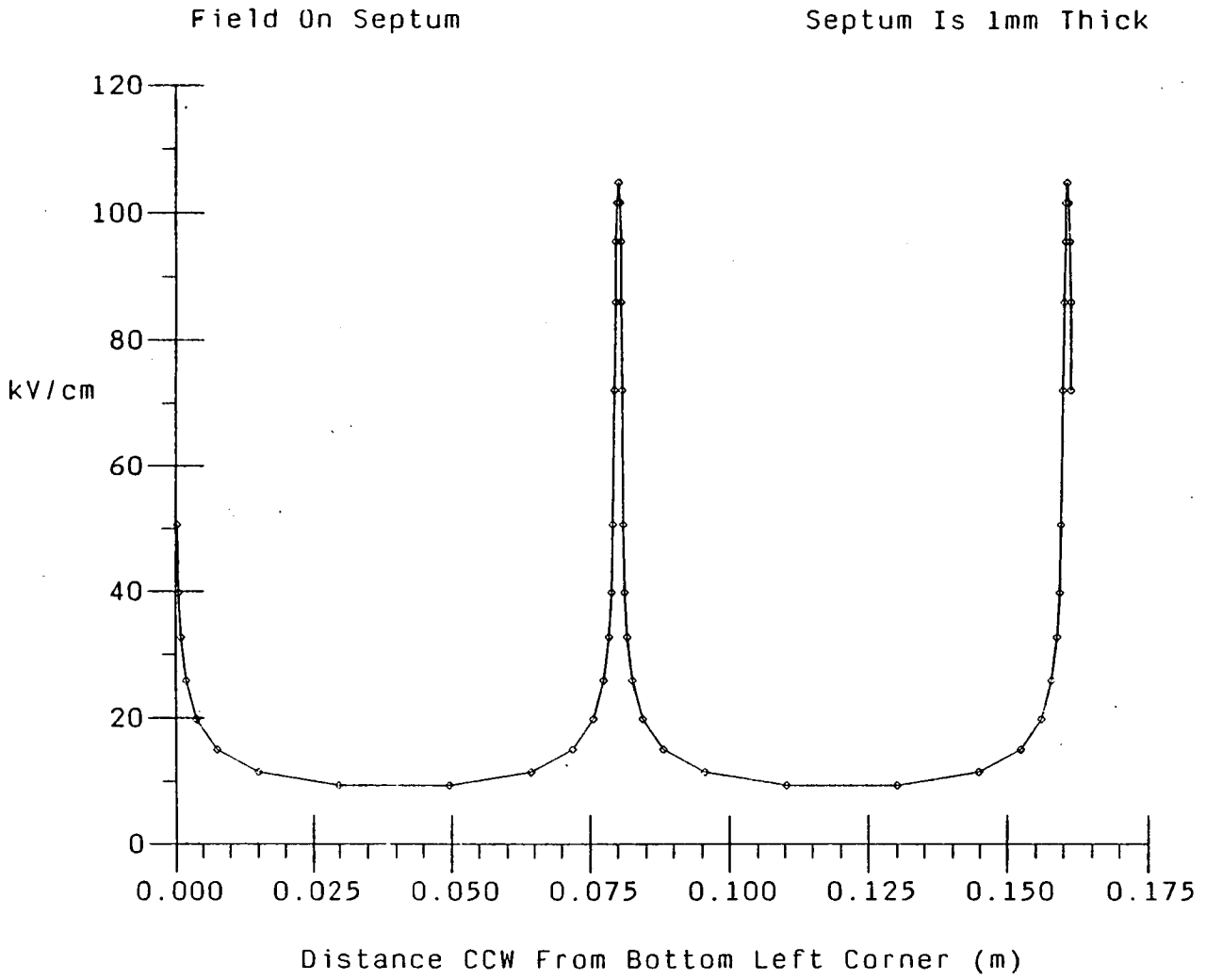

FIGURE 48 Fieldstrength on surface of septum at 20 cm from apex, t = 1 mm, Z_0 = 99.1 Ω

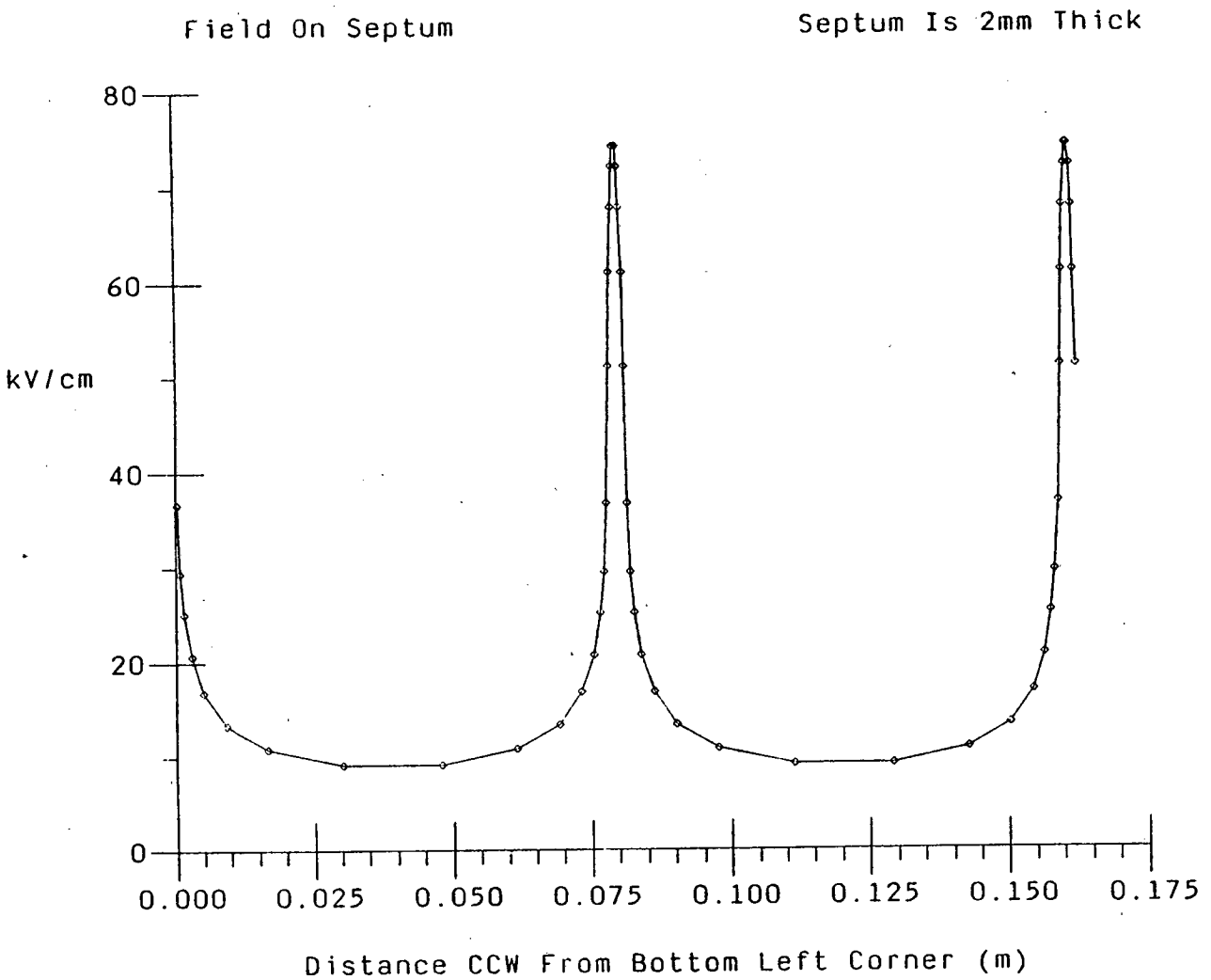

FIGURE 49 Fieldstrength on surface of septum at 20 cm from apex, t = 2 mm, Z_0 = 97.8 Ω

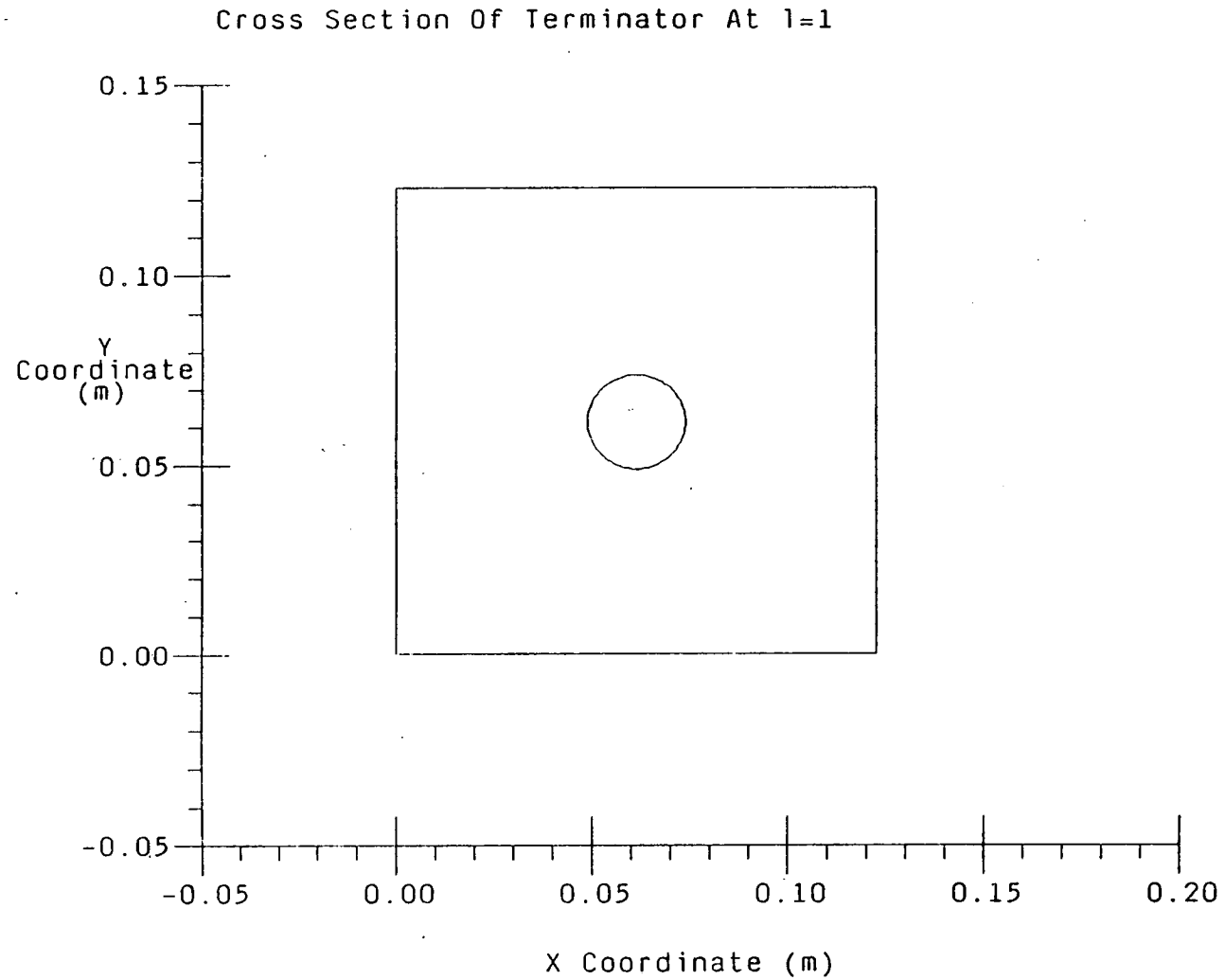

FIGURE 50 Cross-section of termination at l = 1, Figure 41

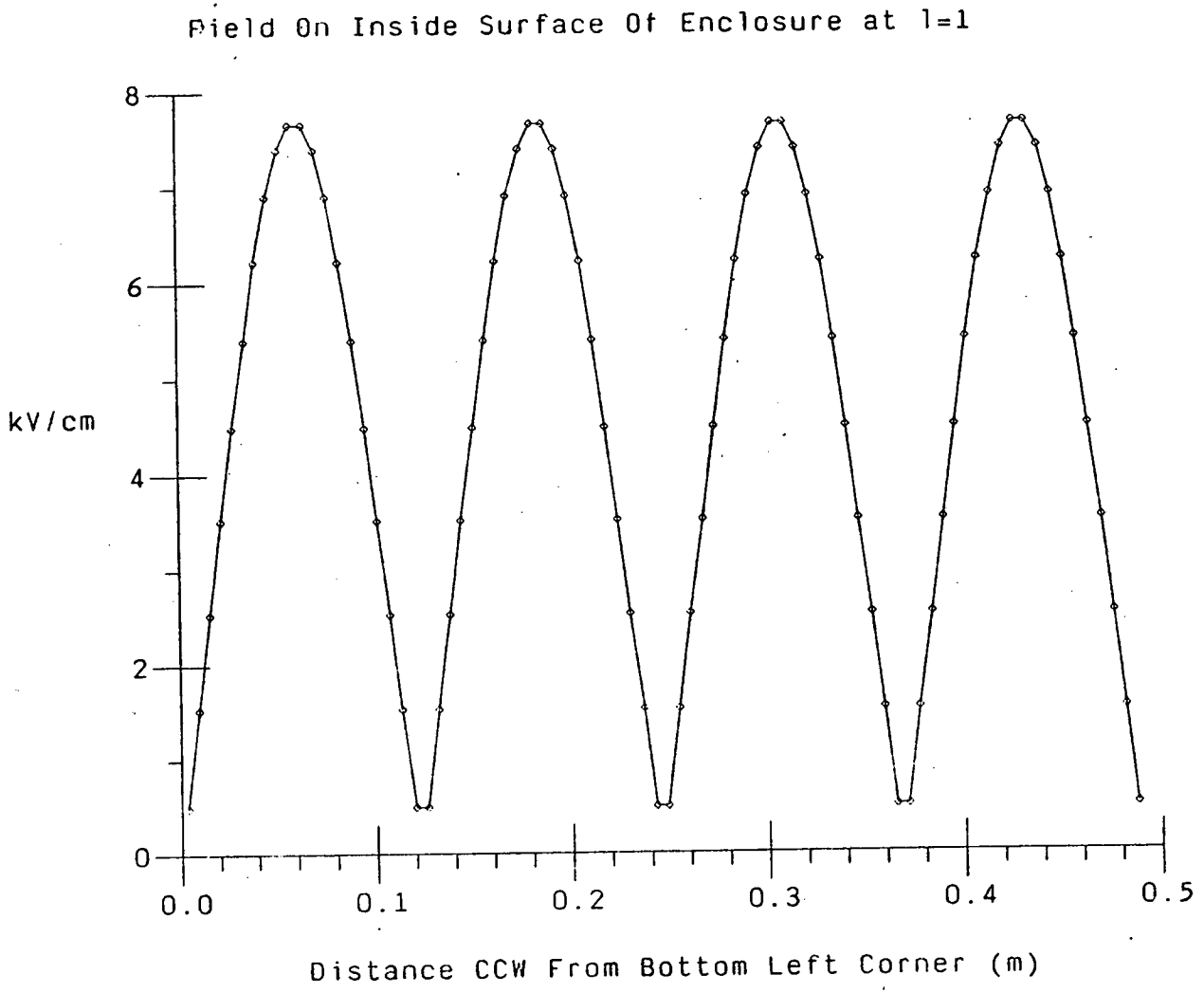

FIGURE 51 Fieldstrength on inside surface of enclosure at l = 1

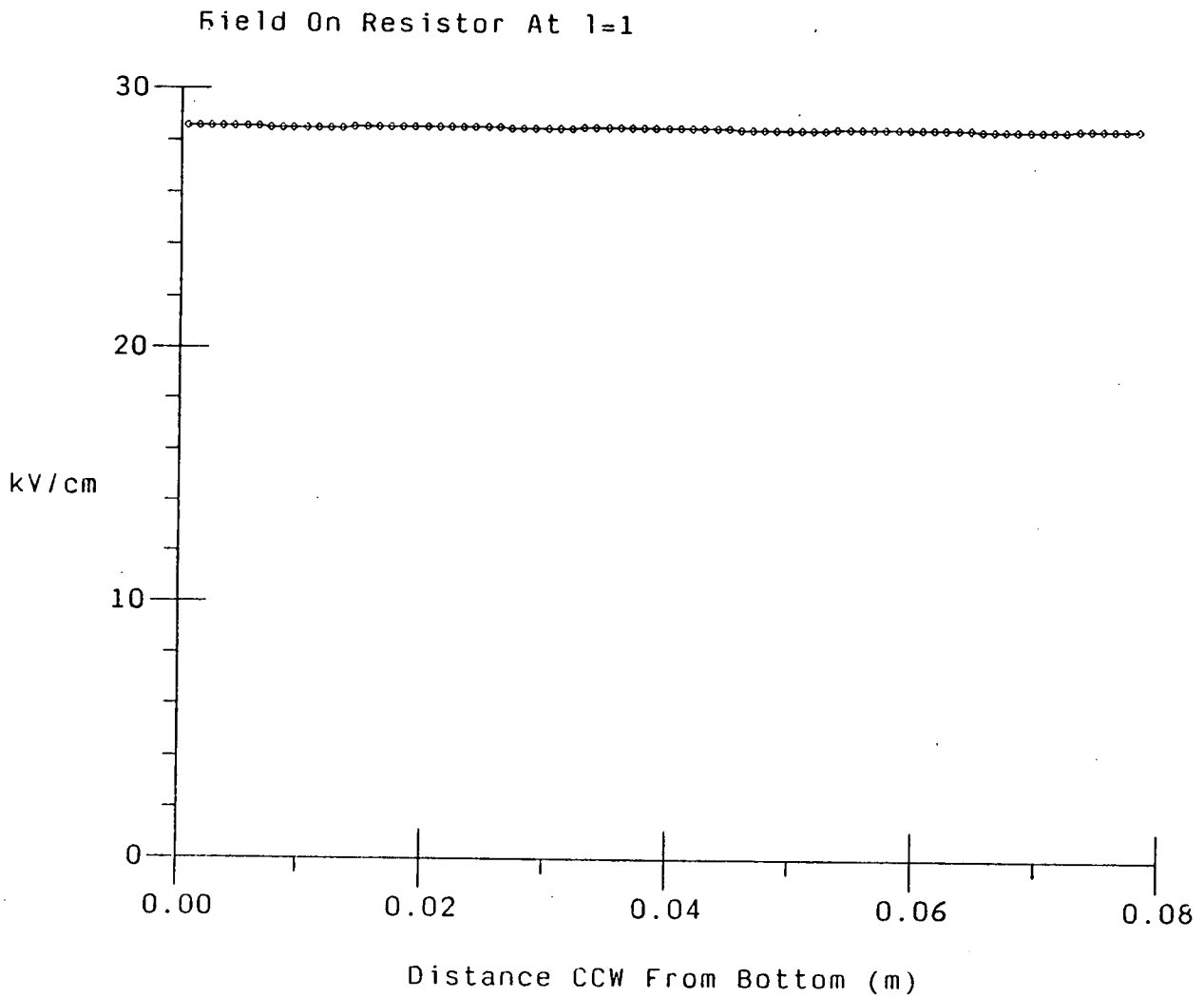

FIGURE 52 Fieldstrength on surface of resistor at l = 1

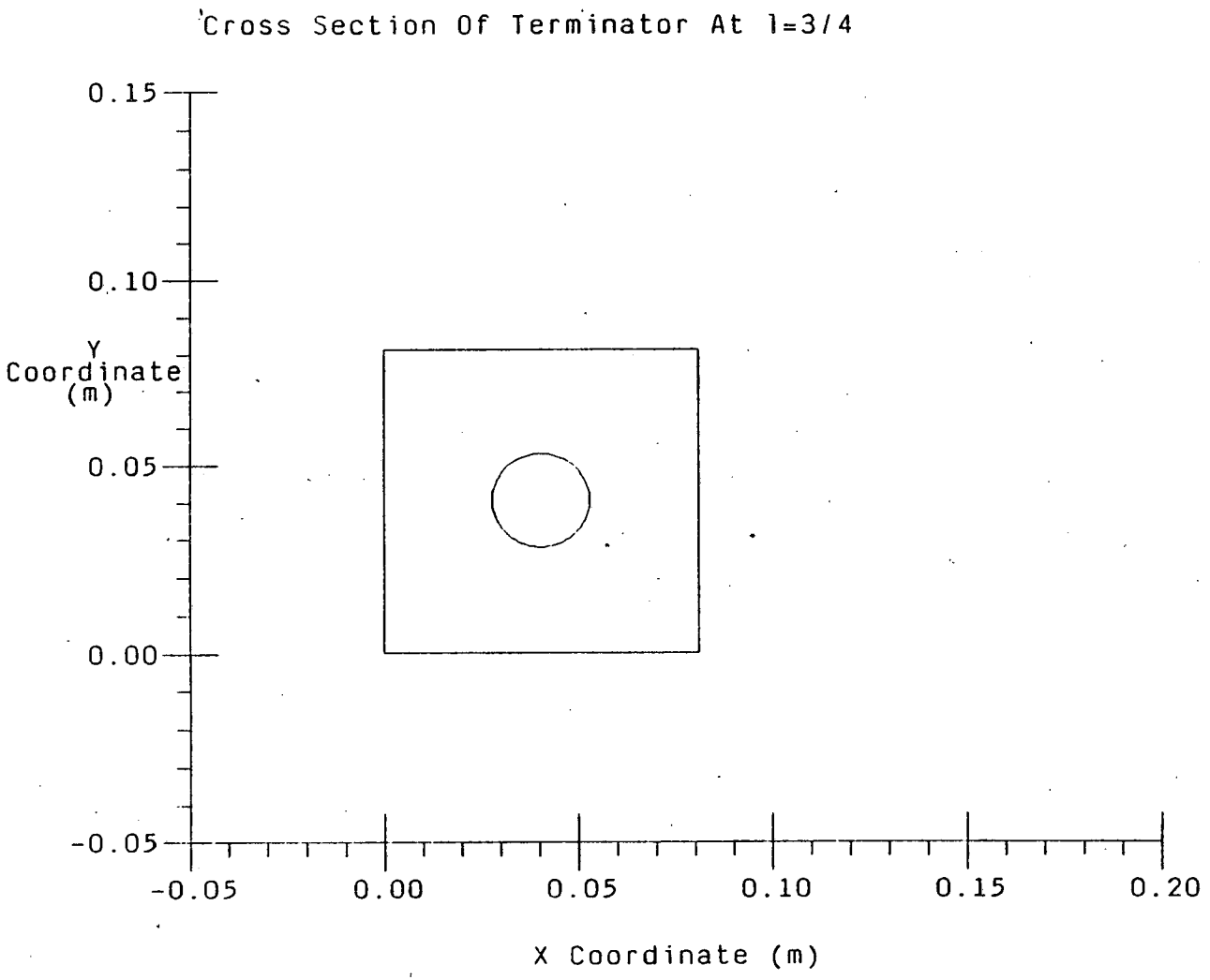

FIGURE 53 Cross-section of termination at l = 3/4, Figure 41

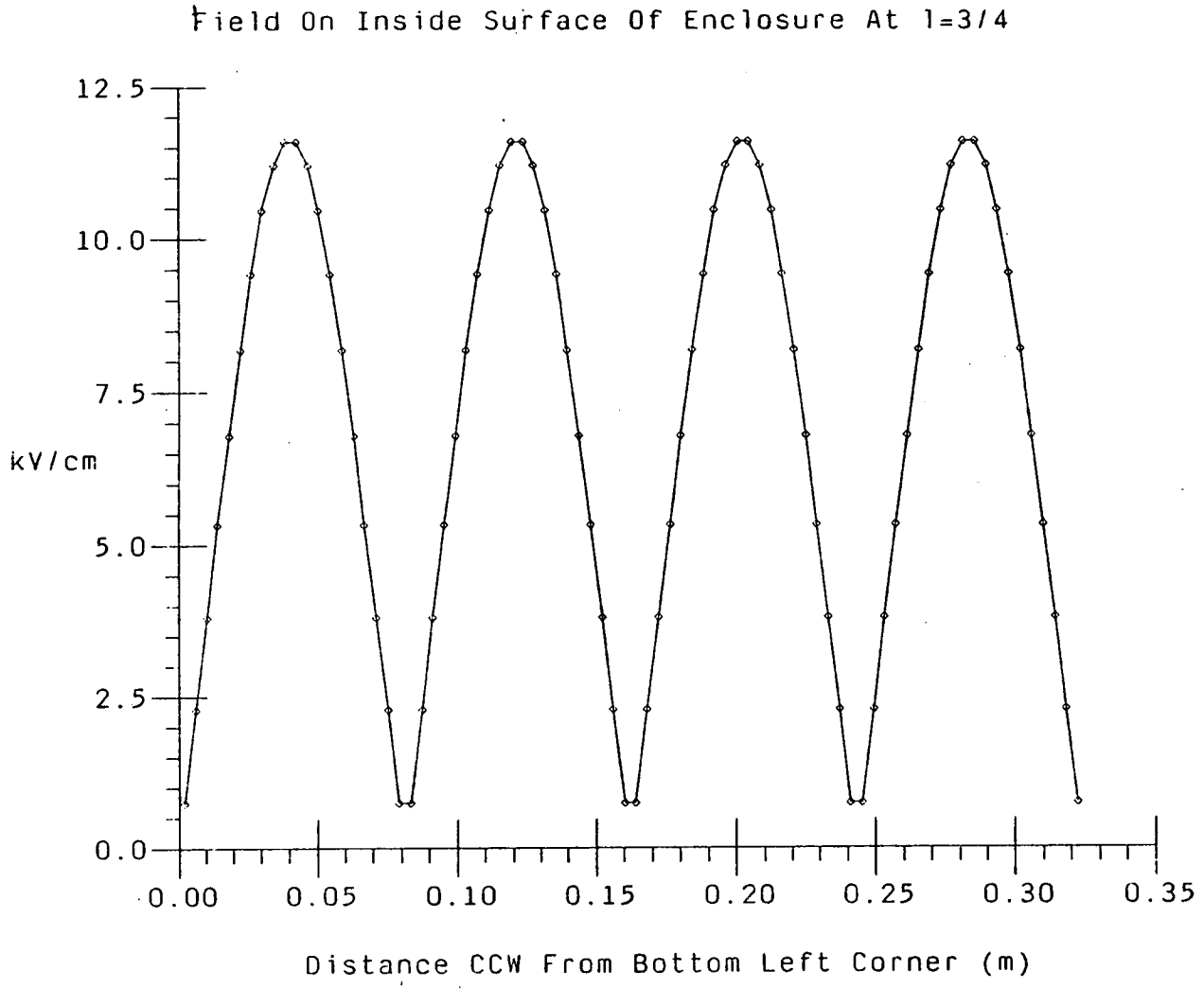

FIGURE 54 Fieldstrength on inside surface of enclosure at l = 3/4

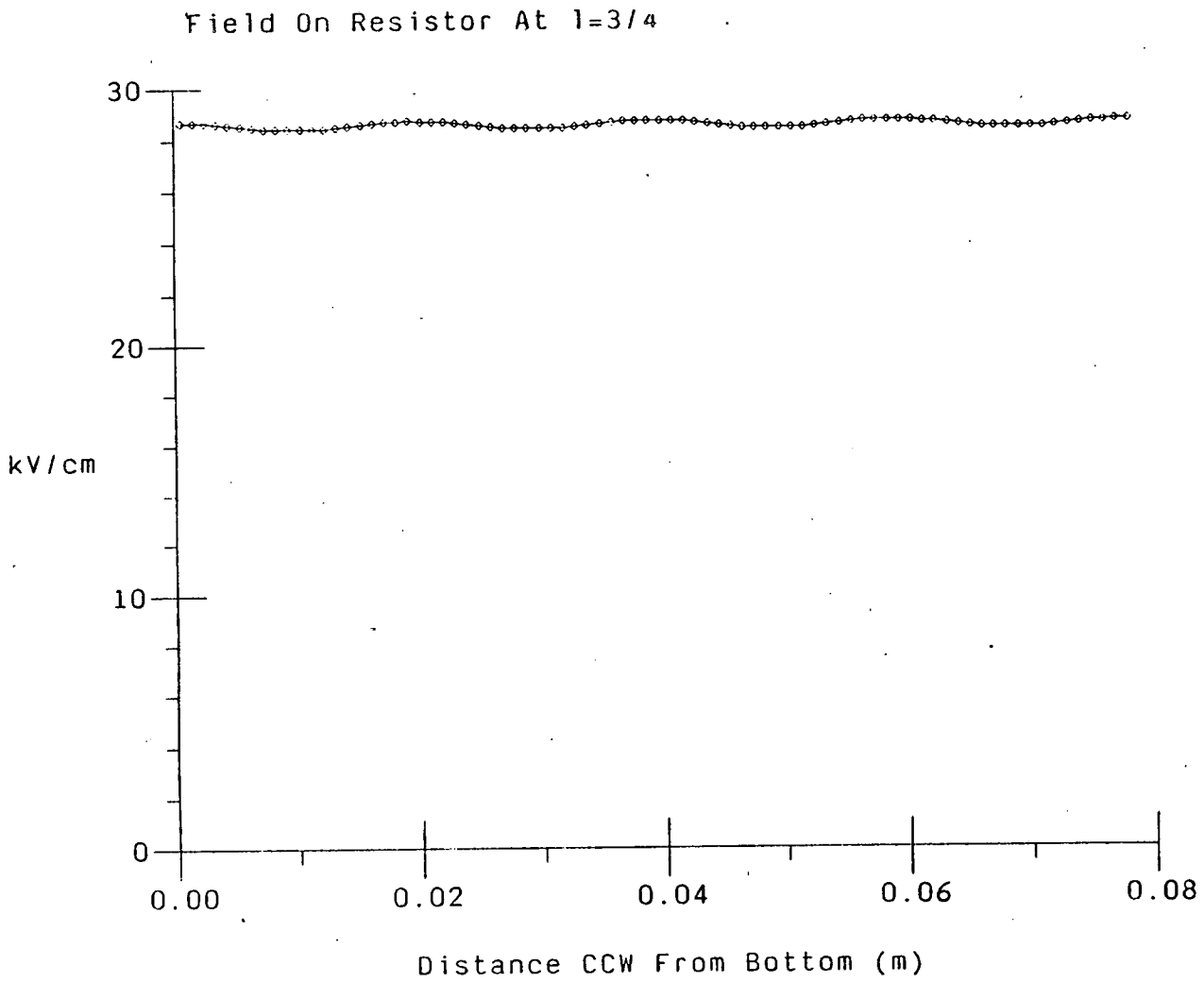

FIGURE 55 Fieldstrength on surface of resistor at l = 3/4

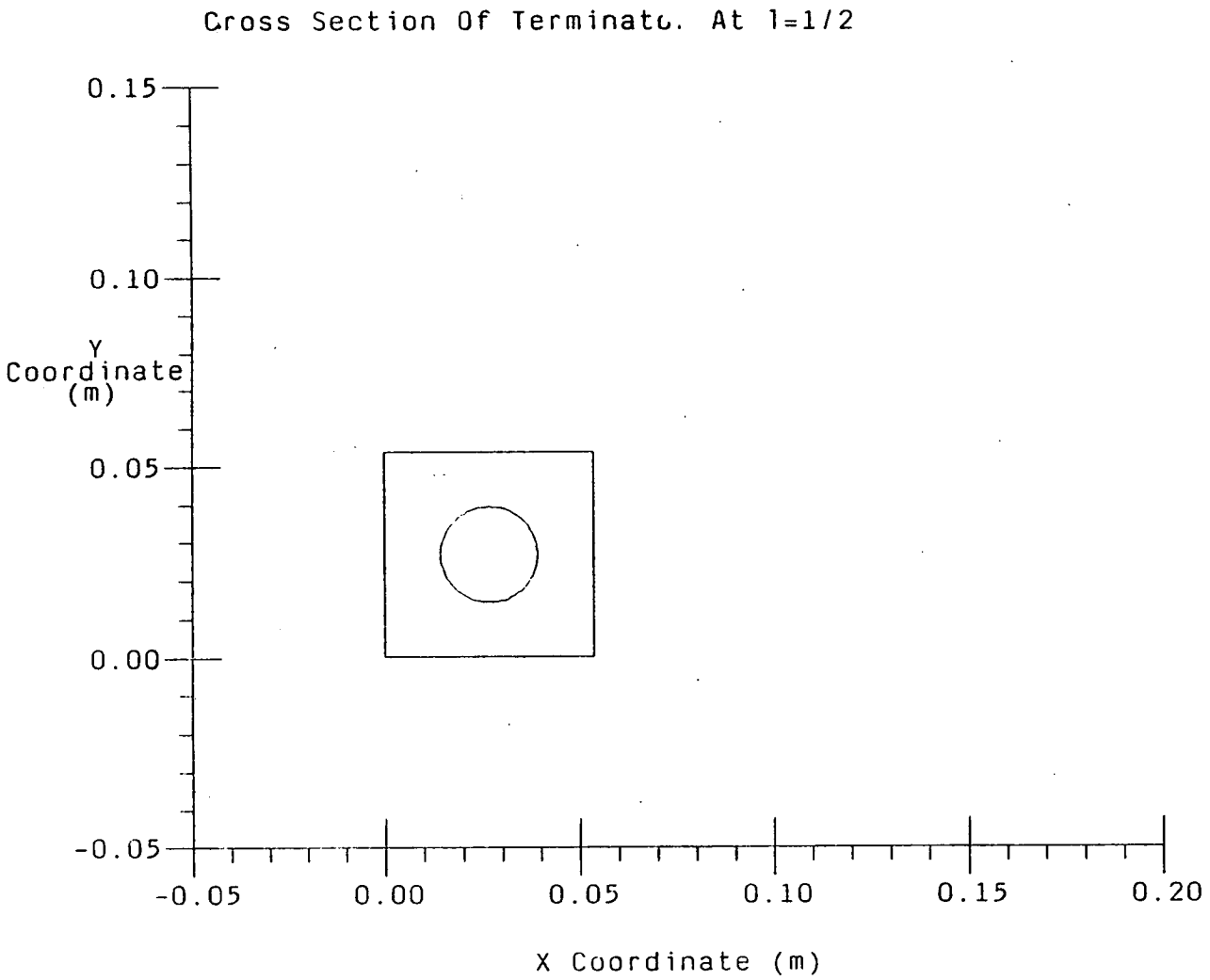

FIGURE 56 Cross-section of terminator at l = ½, Figure 41

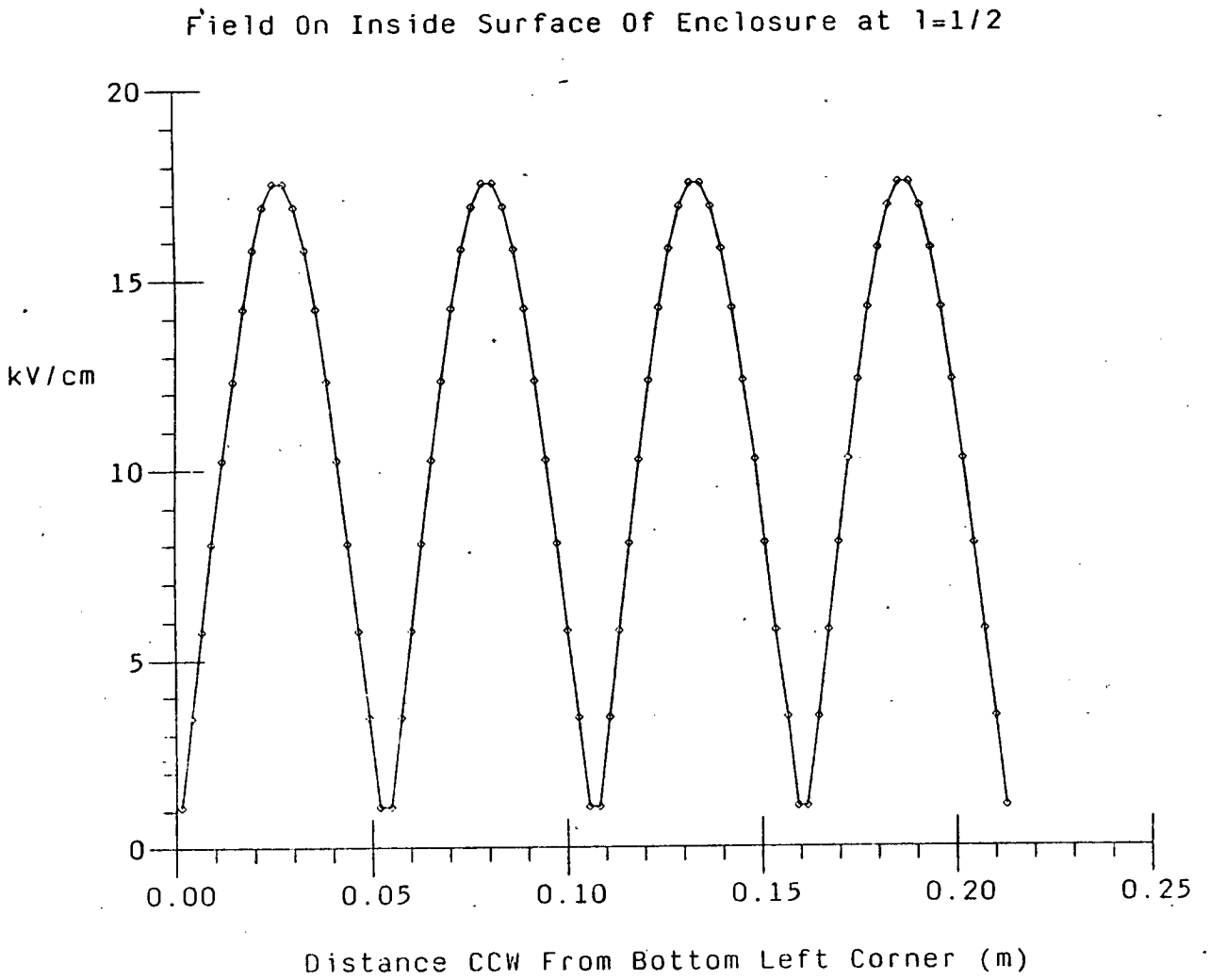

FIGURE 57 Fieldstrength on inside of enclosure at l = ½

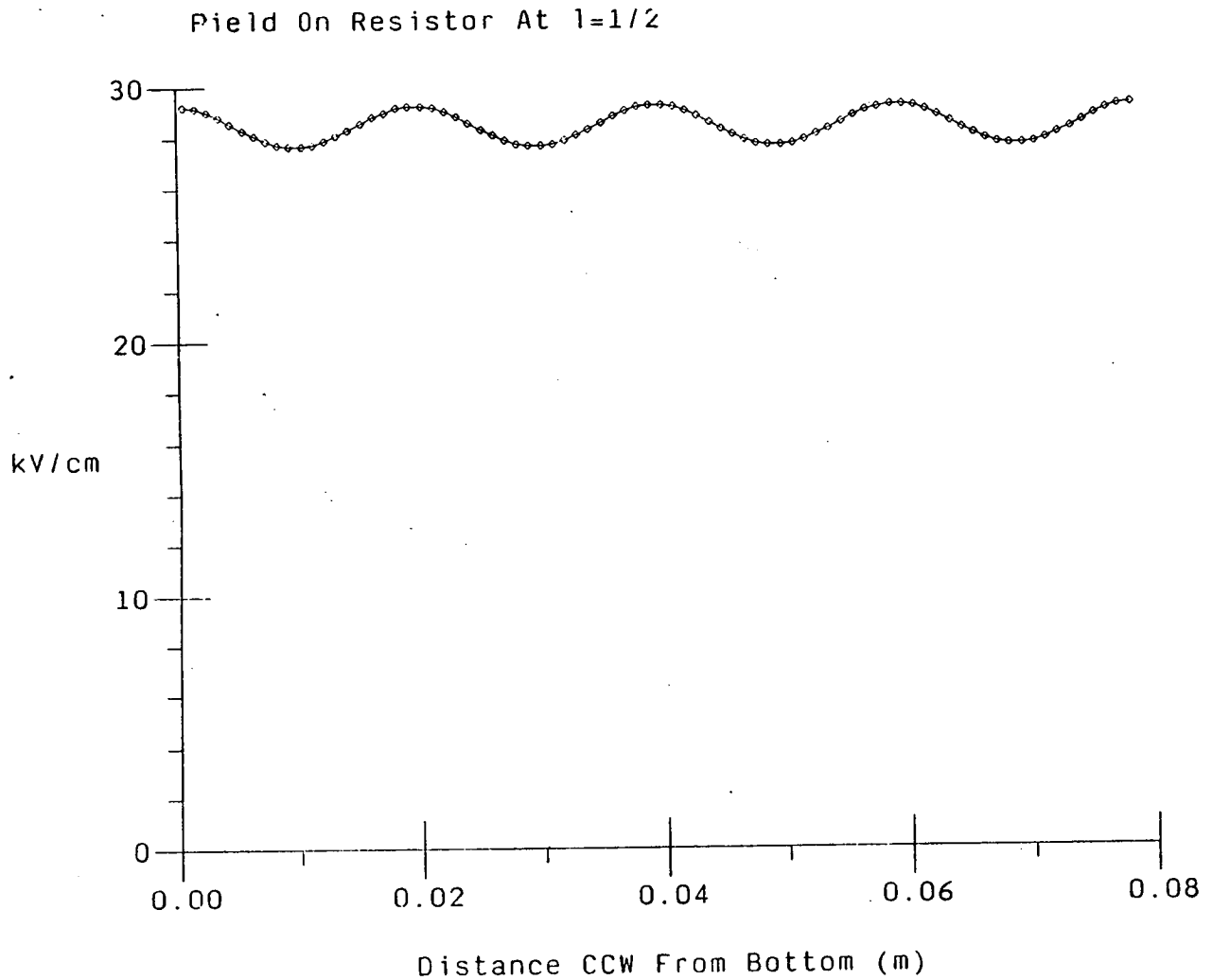

FIGURE 58 Fieldstrength on surface of resistor at l = ½

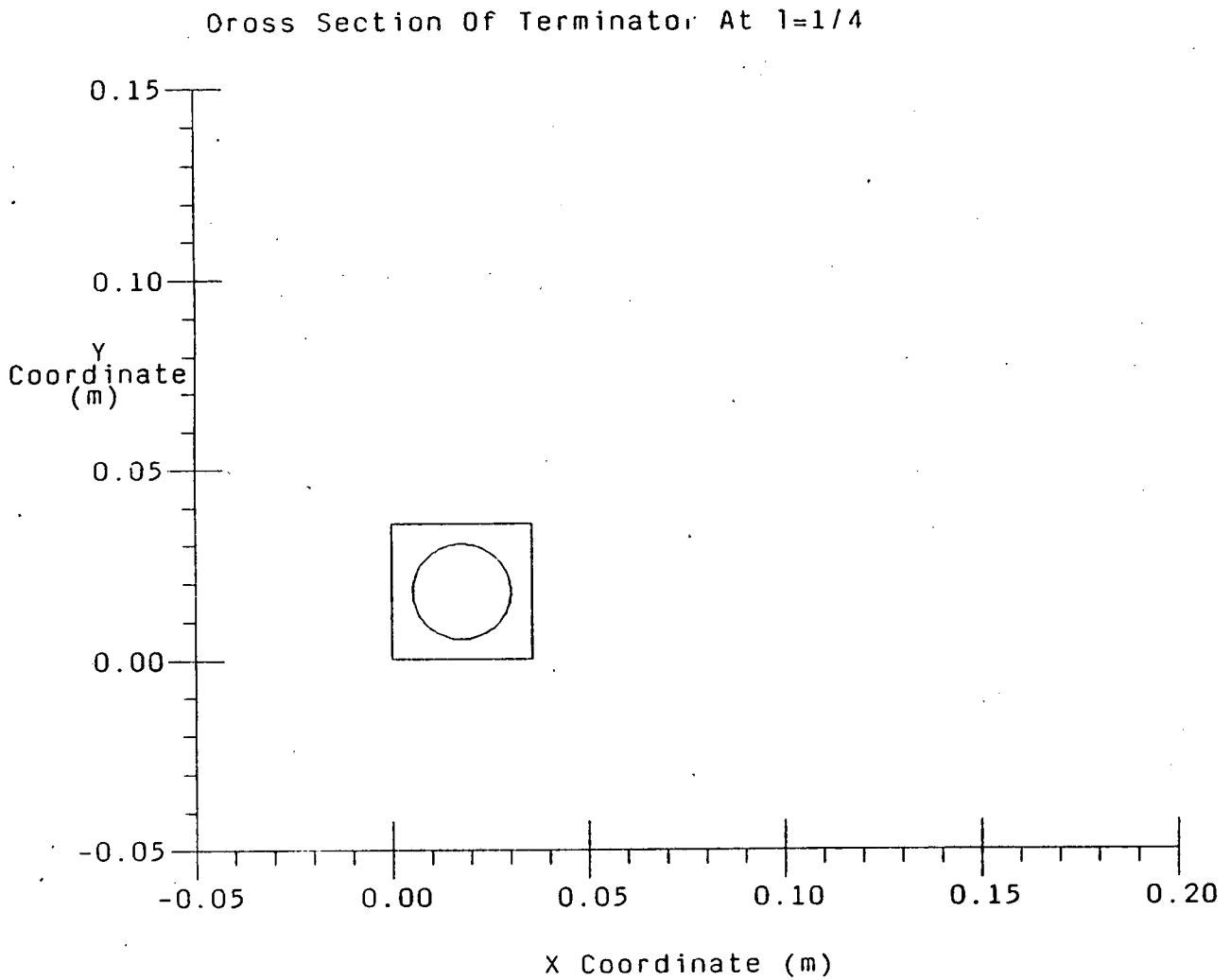

FIGURE 59 Cross-section of terminator at l = ¼, Figure 41

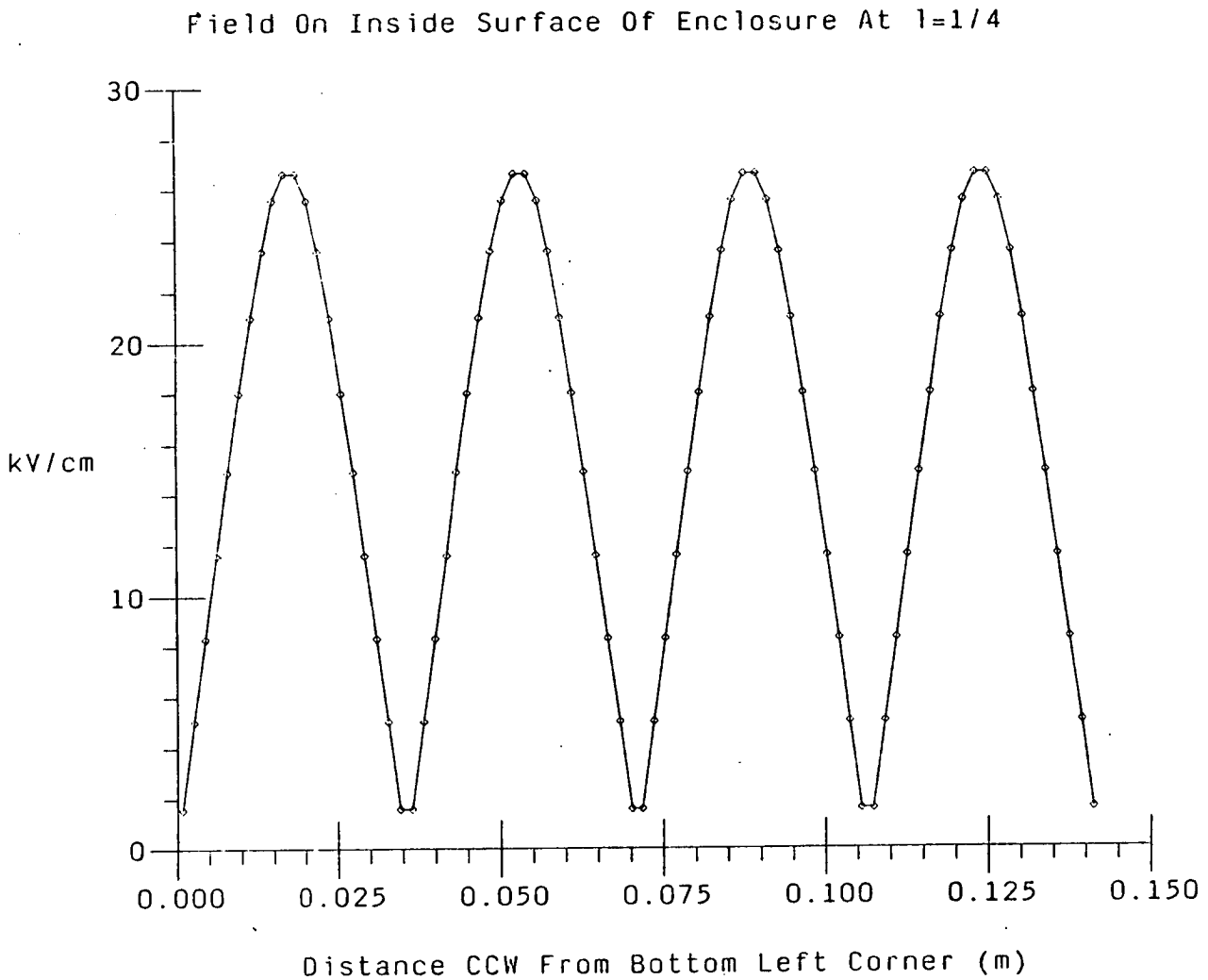

FIGURE 60 Fieldstrength on inside surface of enclosure at l = ¼

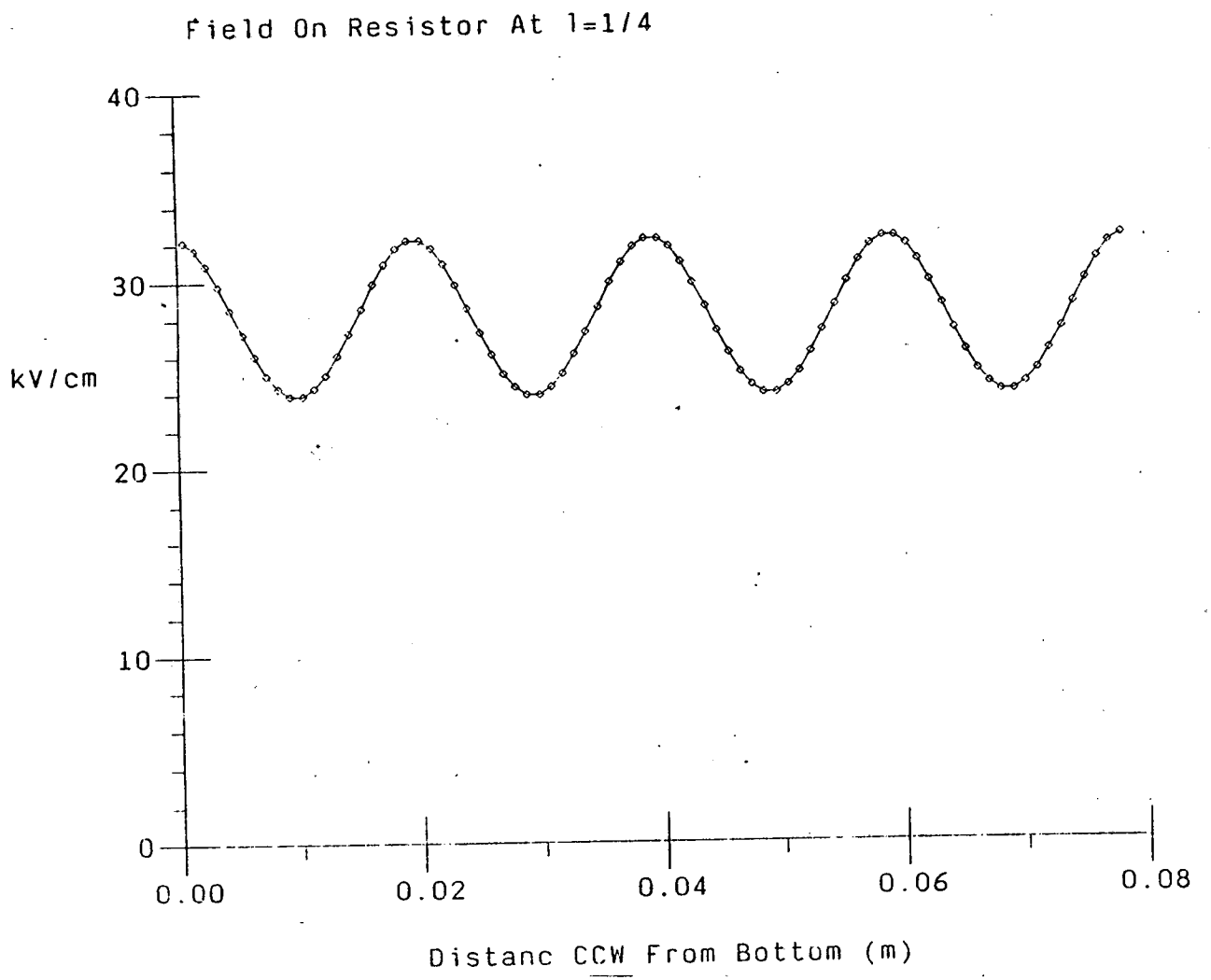

FIGURE 61 Fieldstrength on surface of resistor at l = ¼

10.0 REFERENCES

[1] Hill, D.A. Bandwidth Limitations of TEM Cells due to Resonances. J. Microwave Power 18(2):181-195; 1983.

[2] Wilson, P.F., Ma, M.T. Simple Approximate Expressions for Higher Order Mode Cut-Off and Resonant Frequencies in TEM Cells. IEEE Trans. EMC, EMC-28(3): 125-130; August 1986.

[3] Kanda, M., Electromagnetic Field Distortion due to a Conducting Rectangular Cylinder in a Transverse Electromagnetic Cell. IEEE Trans. EMC-24(3): 294-301; 1982

[4] Weil, C.M.; et al. Frequency Range of Large-Scale TEM Mode Rectangular Strip Lines. Microwave Journal: 93-100; November 1981.

[5] Tippet, J.C. and Chang, D.C., Radiation Characteristics of Dipole Sources (Located Inside a Rectangular Coaxial Transmission Line), NBSIR 75-829, January 1976.

[6] Crawford, M.L. Workman, J.L., Using a TEM Cell for EMC Measurements of Electronic Equipment. NBS Technical Note 1013, Revised July 1981.

[7] Weil, C., Gruner, L., Higher-order Mode Cutoff in Rectangular Striplines. IEEE Trans. Microwave Theory Tech. MTT-32(6): 638-641; June 1984.

[8] Baum, C., Private Communications. December 1977.

[9] Sevat, P.A.A., Design of a Bounded Wave EMP Simulator, (Intended as a second stage simulator for DREO), DREO report 1006, June 1989, Ottawa.

[10] Donaldson, E.E., et al. Field Measurements made in an Enclosure. Proc. IEEE 66(4): 464-472; April 1978.

[11] Tippet, J.C. Model Characteristics of Rectangular Coaxial Transmission Line. Doctorial Thesis Submitted to Faculty of Graduate School, University of Colo, 1978.

[12] Willis, W.L. High Voltage/Pulse Power Technology, Lecture 6, Figure 5. Los Alamos Scientific Laboratory Training Course, LA-UR-80-2082.

[13] Whitson, A.L.,Engineering Techniques for Electromagnetic Pulse Hardness testing. SRI, DNA 3332 F, September 1974.

[14] Sevat, P.A.A., A 600 kV Pulser for the 10 m Transmission Line EMP Simulator of DREO, DREO Report March 1989

[15] Saad, S., et al, Microwave Engineers' Handbook. Volume 1, Artech House Inc.

[16] Willis, W.L. High Voltage/Pulse Power Technology, Lecture 6, Page 24. Los Alamos Scientific Laboratory Training Course, LA-UR-80-2082.

[17] Ramo, S., et al, Fields and Waves in Communication Electronics, John Wiley and Sons, Inc., 1984.

[18] Moreno, T.A.M., Microwave Transmission Design Data, McGraw-Hill, Inc., 1989.

[19] Weil, C.M., The Characteristic Impedance of Rectangular Transmission Lines with Thin Center Conductor and Air Dielectric, IEEE Trans. on MTT, Vol. MTT-26, No. 4, April 1978, pp 238-242.

ER Series 300 Watt Regulated High Voltage DC Power Supplies

Laboratory Performance...

High Power Density...

Enhanced Features

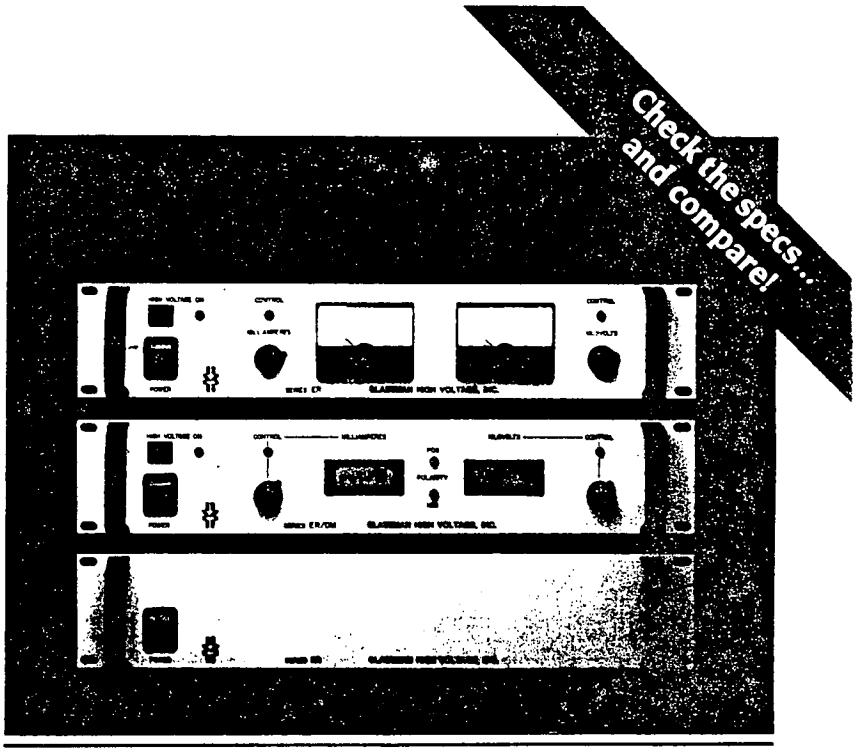

Models from 0 to 2 KV through 0 to 75 KV; 3.5 inch panel height.

The ER Series...the most sophisticated, medium power, high voltage power supply available today. The "designed in" versatility of this standard product line finds itself at home in most applications/environments. With three control panel configurations...analog, digital or blank...and a full complement of standard remote controls, you might think high price. Not in Glassman's case, just high quality.

Features

Air Insulated. As in all standard Glassman power supplies, the ER Series features "air" as the primary dielectric medium. No oil or encapsulation to impede serviceability.

Constant Voltage/Constant Current Operation. Automatic crossover from voltage or current regulated mode dependent on the load conditions.

Low Ripple. Better than 0.03% of rated voltage at full load.

Tight Regulation. Voltage regulation better than 0.005% line or load; current regulation better than 0.05% from short circuit to rated voltage.

Fast Transient Response. Less than 3 milliseconds for a 50% load transient.

Front Panel Controls (Analog and Digital Versions). Ten-turn voltage and current controls with locking vernier dials, AC power ON/OFF and high voltage enable switches.

Remote Control Facilities. As standard, all ER Series power supplies provide output voltage and current program/monitor terminals, TTL high voltage enable/disable, safety interlock terminals, and a +10 volt reference source.

Small Size and Weight. ER Series power supplies consume only 3.5" of vertical panel height. Total weight is 18 pounds.

Innovations in high voltage power supply technology.

GLASSMAN HIGH VOLTAGE INC.
Route #22 East, Salem Industrial Park, P.O. Box 551, Whitehouse Station, N.J. 08889
(201) 534-9007 • TWX 710-480-2839 • FAX (201) 534-5672

Specifications

Input: 105-125 V RMS, 48-63 Hz single phase, <6 A. Connector per IEC 320/VI with mating line cord.

Efficiency: Typically 85% at full load.

Output: Continuous, stable adjustment from zero to rated voltage and current via 10-turn potentiometers, external 0 to 10 V, or external potentiometers. Linearity, ≤1% fs. Repeatability, ≤0.1% fs. Accuracy, 1% of rated + 1% of setting. Resolution is a function of programming method.

Stored Energy: 20 KV model, 1.5 joules; 60 KV model, <4 joules.

Voltage Regulation: <0.005% line and load.

Ripple: <0.03% RMS of rated voltage at full load.

Current Regulation: <0.05% from short circuit to rated voltage at any set current.

Voltage Monitor: 0 to +10 V DC for zero to rated voltage. Accuracy, 1% of reading + 1% of rated voltage.

Current Monitor: 0 to +10 V DC for zero to rated current. Accuracy, 1% of reading + .05% of rated current.

Stability: 0.01% per hour after 1/2 hour warm-up, 0.05% per 8 hours.

Output Voltage Time Constant: Typically 50 ms rise or decay time constant (300 ms for 75 KV model) using TTL (on/off) or remote voltage control with 75% resistive load.

Temperature Coefficient: 0.01%/°C.

Ambient Temperature: -20 to +40°C operating, -40 to + 85°C storage.

Polarity: Positive, negative, or reversible with respect to chassis ground.

Protection: Automatic current regulation protects against all overloads, including arcs and short circuits. Fuses, surge-limiting resistors, and low-energy components provide ultimate protection.

Accessories: Detachable 8-foot shielded HV Coaxial cable (see Model Chart for wire type) and 6-foot detachable line cord provided.

Remote controls: Common, +10 V reference, interlock, current monitor, current program, voltage monitor, voltage program, TTL, and ground.

External Interlock: Open off, closed on.

TTL Enable/Disable: OV off, 5-15 V on.

Warranty

Glassman High Voltage, Inc. warrants standard power supplies to be free from defect in materials and workmanship for three years from date of shipment. OEM and modified standard power supplies are warranted for one year from date of shipment. The company agrees to replace or repair any power supply that fails to perform as specified within the warranty period. Formal warranty available.

Options:

Symbol	Description
100	100 V input, rated 90-110 V RMS, 48-63 Hz.
220	220 V input, rated 200-264 V RMS, 48-63 Hz.
400	48-420 Hz, available on standard model and options 100 and 220.
DM	3-1/2 digit LCD panel meters
NC	Blank front panel (power switch only)
CT	Current trip. Power supply trips off under overload conditions.
ZR	Zero start interlock. Voltage control must be at zero before accepting an enable signal.
SS	Slow start ramp of up to 30 seconds available. Specify time.

Models

Positive Polarity	Negative Polarity	Reversible Polarity	Output Voltage (kV)	Output Current (mA)	Output Cable Provided
Reversible Polarity Only		ER2R150 ER3R100 ER5R60	0-2 0-3 0-5	0-150 0-100 0-60	RG-59 RG-59 RG-59
ER10P30 ER15P20	ER10N30 ER15N20	ER10R30 ER15R20	0-10 0-15	0-30 0-20	RG-8U RG-8U
ER20P15 ER30P10	ER20N15 ER30N10	ER20R15 ER30R10	0-20 0-30	0-15 0-10	RG-8U RG-8U
ER40P7.5 ER50P6	ER40N7.5 ER50N6	ER40R7.5 ER50R6	0-40 0-50	0-7.5 0-6	RG-8U RG-8U
ER60P5 ER75P3	ER60N5 ER75N3	ER60R5 ER75R3	0-60 0-75	0-5 0-3	RG-8U DS2124

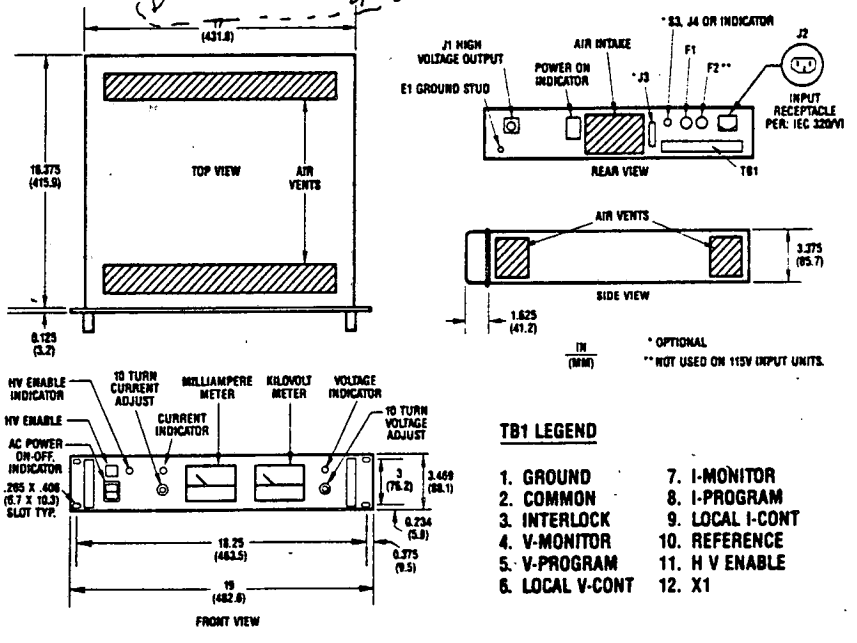

TB1 LEGEND

1. GROUND	7. I-MONITOR
2. COMMON	8. I-PROGRAM
3. INTERLOCK	9. LOCAL I-CONT
4. V-MONITOR	10. REFERENCE
5. V-PROGRAM	11. H V ENABLE
6. LOCAL V-CONT	12. X1

* OPTIONAL
** NOT USED ON 115V INPUT UNITS.

Innovations in high voltage power supply technology.

GLASSMAN HIGH VOLTAGE INC.
Route #22 East, Salem Industrial Park, P.O. Box 551, Whitehouse Station, N.J. 08889
(201) 534-9007 • TWX 710-480-2839 • FAX (201) 534-5672

TDK

TDK HIGH VOLTAGE CERAMIC CAPACITORS

Type UHV: 20kVdc to 50kVdc
Type FD: 5kVac to 10kVac

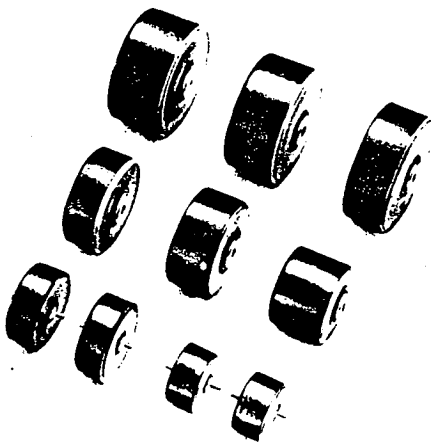

HIGH VOLTAGE CERAMIC CAPACITORS
Type UHV: 20kVdc to 50kVdc

TDK UHV type high voltage ceramic capacitors feature low dissipation and excellent voltage—capacitance characteristics using patented strontium titanate for dielectric material. They are epoxy-encapsulated to meet requirement of high voltage applications.

FEATURES

- Low dissipation factor.
- Excellent voltage-capacitance characteristics.
- Small size.
- Screw terminals for easy mounting.

APPLICATIONS

High voltage power supplies, laser equipment.

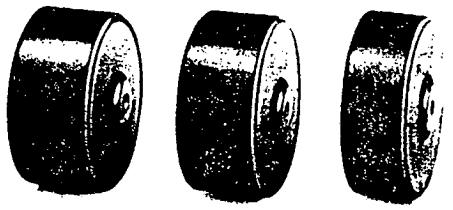

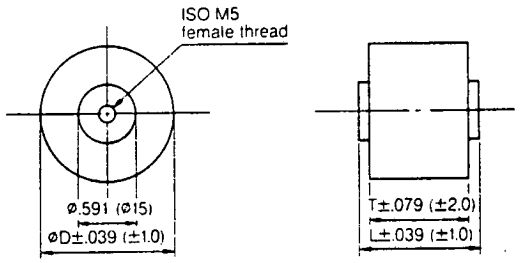

Dimensions in inches (mm)

Fig. 1

SPECIFICATIONS

Rated voltage (kVdc)	Part No.	Rated capacitance (pF) ±10%	Dimensions in inches (mm)		
			øD	T	L
20	**UHV-1A**	1400	1.50 (38)	.748 (19)	.906 (23)
	UHV-2A	2500	1.89 (48)	.748 (19)	.906 (23)
	UHV-3A	4000	2.36 (60)	.748 (19)	.906 (23)
30	**UHV-4A**	940	1.50 (38)	.866 (22)	1.02 (26)
	UHV-5A	1700	1.89 (48)	.866 (22)	1.02 (26)
	UHV-6A	2700	2.36 (60)	.866 (22)	1.02 (26)
40	**UHV-7A**	700	1.50 (38)	1.10 (28)	1.26 (32)
	UHV-8A	1300	1.89 (48)	1.10 (28)	1.26 (32)
	→ **UHV-9A**	2000	2.36 (60)	1.10 (28)	1.26 (32)
50	**UHV-10A**	560	1.50 (38)	1.22 (31)	1.38 (35)
	UHV-11A	1000	1.89 (48)	1.22 (31)	1.38 (35)
	UHV-12A	1700	2.36 (60)	1.22 (31)	1.38 (35)

- Operating temperature range: −30°C to +85°C
- Capacitance: Within the specified tolerance at 25°C, 1 kHz, 1Vrms.
- Withstanding voltage: No breakdown at 1.5 times of rated voltage, 60sec.
- Dissipation factor (tan δ): 0.1% max. at 25°C, 1kHz, 1Vrms.
- Insulation resistance: 100,000MΩ min. at 1kVdc, 60sec.
- Temperature characteristic: Z5T: Maximum capacitance change from the 25°C value shall be +22%, −33% over temperature range of 10°C to 85°C
- AC corona starting voltage: 50% of rated voltage (rms) min. at 50Hz
- Voltage-capacitance characteristics: Capacitance shall not exceed 10% from the initial value when rated voltage is applied.

HIGH VOLTAGE CERAMIC CAPACITORS
Type UHV: 20kVdc to 50kVdc

Temperature characteristics of capacitance

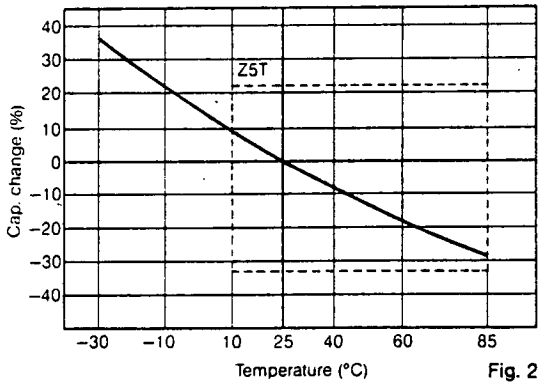

Fig. 2

Temperature characteristics of tan δ

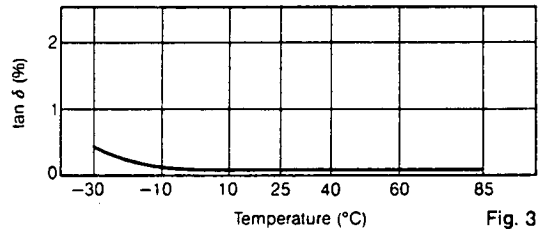

Fig. 3

DC voltage characteristics of capacitance

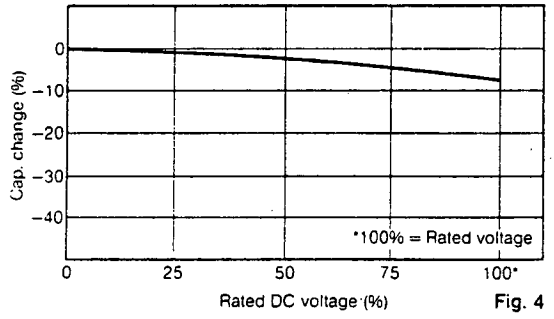

Fig. 4

Life test

Cap. change

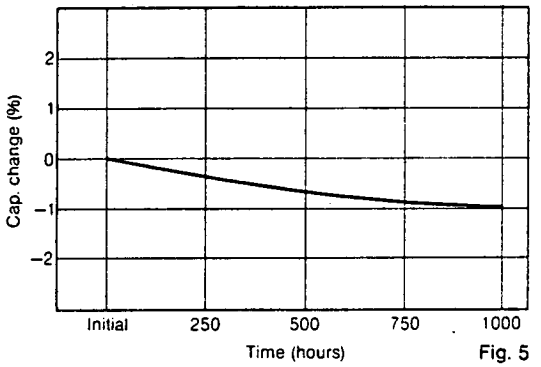

Fig. 5

tan δ

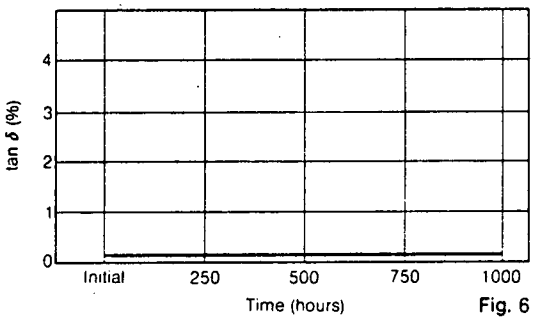

Fig. 6

AC Corona starting voltage

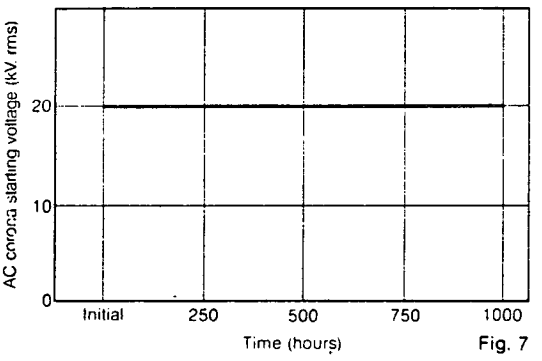

Fig. 7

- Sample: UHV-5A sampling, n = 10
- Test conditions: Sample shall be placed in a chamber at 60°C ± 3°C with an application of 110% of rated voltage for 1,000 hours.

HIGH VOLTAGE CERAMIC CAPACITORS
Type UHV: 20kVdc to 50kVdc

Humidity test

Cap. change

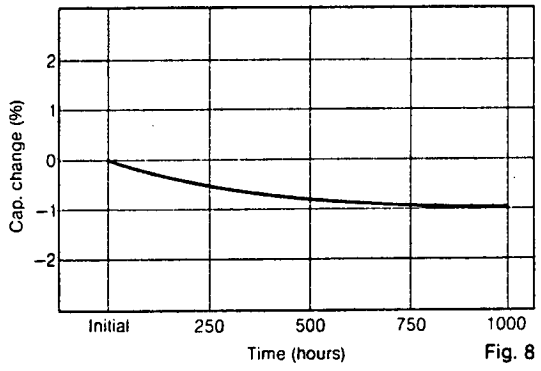

Fig. 8

tan δ

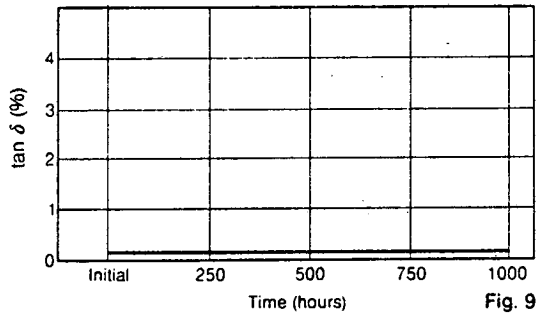

Fig. 9

AC Corona starting voltage

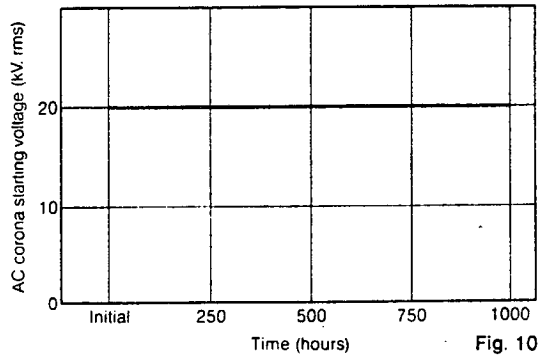

Fig. 10

- Sample: UHV-5A sampling, n = 10
- Test conditions: Sample shall be placed in a chamber at 40°C ±2°C at 90 to 95% RH for 1,000 hours. It shall be taken out every 250 hours and characteristics tested after having been left at normal temperature and humidity for 30 minutes.

Heat cycle test

Cap. change

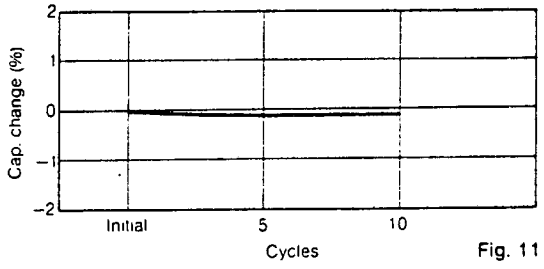

Fig. 11

tan δ

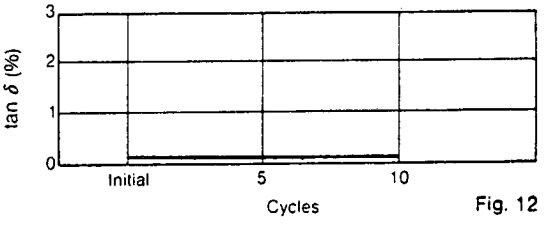

Fig. 12

AC Corona starting voltage

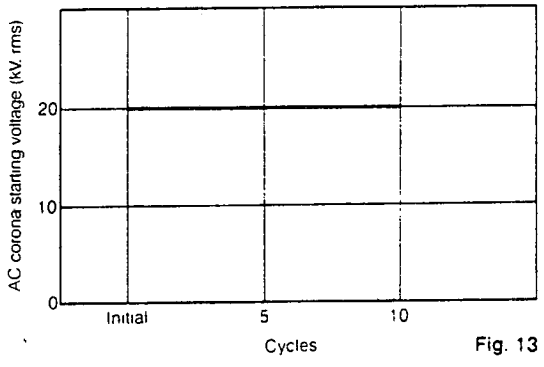

Fig. 13

- Sample: UHV-5A sampling, n = 10
- Test conditions: Sample shall be placed in a chamber and the temperature cycle shown in Fig. 14 repeated 10 times.

Heat cycle test condition

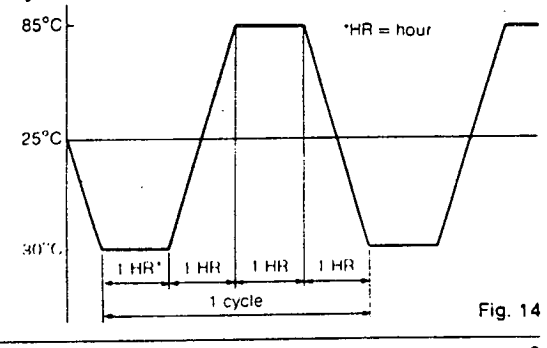

Fig. 14

HIGH VOLTAGE CERAMIC CAPACITORS
Type UHV: 20kVdc to 50kVdc

Discharge test

Capacitance change

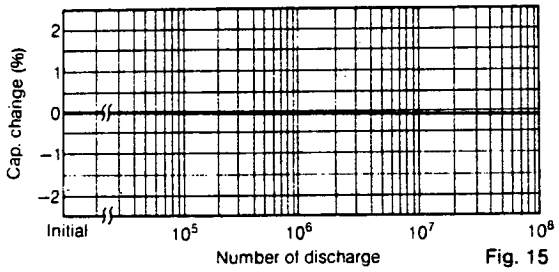

Fig. 15

tan δ

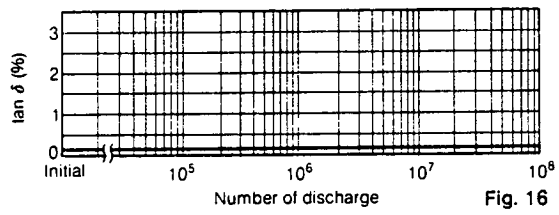

Fig. 16

AC corona starting voltage

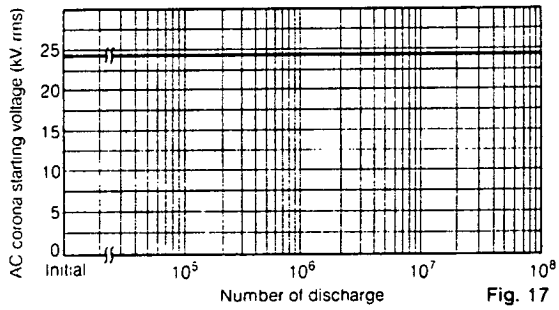

Fig. 17

- Sample: UHV-9A sampling, n = 2
- Test conditions: Sample shall be tested in a circuit shown in Fig. 18 in insulating oil at room temperature.
- Charging voltage: 40kVdc
- Charging/discharging frequency: 10 pulses per second

Discharge test circuit

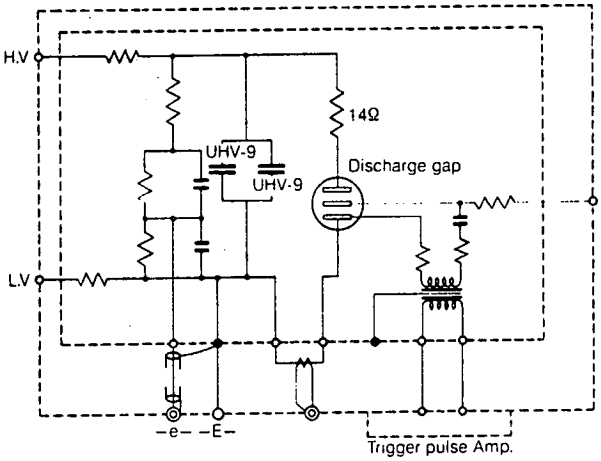

Fig. 18

Discharge test current wave form

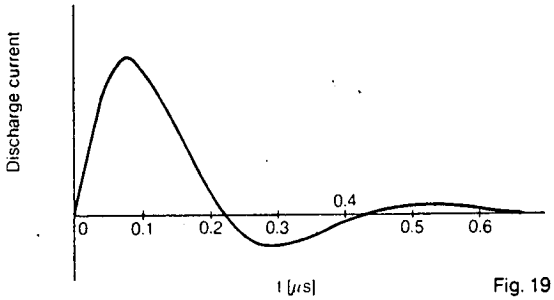

Fig. 19

HIGH VOLTAGE/HIGH POWER CERAMIC CAPACITORS AND HIGH VOLTAGE RESISTORS

CATALOG NO. 62-09

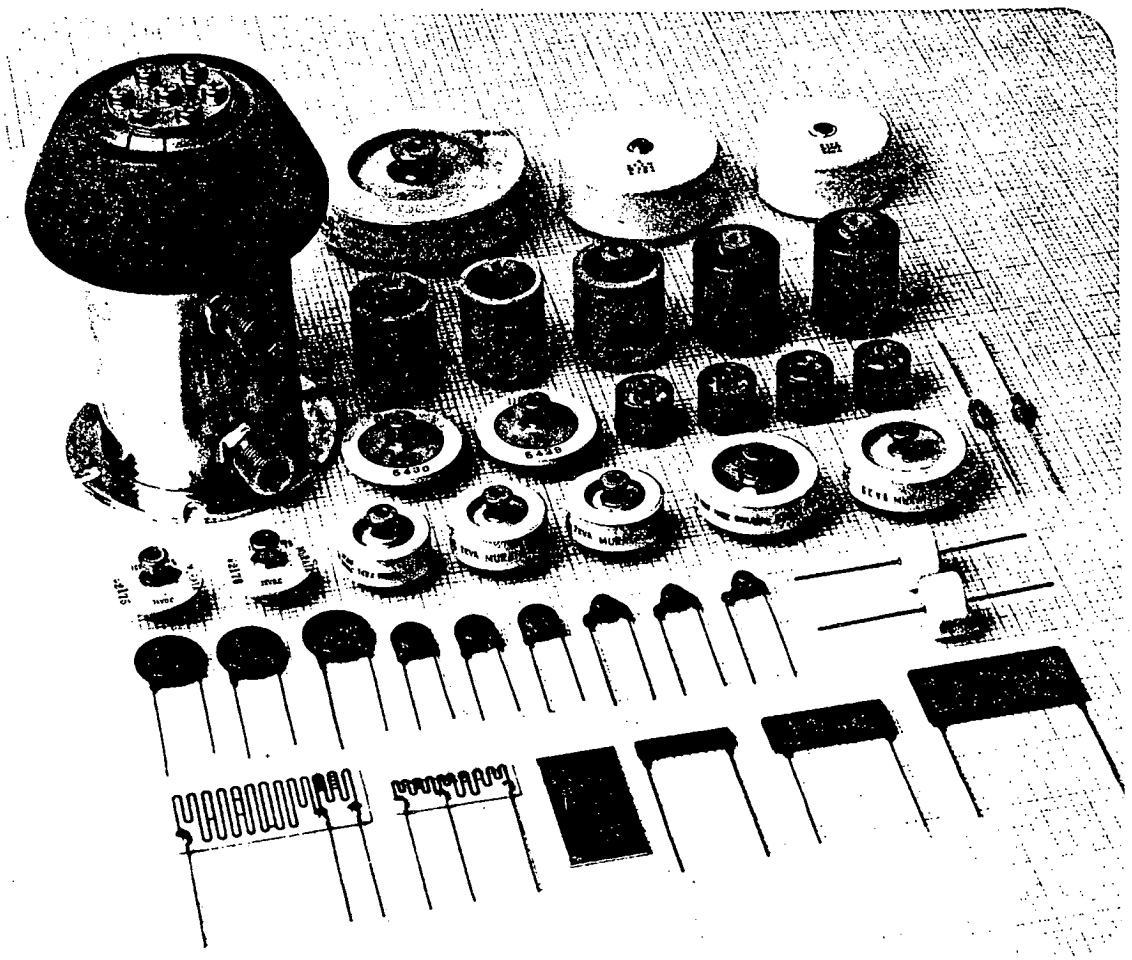

MURATA ERIE NORTH AMERICA

HIGH VOLTAGE
CERAMIC DISC CAPACITORS
DHS SERIES E.I.A. CLASS I

10 to 40 KVDC

DIMENSIONS: in. (mm)

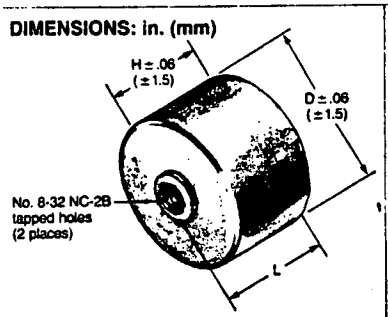

Murata Erie's new High Voltage Ceramic Capacitors DHS N4700 series is designed to meet the stringent requirements of high voltage applications and feature a low dissipation factor and a low voltage coefficient.

FEATURES

- **Epoxy resin encapsulated**
- **Small size**
- **Low dissipation factor and low heating value**
- **Linear temperature characteristic**
- **Low DC, AC-voltage coefficient**

APPLICATIONS

- **HV DC power supplies**
- **Lightning arrestor voltage distribution systems**
- **Electron microscopes, synchroscopes**
- **Gas lasers**
- **Electrostatic copying machines**

PART NUMBERING SYSTEM

TYPE	TEMP. CHAR.	CAPACITANCE	TOL.	VOLTAGE
DHS20	N4700	561	M	10KV

TYPE DHS20 — CAPACITOR TYPE AND SIZE

TEMP. CHAR. N4700 — TEMPERATURE CHARACTERISTICS AND T.C. TOLERANCES
Per standard EIA Specifications
See Page 6

CAPACITANCE 561 — CAPACITANCE VALUE
Expressed in picofarads and identified by a three-digit number. First two digits represent significant figures. Last digit specifies the number of zeros to follow.

TOL. M — CAPACITANCE TOLERANCE
M = ± 20%

VOLTAGE 10KV — VOLTAGE
Identified by a two-digit number in KVDC.

	CAPACITANCE (pF)	WORKING VOLTAGE KVDC	WORKING VOLTAGE KVAC (60Hz)	TEST VOLTAGE (KVDC)	DIMENSIONS: in. (mm) D	L	H
DHS20 N4700 561M-10KV	560	10	4	15	.787 (20)	.63 (16)	.47 (12)
DHS30 N4700 122M-10KV	1,200				1.18 (30)		
DHS30 N4700 182M-10KV	1,800				1.18 (30)		
DHS38 N4700 282M-10KV	2,800				1.49 (38)		
DHS52 N4700 502M-10KV	5,000				2.04 (52)		
DHS60 N4700 802M-10KV	8,000				2.36 (60)		
DHS20 N4700 371M-15KV	370	15	6	23	.787 (20)	.71 (18)	.55 (14)
DHS30 N4700 801M-15KV	800				1.18 (30)		
DHS30 N4700 112M-15KV	1,100				1.18 (30)		
DHS38 N4700 192M-15KV	1,900				1.49 (38)		
DHS52 N4700 342M-15KV	3,400				2.04 (52)		
DHS60 N4700 532M-15KV	5,300				2.36 (60)		
DHS20 N4700 281M-20KV	280	20	8	30	.787 (20)	.95 (24)	.787 (20)
DHS30 N4700 601M-20KV	600				1.18 (30)		
DHS30 N4700 881M-20KV	880				1.18 (30)		
DHS38 N4700 142M-20KV	1,400				1.49 (38)		
DHS52 N4700 252M-20KV	2,500				2.04 (52)		
DHS60 N4700 402M-20KV	4,000				2.36 (60)		
DHS20 N4700 191M-30KV	190	30	12	45	.787 (20)	1.10 (28)	.95 (24)
DHS30 N4700 401M-30KV	400				1.18 (30)		
DHS30 N4700 591M-30KV	590				1.18 (30)		
DHS38 N4700 941M-30KV	940				1.49 (38)		
DHS52 N4700 172M-30KV	1,700				2.04 (52)		
DHS60 N4700 272M-30KV	2,700				2.36 (60)		
DHS20 N4700 141M-40KV	140	40	16	60	.787 (20)	1.42 (36)	1.26 (32)
DHS30 N4700 301M-40KV	300				1.18 (30)		
DHS30 N4700 441M-40KV	440				1.18 (30)		
DHS38 N4700 701M-40KV	700				1.49 (38)		
DHS52 N4700 132M-40KV	1,300				2.04 (52)		
DHS60 N4700 202M-40KV	2,000				2.36 (60)		

TYPICAL MARKING

Manufacturer's Identification
Capacitance (in 3-digit code)
Tolerance (EIA Code)
Rated Voltage
Date Code of Mfg.
T.C.

HIGH VOLTAGE CERAMIC DISC CAPACITORS DHS SERIES SPECIFICATIONS

10 to 40 KVDC

Temperature Range
Operating: −30 to +85°C
Storage: −40°C to +125°C

Capacitance and Tolerance
Capacitance change shall exceed ±20% when measured at 1KHz±0.1KHz at 25°C with not more than 5±0.05Vrms, AC applied during measurement.

Dissipation Factor
The maximum dissipation factor for these capacitors shall be 0.5%
Dissipation factor shall be measured at a frequency of 1KHz±0.1KHz at 25°C with not more than 5±0.5Vrms, AC applied during measurements.

Temperature Characteristics

Characteristic	Temp. Range	Base Temp.	Temp. Coeff.
N4700	−30°C to +85°C	20°	(−4,700±1,000) × 10^{-6}/°C

Dielectric Strength Test
These capacitors shall withstand the specified test voltage for 1 minute through a current-limiting resistor of 1,000Ω.

Insulation Resistance
The minimum value of insulation resistance shall be not less than 10,000MΩ at 25°C.
Measurements shall be made after a 1 minute charge at 500VDC voltage through a current limiting resistor which shall be not greater than 10MΩ.

Humidity Resistance
After exposure for a period of 100 hours to an atmosphere of 95% relative humidity at a temperature of +40°C, capacitors shall have a minimum insulation resistance of 5,000MΩ and a maximum dissipation factor of 1.5%. Twenty-four hours after removal from the test chamber, capacitors shall be measured in accordance with section 3 and 6.

Life Test
These capacitors shall withstand a test potential of 1.5 times the rated DC voltage for a period of 1,000 hours at an ambient temperature of +85°C.

Encapsulation
Ceramic is enclosed in a molded epoxy resin.

TYPICAL TEMPERATURE CHARACTERISTICS

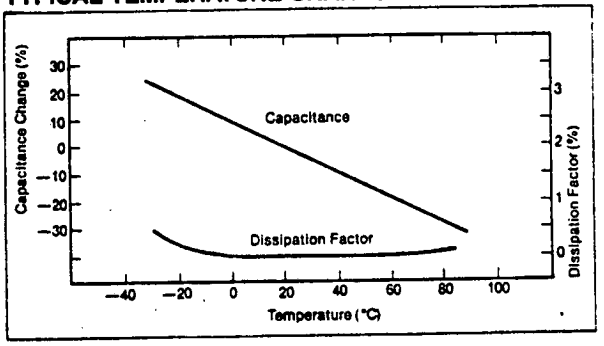

TYPICAL VOLTAGE COEFFICIENT

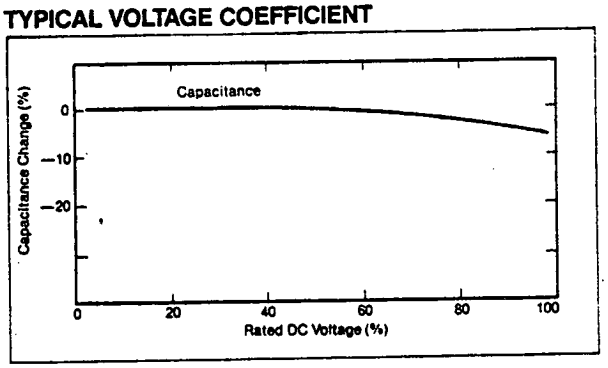

TYPICAL FREQUENCY CHARACTERISTICS

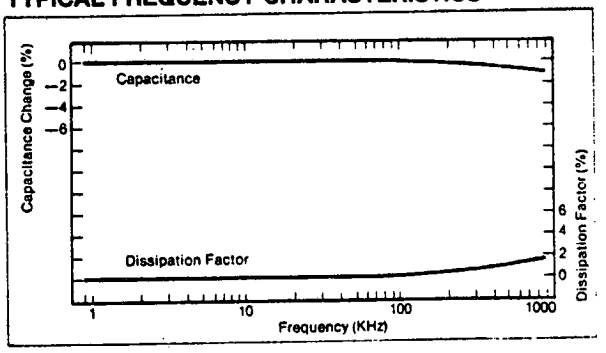

Corona Test

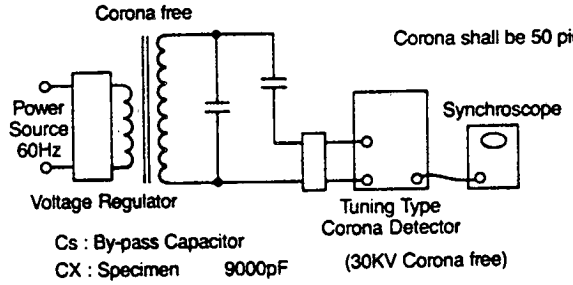

Corona shall be 50 picocoulomb max. in direct reading at
2KVrms (10KV rated voltage)
3KVrms (15KV rated voltage)
4KVrms (20KV rated voltage)
6KVrms, (30KV rated voltage)
8KVrms (40KV rated voltage)

HIGH VOLTAGE CERAMIC CAPACITORS
DHS SERIES E.I.A. CLASS III

10 to 40 KVDC

DIMENSIONS:
in. (mm)

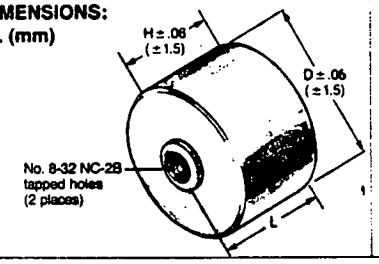

FEATURES

- Epoxy resin encapsulated
- Small size
- Highly reliable internal construction
- Wide selection of values
- Up to 40 KVDC working voltage

APPLICATIONS

- Electrostatic copying machines
- Electron microscopes, synchroscopes
- CRT power supplies
- Lightning arrestor voltage distribution systems
- HVDC power supplies

PART NUMBERING SYSTEM

TYPE	TEMP. CHAR.	CAPACITANCE	TOL.	VOLTAGE
DHS20	Z5V	681	Z	10KV

CAPACITOR TYPE AND SIZE

TEMPERATURE CHARACTERISTICS
Temperature Range Z5 = +10°C to +85°C
MAX. CAP. CHANGE OVER TEMP. RANGE
V = +22%, −82%

CAPACITANCE VALUE
Expressed in picofarads and identified by a three-digit number. First two digits represent significant figures. Last digit specifies the number of zeros to follow.

CAPACITANCE TOLERANCE
Z = +80%, −20%

VOLTAGE
Identified by a two-digit number in KVDC.

PART NUMBER	CAPACITANCE (pF)	WORKING VOLTAGE KVDC	TEST VOLTAGE KVDC	DIMENSIONS: in. (mm) D max.	L	H
DHS20 Z5V 681Z-10KV	680	10	15	.787 (20)	.75 (19)	.66 (17)
DHS24 Z5V 122Z-10KV	1,200			.94 (24)	.74 (19)	.66 (17)
DHS30 Z5V 202Z-10KV	2,000			1.18 (30)	.75 (19)	.66 (17)
DHS38 Z5V 322Z-10KV	3,200			1.49 (38)	.74 (19)	.66 (17)
DHS43 Z5V 472Z-10KV	4,700			1.69 (43)	.75 (19)	.66 (17)
DHS52 Z5V 6527-10KV	6,500			2.04 (52)	.74 (19)	.66 (17)
DHS57 Z5V 832Z-10KV	9,300			2.24 (57)	.75 (19)	.66 (17)
DHS60 Z5V 932Z-10KV	9,300			2.36 (60)	.74 (19)	.66 (17)
DHS20 Z5V 471Z-15KV	470	15	23	.787 (20)	.90 (23)	.82 (21)
DHS24 Z5V 801Z-15KV	800			.94 (24)	.90 (23)	.82 (21)
DHS30 Z5V 132Z-15KV	1,300			1.18 (30)	.90 (23)	.82 (21)
DHS38 Z5V 222Z-15KV	2,200			1.49 (38)	.90 (23)	.82 (21)
DHS43 Z5V 322Z-15KV	3,200			1.69 (43)	.90 (23)	.82 (21)
DHS52 Z5V 462Z-15KV	4,600			2.04 (52)	.90 (23)	.82 (21)
DHS57 Z5V 582Z-15KV	5,800			2.24 (57)	.90 (23)	.82 (21)
DHS60 Z5V 652Z-15KV	6,500			2.36 (60)	.90 (23)	.82 (21)
DHS20 Z5V 351Z-20KV	350	20	30	.787 (20)	1.02 (26)	.94 (24)
DHS24 Z5V 601Z-20KV	600			.94 (24)	1.02 (26)	.94 (24)
DHS30 Z5V 102Z-20KV	1,000			1.18 (30)	1.02 (26)	.94 (24)
DHS38 Z5V 162Z-20KV	1,600			1.49 (38)	1.02 (26)	.94 (24)
DHS43 Z5V 242Z-20KV	2,400			1.69 (43)	1.02 (26)	.94 (24)
DHS52 Z5V 332Z-20KV	3,300			2.04 (52)	1.02 (26)	.94 (24)
DHS57 Z5V 432Z-20KV	4,300			2.24 (57)	1.02 (26)	.94 (24)
DHS60 Z5V 482Z-20KV	4,800			2.36 (60)	1.02 (26)	.94 (24)
DHS20 Z5V 261Z-30KV	260	30	45	.787 (20)	1.33 (34)	1.25 (32)
DHS24 Z5V 461Z-30KV	460			.94 (24)	1.33 (34)	1.25 (32)
DHS30 Z5V 781Z-30KV	780			1.18 (30)	1.33 (34)	1.25 (32)
DHS38 Z5V 122Z-30KV	1,200			1.49 (38)	1.33 (34)	1.25 (32)
DHS43 Z5V 182Z-30KV	1,800			1.69 (43)	1.33 (34)	1.25 (32)
DHS52 Z5V 252Z-30KV	2,500			2.04 (52)	1.33 (34)	1.25 (32)
DHS57 Z5V 3327-30KV	3,300			2.24 (57)	1.33 (34)	1.25 (32)
DHS60 Z5V 362Z-30KV	3,600			2.36 (60)	1.33 (34)	1.25 (32)
DHS20 Z5V 181Z-40KV	180	40	60	.787 (20)	1.61 (41)	1.53 (39)
DHS24 Z5V 341Z-40KV	340			.94 (24)	1.61 (41)	1.53 (39)
DHS30 Z5V 571Z-40KV	570			1.18 (30)	1.61 (41)	1.53 (39)
DHS38 Z5V 921Z-40KV	920			1.49 (38)	1.61 (41)	1.53 (39)
DHS43 Z5V 132Z-40KV	1,300			1.69 (43)	1.61 (41)	1.53 (39)
DHS52 Z5V 192Z-40KV	1,900			2.04 (52)	1.61 (41)	1.53 (39)
DHS57 Z5V 242Z-40KV	2,400			2.24 (57)	1.61 (41)	1.53 (39)
DHS60 Z5V 272Z-40KV	2,700			2.36 (60)	1.61 (41)	1.53 (39)

TYPICAL MARKING

Manufacturer's Identification
Capacitance (in pF)
Tolerance (EIA Code)
Rated Voltage
Date Code of Mfg.

HIGH VOLTAGE CERAMIC CAPACITORS
DHS SERIES SPECIFICATIONS

10 to 40 KVDC

Temperature Range
Operating: −30°C to +85°C
Storage: −40°C to +125°C

Capacitance and Tolerance
Characteristic: Z5V
Temp. Range: −10°C to +85°C
Cap. Change: Within +22%, −82% of 25°C value (Within a given lot, ±10% of the mean value is typical)
Capacitance shall be measured at a frequency of 1KHz ± 0.1KHz at 25°C with not more than 5 ± 0.5Vrms AC applied during measurement.

Dissipation Factor
The maximum dissipation factor for these capacitors shall be 1.5%.

Dissipation factor shall be measured at a frequency of 1KHz ± 0.1KHz at 25°C with not more than 5 ± 0.5Vrms AC applied during measurements.

Dielectric Strength Test
These capacitors shall withstand the specified test voltage for 1 minute through a current-limiting resistor of 1000Ω.

Ultimate Voltage Breakdown Test
These capacitors shall be capable of withstanding a DC potential of twice the rated DC voltage for a period of 10 seconds. The test voltage shall be applied at a rate not greater than 10KV/second.

Insulation Resistance
The minimum value of insulation resistance shall be not less than 10,000MΩ.

Measurements shall be made after a 1 minute charge at 500V DC voltage through a current limiting resistor which shall be not greater than 10MΩ.

Humidity Resistance
After exposure for a period of 100 hours to an atmosphere of 95% relative humidity at a temperature of +40°C, capacitors shall have a minimum insulation resistance of 5000MΩ and a maximum dissipation factor of 2%. Twenty-four hours after removed from the test chamber, capacitors shall be measured in accordance with Section 3 and 6.

Life Test
These capacitors shall withstand a test potential of 1.5 times the rated DC voltage for a period of 1000 hours at an ambient temperature of +85°C.

Encapsulation
Ceramic is enclosed in a molded epoxy resin.

TYPICAL TEMPERATURE CHARACTERISTICS

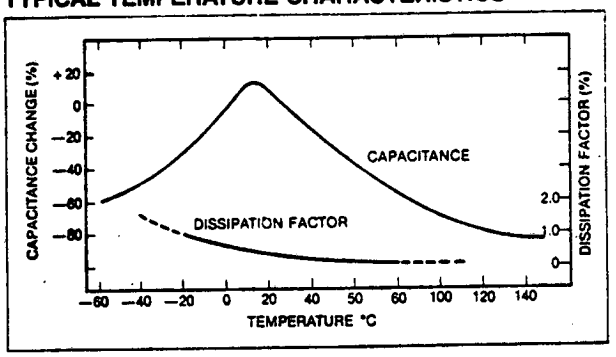

TYPICAL FREQUENCY CHARACTERISTICS

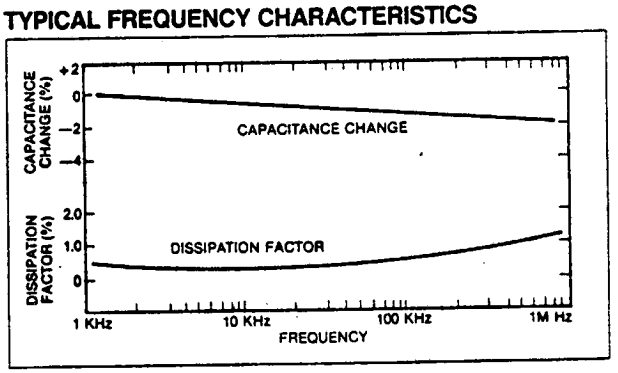

TYPICAL VOLTAGE COEFFICIENT

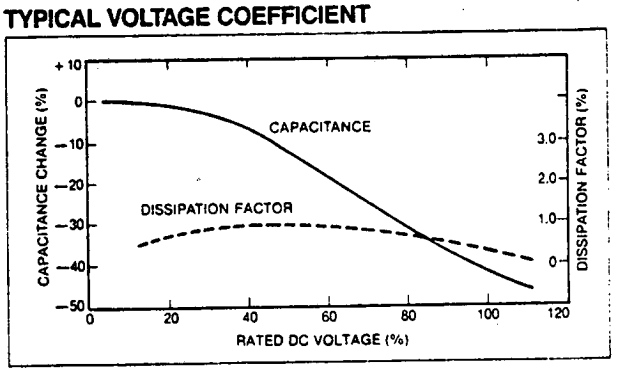

Corona Test

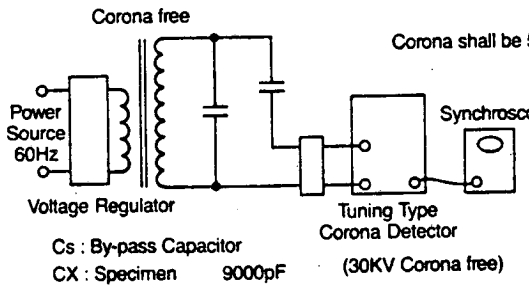

Corona shall be 50 picocoulomb max. in direct reading at
2KVrms (10KV rated voltage)
3KVrms (15KV rated voltage)
4KVrms (20KV rated voltage)
6KVrms (30KV rated voltage)
8KVrms (40KV rated voltage)

The Carborundum Company
Electronic Ceramics Division
P.O. Box 664
Niagara Falls, New York 14302
Telephone 716-278-2521
Fax 716-278-6270

Carborundum® Non-Inductive Resistors

Carborundum® resistors are problem solvers for:
Impulse generators
Electronic generators
Capacitor discharging
Protecting silicon rectifiers
High-frequency circuits
High-voltage circuits
X-ray equipment
RF dummy loads
Capacitor current limiting
Parasitic oscillation protection
High-frequency circuits
High-current circuits
. . . just to name a few uses.

Carborundum ceramic non-inductive resistors are supplied in a wide variety of sizes and wattages. Listed below is a short summary of additional standard groupings available. Individual data bulletins listing complete descriptions and specifications are available on request. Write for the units you are interested in.

Connectors and Terminals
Complete descriptions on finger stock connector caps, radial terminal lugs and anti-corona ring pulse power terminals are available on request.

Carborundum Resistors are Supplied in Three Versions
Type AS for its ability to absorb high amounts of energy and for its non-inductive property at high voltage.
Type SP for great AC power handling capacity at either power frequencies or at many megahertz.
Type A for a high power non-inductive resistor when high resistance is required.

†*Allowable peak energy/voltage will depend on the resistance value.*

Series 234 and 231 Resistors

Carborundum Series 234 and 231 resistors are a small size non-inductive bulk type resistor (there are no spirals or windings), capable of dissipating a full 10 watts of power (Type SP) or absorbing 275 joules of energy (Type AS).

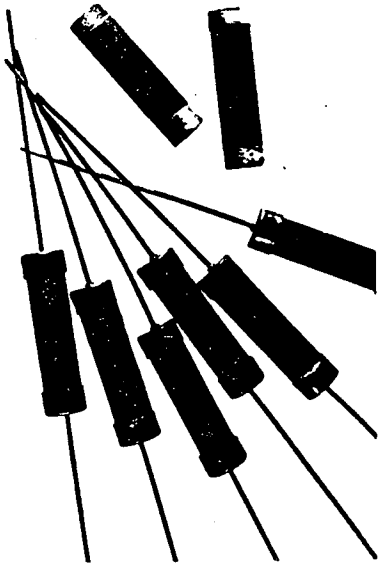

Specifications	234SP	234AS	231SP	231AS
Resistance, ohms ±5%, ±10%, ±20%	1-330	12-5000	1-1000	25-6250
Peak voltage†	500 volts	2.5kv	375 volts	1.5kv
Power at 40°C	10 watts	3 watts	2.5 watts	1.5 watts
Derate linearly to 0 watts at:	350°C	230°C	350°C	230°C
Max. operating temperature	350°C	230°C	350°C	230°C
Peak energy†	30 joules	275 joules	15 joules	75 joules

Characteristics	234SP	234AS	231SP	231AS
Short time overload				
10 cycles of 1000% rated power	5% max.	1% max.	3.5% max.	1% max.
5 sec. on, 90 sec. off				
Life test 1000 hr. rated power	5% max.	5% max.	5% max.	5% max.
Temperature coefficient	±0.075%/°C	-0.075%/°C	±0.075%/°C	-0.075%/°C

Type 234

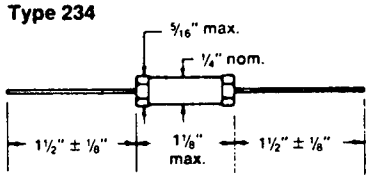

Type 231

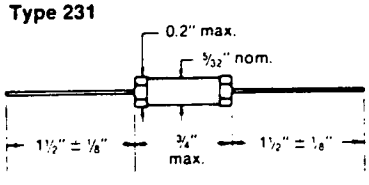

CARBORUNDUM

Form A-7049 Effective: 9/88
Supersedes 2/88

Series 800 and 1000

This general line is available in a wide variety of sizes and terminations. They retain the non-inductive and heavy load characteristics of all Carborundum ceramic resistors. These resistors can handle up to 1000 watts, 165 KJ and 165 KV in resistance values from 1 ohm to 1 megohm.

Parts are specified by the four or five character type number (for example

885SP, 888AS, 890A), the first two digits of the resistance, a single digit to indicate the power of ten multiplier, and a "J" for ±5%, a "K" for ±10%, or an "L" for ±20%. Where the resistance is less than ten ohms, the power of ten multiplier is not used, and an "R" replaces the decimal point. Thus R50 = 0.50 ohm, 7R5 = 7.5 ohm, 220 = 22.0 ohm, 152 = 1500 ohm, etc.

Standard construction for type SP resistors provides aluminum metalization, while type A resistors have nickel metalization. * Type AS resistors have silver metalization with a dielectric coating. These standard features are designated by the suffix "DS".

The AS resistor can also be supplied for oil applications with the suffix "GO" or "HO" which provide a radial or horizontal tab terminated resistor, coated for use in oil. The suffix "N" provides a no arc terminal with a dielectric coating for applications requiring high energy or current density performance. Consult customer service for additional options and part number and performance detail. A typical part number would be 886AS501KDS. This represents a type AS resistor, 5" long x 3/4" diameter, 500 ± 10% ohms, with dielectric coating, and silver terminations.

Electrical Specifications

Length and Diameter	Type	Resistance Available ohms Min.	to	Max.	Average Power @40°C (watts)	Peak Energy (joules)†	Peak Voltage (volts)†
2" x ½"	884SP	1.0		200	22.5	250	1,000
2½" x ¾"	885SP	1.0		130	45	250	1,000
	885AS . . DS*	6.0		1200	15	2,800	8,000
	885A	1500		220K	15	750	3,750
5" x ¾"	886SP	1.0		330	90	500	4,000
	886AS . . DS*	15.0		3300	30	7,000	20,000
	886A	3900		390K	30	1,500	10,000
6" x 1"	887SP	1.0		330	150	1,600	4,000
	887AS . . DS*	12.0		3300	50	13,000	30,000
	887A	3900		390K	50	6,000	12,000
6" x 1½"	1026AS . . DS*	5.0		1200	70	37,000	30,000
8" x 1"	888SP	1.0		390	190	2,100	6,000
	888AS . . DS*	15.0		3900	75	16,500	45,000
	888A	4700		470K	60	7,500	15,000
8" x 1½"	1028A . . DS*	6.5		1875	100	46,000	45,000
12" x 1"	889SP	1.0		680	275	3,200	10,000
	889AS . . DS*	25.0		6800	100	27,000	75,000
	889A	8200		680K	90	12,500	25,000
12" x 1½"	1032AS . . DS*	9.0		2500	150	75,000	75,000
18" x 1"	890SP	1.0		1000	375	4,200	16,000
	890AS . . DS*	40.0		10K	150	43,000	120,000
	890A	12K		1M	125	20,000	40,000
18" x 1½"	1038AS . . DS*	15.0		3800	225	119,000	120,000
18" x 2"	891SP	1.0		450	750	15,000	16,000
24" x 2"	892SP	1.0		600	1000	17,500	22,000
24" x 1½"	1044AS . . DS*	20.0		4800	300	164,000	165,000

Characteristics	Type SP	Type AS	Type A
Maximum operating temperature: °C	350	230	230
Temperature coefficient: percent per degree C, -55°C to maximum rated temperature	±0.075	-0.075	-0.20
Voltage coefficient: Maximum percent per kilovolt per inch active length (overall length less termination)	1.0	1.0	—
Short time overload: Maximum percent change after 5 cycles 10 times rated power, 5 seconds on, 90 seconds off	2.0	2.0	—
Moisture resistance: Maximum percent change when tested per MIL-STD-202 method 103	2.5	2.5	2.5

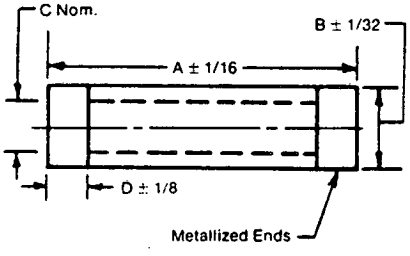

Standard Sizes

Type	A	B	C (SP&AS)	C (A)	D
884 SP	2.0	0.50	0.22	—	0.25
885 SP, AS, & A	2.5	0.75	0.50	0	0.50
886 SP, AS, & A	5.0	0.75	0.50	0	0.62
887 SP, AS & A	6.0	1.00	0.75	0.5	0.50
888 SP, AS, & A	8.0	1.00	0.75	0.5	0.88
889 SP, AS, & A	12.0	1.00	0.75	0.5	0.88
890 SP, AS & A	18.0	1.00	0.75	0.5	0.88
891 SP	18.0	2.00	1.50	—	1.00
892 SP	24.0	2.00	1.50	—	1.00
1026 AS	6.0	1.50	1.00	—	0.50
1028 AS	8.0	1.50	1.00	—	0.88
1032 AS	12.0	1.50	1.00	—	0.88
1038 AS	18.0	1.50	1.00	—	0.88
1044 AS	24.0	1.50	1.00	—	0.88

Special sizes are available: consult factory.

UNCLASSIFIED

SECURITY CLASSIFICATION OF FORM
(highest classification of Title, Abstract, Keywords)

DOCUMENT CONTROL DATA

(Security classification of title, body of abstract and indexing annotation must be entered when the overall document is classified)

1. **ORIGINATOR** (the name and address of the organization preparing the document. Organizations for whom the document was prepared, e.g. Establishment sponsoring a contractor's report, or tasking agency, are entered in section 8.)

Defence Research Establishment Ottawa
Ottawa, Ontario
K1A 0Z4

2. **SECURITY CLASSIFICATION** (overall security classification of the document including special warning terms if applicable)

UNCLASSIFIED

3. **TITLE** (the complete document title as indicated on the title page. Its classification should be indicated by the appropriate abbreviation (S,C or U) in parentheses after the title.)

DESIGN OF A TEM CELL EMP SIMULATOR (U)

4. **AUTHORS** (Last name, first name, middle initial)

SEVAT, PETER

5. **DATE OF PUBLICATION** (month and year of publication of document)	6a. **NO. OF PAGES** (total containing information. Include Annexes, Appendices, etc.)	6b. **NO. OF REFS** (total cited in document)
JUNE 1991	114	110

7. **DESCRIPTIVE NOTES** (the category of the document, e.g. technical report, technical note or memorandum. If appropriate, enter the type of report, e.g. interim, progress, summary, annual or final. Give the inclusive dates when a specific reporting period is covered.)

DREO REPORT

8. **SPONSORING ACTIVITY** (the name of the department project office or laboratory sponsoring the research and development. Include the address.)

Defence Research Establishment Ottawa
Electronics Division, Nuclear Effects Section
Ottawa, Ontario K1A 0Z4

9a. **PROJECT OR GRANT NO.** (if appropriate, the applicable research and development project or grant number under which the document was written. Please specify whether project or grant)	9b. **CONTRACT NO.** (if appropriate, the applicable number under which the document was written)
041LT	

10a. **ORIGINATOR'S DOCUMENT NUMBER** (the official document number by which the document is identified by the originating activity. This number must be unique to this document.)	10b. **OTHER DOCUMENT NOS.** (Any other numbers which may be assigned this document either by the originator or by the sponsor)
DREO REPORT 1084	

11. **DOCUMENT AVAILABILITY** (any limitations on further dissemination of the document, other than those imposed by security classification)

(X) Unlimited distribution
( ) Distribution limited to defence departments and defence contractors; further distribution only as approved
( ) Distribution limited to defence departments and Canadian defence contractors; further distribution only as approved
( ) Distribution limited to government departments and agencies; further distribution only as approved
( ) Distribution limited to defence departments; further distribution only as approved
( ) Other (please specify):

12. **DOCUMENT ANNOUNCEMENT** (any limitation to the bibliographic announcement of this document. This will normally correspond to the Document Availability (11). however, where further distribution (beyond the audience specified in 11) is possible, a wider announcement audience may be selected.)

UNCLASSIFIED

SECURITY CLASSIFICATION OF FORM

UNCLASSIFIED

SECURITY CLASSIFICATION OF FORM

13. ABSTRACT (a brief and factual summary of the document. It may also appear elsewhere in the body of the document itself. It is highly desirable that the abstract of classified documents be unclassified. Each paragraph of the abstract shall begin with an indication of the security classification of the information in the paragraph (unless the document itself is unclassified) represented as (S), (C), or (U). It is not necessary to include here abstracts in both official languages unless the text is bilingual).

(U) This report is a compilation of design criteria for a Transverse Electromagnetic (TEM) cell, an EMP generator and a terminating network. From this information, two detailed designs are presented, one for a 50 Ω and the other for a 100 Ω cell. Both these designs integrate the three sections mentioned above into one shielded system.

14. KEYWORDS, DESCRIPTORS or IDENTIFIERS (technically meaningful terms or short phrases that characterize a document and could be helpful in cataloguing the document. They should be selected so that no security classification is required. Identifiers, such as equipment model designation, trade name, military project code name, geographic location may also be included. If possible keywords should be selected from a published thesaurus. e.g. Thesaurus of Engineering and Scientific Terms (TEST) and that thesaurus-identified. If it is not possible to select indexing terms which are Unclassified, the classification of each should be indicated as with the title.)

Electromagnetic

EMP

TEM CELL